EFFECTS OF PROLONGED GLUCOSE INFUSION ON INSULIN SIGNAL TRANSDUCTION AND GLUCOSE TRANSPORT IN RAT SKELETAL MUSCLE

Einfluss einer Dauerinfusion von Glucose auf Insulinsignaltransduktion und Glukosetransport im Skelettmuskel der Ratte

DISSERTATION

der Fakultät für Chemie und Pharmazie
der Eberhard-Karls-Universität Tübingen

zur Erlangung des Grades eines Doktors
der Naturwissenschaften

2000

vorgelegt von
Basel Houdali

Tag der mündlichen Prüfung:	15. Juni 2000
Dekan:	Prof. Dr. U. NAGEL
1. Berichterstatter:	Prof. Dr. H.P.T. AMMON
2. Berichterstatter:	Prof. Dr. K. RETT

Die vorliegende Arbeit wurde im Mai 1997 unter der Anleitung von Herrn Professor Dr. H.P.T. Ammon und Herrn Prof. Dr. Kristian Rett am Pharmazeutischen Institut und in der Medizinischen Klinik und Poliklinik / Abteilung Innere Medizin IV (Diabetologie) begonnen und im Mai 2000 abgeschlossen.

Herrn Prof. Dr. Ammon, Herrn Prof. Dr. Rett und Herrn Prof. Dr. Häring danke ich für die Überlassung des Themas und die Ermöglichung dieser Dissertation.

Herrn Prof. Dr. Schleicher danke ich für die Laborbetreuung, für die wissenschaftlichen Anregungen und Diskussionen sowie für die ständige Hilfsbereitschaft bei Problemen aller Art.

Mein besonderer Dank gilt Herrn Prof. Dr. Rett für sein ständiges Interesse am Fortgang dieser Arbeit, seine immer freundliche Art und seine fachliche und sonstige Unterstützung.

Herrn Dr. Machicao danke ich für seine Unterstützung, für die Zurverfügungstellung seines PCR-Labors und für das Korrekturlesen dieser Arbeit.

Herrn Dr. Lehmann und Herrn Alexander Beck danke ich für die Unterstützung bei der Kapillarelectrophorese.

Herrn PD Dr. Dr. H.G. Wahl danke ich für die Ermöglichung der gaschromatographischen Analyse der Fettsäurezusammensetzung im Skelettmuskel.

Bei allen Mitgliedern der beiden Arbeitskreise, insbesondere bei Herrn Dr. Wolfgang Schechinger möchte ich mich für das freundliche und fröhliche Arbeitsklima, die gute Zusammenarbeit und die geistige Unterstützung bedanken.

Der Deutschen Diabetes Stiftung, der Firma Bayer AG, der Fortüne Einrichtung der Universitätsklinik Tübingen und der Friedrich-Ebert-Stiftung danke ich für die finanzielle Unterstützung.

Für meine Eltern und meine Frau
in Liebe und Dankbarkeit

Meine akademischen Lehrer waren die Herrn Professoren:

A. Nahrstedt	Pharmazeutische Biologie
H. Glasl	Pharmazeutische Biologie
G. Blaschke	Pharmazeutische Chemie
B. Unterhalt	Pharmazeutische Chemie
W. Meyer zu Reckendorf	Pharmazeutische Analytik
E.J. Verspohl	Pharmakologie
R. Gröning	Pharmazeutische Technologie
P. Rohdewald	Klinische Chemie
M. Stockhausen	Mathematik
L. Reimer	Physik
G. Peters	Mikrobiologie

Lebenslauf

Name:	Houdali
Vorname:	Basel
Adresse:	Ovellackerhof 2, 45891 Gelsenkirchen
Geboren:	24.12.1970 in Kuwait
Schule:	1977-1981 Grundschule in Kuwait
	1981-1985 Intermediate School in Kuwait
	1985-1989 High School in Kuwait
Schulabschluss:	General Secondary School Education im Mai 1989
Studium:	Sept. 1989 - Mai 1990 Studium der Chemie-ingenieurwissenschaft in Kuwait
	Im Sommer 1990 Wechsel nach Deutschland
	Juni 1990 - Jan. 1991 Sprachschule in Erlangen
	Feb. 1991 - Dez. 1991 Studienkolleg in Münster
	SS 1992 Studium der Pharmazie in Münster
Studiumabschluss:	Im November 1997 Abschluss der Pharmazeutischen Prüfung
Promotion:	Mai 1997 - Mai 2000 Promotionarbeit bei Prof. Dr. Ammon, Lehrstuhl Pharmakologie für Naturwissenschaftler, Tübingen und Prof. Dr. Häring, Innere Medizin/Abteilung IV and der Medizinischen Klinik und Poliklinik der Universität Tübingen zum Thema: ”Effects of Prolonged Glucose Infusion on Insulin Signal Transduction and Glucose transport in Rat Skeletal Muscle”
Förderung:	Jan. - Juni 1998 Friedrich-Ebert-Stiftung Juni - April 1999 Bayer AG April1999 - Mai 2000 Fortüne / Universität Tübingen Ab Juli 1999 auch Deutsche Diabetes Stiftung / München

4 RESULTS

ABBREVIATIONS

°C	Grade centigrade
A	Ampère (current unit)
AKT	Viral oncoprotein homology, also PKB
ATP	Adonosin triphosphate
AUC	Area under the curve
bp	Base pair
BSA	Bovine serum albumin
C	Control animals
CE	Cholestrol esters
CZE	Capillary zone electrophoresis
d	Day
DAG	Diacylglycerol
DG	Diglycerides
DHPRα1	Dihydropyridine receptor α1-subunit
dNTP	Desoxynucleotide
ECL	Enhanced chemiluminescence
FAME	Fatty acid methyl esters
FFA	Free fatty acids
g	Gravitation force
GFAT	Glutamine:fructose-6-phophate amidotransferase
GIR	Glucose infused rats
Glc-6-p	Glucose-6-phosphate
GLUT1	Glucose transporter isoform 1
GLUT4	Glucose transporter isoform 4
Grb-10	Growth factor receptor binding protein-10
Grb2	Growth factor receptor binding protein-2
H	Hour
HGO	Hepatic glucose output
HRP	Horseradish peroxidase
IDDM	Insulin dependent diabetes mellitus
IgG	Immunoglobulin G
IP	Immunoprecipitation
IR	Insulin receptor
IRS-1-4	Insulin receptor substrate 1-4
KDa	Kilo Dalton
min	Minute
Na/K-ATPaseα1	Sodium/potassium exchange enzyme α1-subunit
NIDDM	Non-insulin dependent diabetes mellitus
O-GlcNAc transferase	UDP-GlcNAc β-N-acetylglucosaminyltransferase
P	Phosphor
P110	Protein 110 KDa
P85	Protein 85 KDa
PBS	Phosphate buffered saline
PDK1-2	Phosphoinositol dependent kinase 1-2
PE	Polyethylene
PH	Pleckstrin homology
PI	Phosphatidylinositol
PI3-K	Phosphatidylinositol-3-Kinase
PIP_3	Phosphatidylinositol triphosphate

ABBREVIATIONS

PKB	Protein kinase B
PKC	Protein Kinase C
PL	Phospholipids
PMSF	Phenylmethylsulfonyl fluoride
ppm	Parts per million
PTB	Phosphotyrosine binding domain
P-Tyrosine	Phospho-tyrosine
RAC	Protein kinase related to A and C kinases, also PKB
rpm	Revolutions per minute
RT-PCR	Reverse transcriptase-polymerase chain reaction
s	Second
SDS-PAGE	Sodium dedecyl sulfate-polyacrylamide gel electrophoresis
SEM	Standard error of the mean
Ser	Serine
SH2	Src homology 2
SH3	Src homology 3
SHC	Src homology and collagen
SH-PTP2	Src homolgy-Protein tyrosine phosphatase 2
SIR	saline infused rats
SOS	Son-Of-Sevenless
Src	Rous asian sarcoma tyrosine kinase
$T_{1/2}$	half-time life
TG	Triglycerides
TPA	12-O-tetradecanoylphorbol-13-acetate
TT	Transversal tubules membranes
Tyr	Tyrosine
UDP	Uridin diphosphate
UDP-GalNAc	UDP-N-acetylgalactosamine
UDP-GlcNAc	UDP-N-acteylglucosamine
vs.	Versus

1 INTRODUCTION

1.1 Glucose Homeostasis

Glucose represents an essential energy substrate for many tissues. The maintenance of narrow-controlled blood glucose concentrations (glucose homeostasis) is central for a constant provision of glucose to the brain. Glucose homeostasis is a physiologically well-balanced mechanism depending on three coordinated and simultaneously ongoing processes involving insulin secretion by the pancreas, hepatic glucose output and glucose uptake by splanchnic (liver and gut) and peripheral tissues (muscle and fat).

1.2 Insulin Signal Transduction

Glucose uptake in peripheral tissues is mediated by glucose transporters (see below). Insulin stimulates the translocation of glucose transporters to the surface of muscle and adipose cells, which increases glucose uptake in these tissues. Considerable advances have been recently made in identifying the mechanism of insulin-stimulated glucose uptake.

1.2.1 The Insulin Receptor

Insulin signal transduction into muscle and fat involves coupling of ligand-receptor and its interaction to many intracellular events. The eventual outcome is increased glucose uptake as well other metabolic and mitogenic consequences (Denton & Tavare , 1995).
The insulin receptor (IR) belongs into the family of transmembraneous receptors with tyrosine kinase domain. IR consists of two extracellular α-subunits and two β-subunits, which transverse the membrane and are linked by disulfide bonds (s. fig. 1.2.1). The insulin receptor can be divided into three structural regions: an extracellular segment, where binding to insulin occurs, a transmembrane domain, which is a passive lipid anchor and an intracellular domain consisting of a regulatory domain and a tyrosine kinase domain capable of autophosphorylation as well as phosphorylation of intracellular substrates on their tyrosine residues (Haring, Kasuga, et al. 1982), (Kasuga, Zick, et al. 1982).
Binding of insulin to its receptor induces a conformational change of the subunits bringing them into close proximity, which in turn facilitates pair trans-phosphorylation of each subunit (by the other). Autophosphorylation on tyrosine residues located on an activation loop displaces the latter from the catalytic site allowing access to intracellular substrates (Ashcroft & Ashcroft, Insulin, Oxford press, 1992). The insulin receptor is internalized upon binding to insulin. Insulin is then dissociated in endosomes from its receptor and degraded subsequently. The insulin receptor is then redistributed to the cell surface (Carpentier 1992).

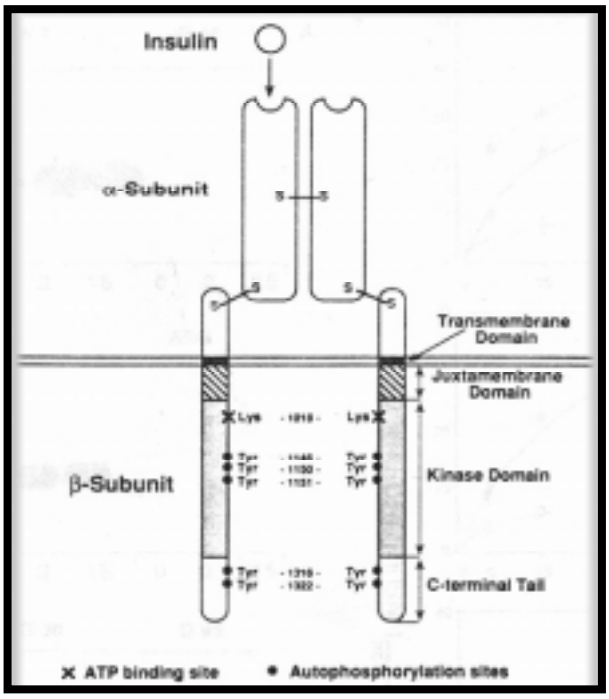

Figure 1.2.1 Schematic presentation of the insulin receptor showing the two extracellular α-subunits and the cytosolic β-subunits. Specific tyrosine phosphorylation sites (Tyr) are indicated. From (Carpentier 1992).

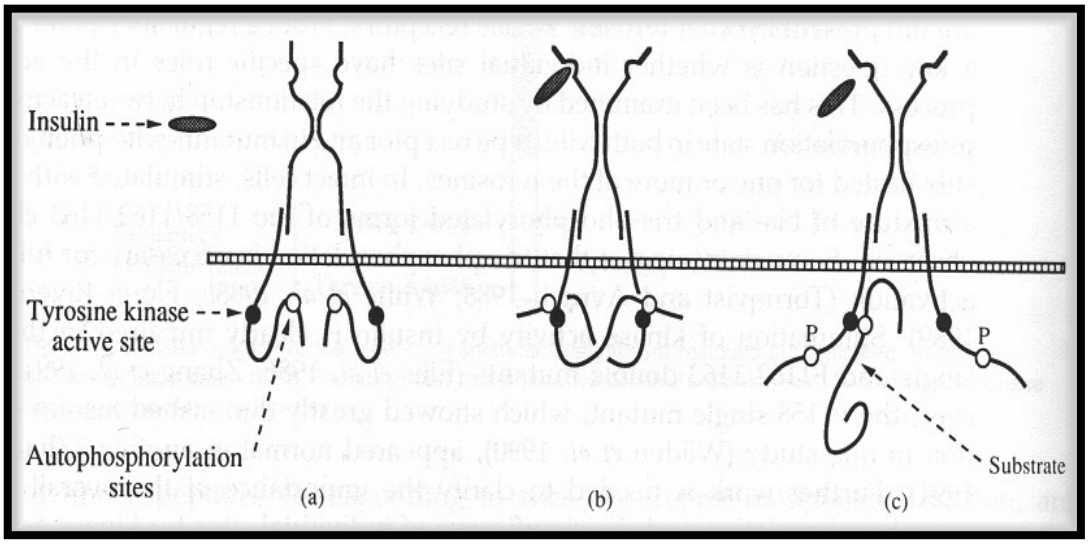

Figure 1.2.2 Schematic presentation of the activation model of IR. (a) in basal state, autophosphorylation site is obscured by an activation loop. (b) Binding of insulin to its receptor induces conformational changes allowing cross phosphorylation of β-subunits. (c) Autophosphorylation induces further conformational changes making phosphorylated sites accessible for intracellular substrates. From (Ashcroft & Ashcroft, Insulin, Oxford Express, 1992).

1.2.2 Formation of Signaling Complexes for the Intracellular Propagation of Insulin Action

Autophosphorylation of IR creates binding sites for signaling molecules to interact specifically with phosphotyrosine. Tyrosine phosphorylated sites on IR are recognized by conserved phosphotyrosine binding domains (PTB) like Src homology 2 domain (*Rous asian sarcoma tyrosine kinase*) (SH2) and Src homology 3 (SH3) as well as pleckstrin homology domain (PH) in signaling molecules. Tyrosine phosphorylated proteins are discriminated by the local residues surrounding of phosphorylated tyrosine. SH2 domains bind to short amino acid sequence containing phosphotyrosine, SH3 domains bind to proline-rich sequences, whereas PH domains can bind to membrane phospholipids and phosphorylation sites that can bind to SH2 (Kellerer, Lammers, et al. 1999).
A variety of signaling molecules with PTB domains (Kellerer, Lammers, et al. 1999) binds to phosphorylated IR. Apart from other proteins with adapter function like growth factor receptor binding protein-10 (Grb-10) and src homologous and collagen (SHC), which couple insulin to a complex network of actions, phosphorylated insulin receptor binds to members of insulin receptor substrate family (IRS-1,-2,-3,-4) and phosphorylates them on tyrosine residues (White 1997), (Shoelson, Chatterjee, et al. 1992), (Holman & Kasuga 1997), (Zhou, Chen, et al. 1999).
Among the latter, IRS-1 is the major cytosolic insulin receptor substrate of approximately 160-180 KDa and 22 potential tyrosine phosphorylation sites.
Once IRS-1 becomes tyrosine phosphorylated, it interacts with SH2 domains of several intracellular targets representing a point of divergence for insulin actions.
IRS-1 binding proteins identified thus far include SHC, $p21^{ras}$ activated complex (Czech 1995), Grb2/SOS (Baltensperger, Kozma, et al. 1993), the protein tyrosine phophatase SH-PTP2 as well as the regulatory subunit of the serine/lipid kinase phosphatidylinositol 3-kinase (Myers, Backer, et al. 1992).

1.2.3 Phosphatidylinositol 3-Kinase is a Hallmark in the Insulin Signaling Pathway

The PI3-K is a heterodimeric enzyme consisting of two subunits, p85α and p110α (Shepherd, Withers, et al. 1998). The p110α subunit is the catalytic subunit with a phospholipid- and a serine kinase activity, whereas the p85α subunit represents the regulatory domain containing two SH2 domains and one SH3 domain. In human skeletal muscle, different isoforms of the regulatory subunit have been identified, which are differently regulated by insulin (Shepherd, Withers, et al. 1998).
PI3-K phosphorylates the inositol ring at position D-3 yielding PI-3-phosphate from PI, PI-3,4-diphosphate from PI 4-phosphate and PI-3,4,5-triphosphate from PI-4,5-biphosphate (Corvera, D'Arrigo, et al. 1999). Insulin was shown to enhance the enzyme activity of IRS-1 associated PI3-K resulting in an increase in phosphatidylinositol triphosphate (PIP_3) (Chen, Friel, et al. 1993). The physiological functions of products phosphorylated by PI3-K is not clearly understood. The generation of PIP_3 is believed to be physiologically most important (Holman & Kasuga 1997). PIP_3 interacts with downstream of PI3-K, particularly since PIP_3 is not a substrate for phospholipases.

PIP_3 interacts with a serine/threonine kinase called AKT or Protein kinase B (PKB) and phospholipid dependent kinases (PDK1 and PDK2) (Burgering & Coffer 1995), (Vanhaesebroeck & Alessi 2000).

1.2.4 Downstream Targets of PI 3-Kinase

The insulin sensitive PKB represents a downstream component of PI3-Kinase. PKB is activated upon phosphorylation on serine 473 and threonine 306, which is induced by PDK1 and PDK2 (Vanhaesebroeck & Alessi 2000). Activation of PKB by a PI3-K-dependent mechanism leads to many cellular effects such as cell differentiation, glycogen synthesis and GLUT4 translocation (Downward 1998). Overexpression of PKB promotes glucose transport and GLUT1 and GLUT4 translocation in 3T3-L1 adipocytes (Cong, Chen, et al. 1997), (Kohn, Summers, et al. 1996) and glucose transport in L6 myotubes (Ueki, Yamamoto-Honda, et al. 1998). Furthermore, overexpression of an inhibitory mutant of PKB inhibits insulin-stimulated translocation of GLUT4 (Cong, Chen, et al. 1997).

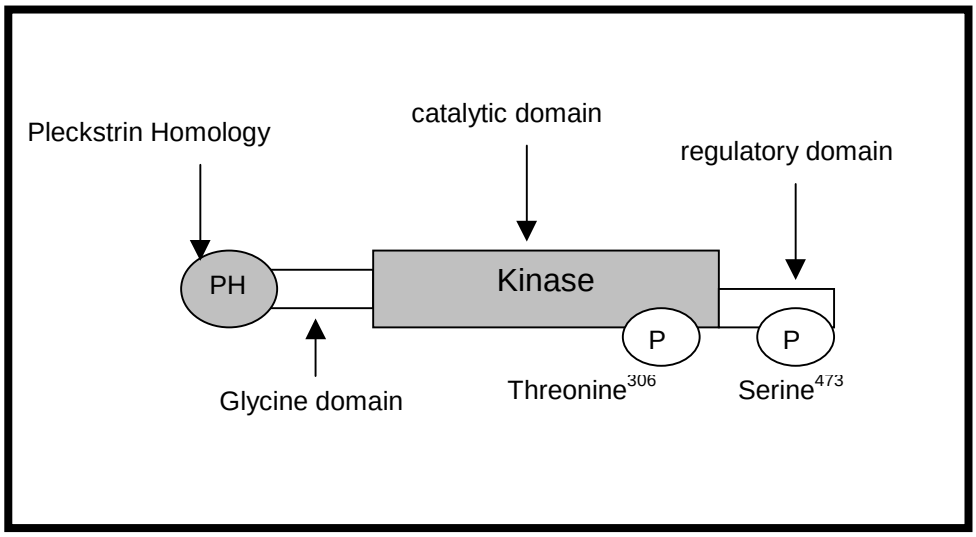

Figure 1.2.3 Schematic presentation of PKB showing phosphorylation sites on regulatory domain and kinase domain.

1.2.5 The Protein Kinase C Family (PKC)

Protein kinases C play a key role as a target for second messengers transducting signals from plasma membrane to cellular processes (Hunter 1995). PKCs play a central pathogenic role in hypertension, atherogenesis, cancer promotion (McCarty 1996) and diabetic complications (Koya & King 1998), (Murphy, McGinty, et al. 1998).

PKCs represent a family of 11 structurally and functionally related isoforms of serine/threonine kinases (α, βI, βII, γ, δ, ε, θ, η, ζ, λ, and μ (human) and its murine homolog D), (Mellor & Parker 1998), (Newton 1995). PKC isoforms are divided into three subgroups due to their activation by second messengers (Newton 1995). Conventional or classical PKCs (cPKC) (α, βI, βII, γ) are Ca^{2+} and Diacylglycerol (DAG) dependent, new or novel PKCs (nPKC) (δ, ε, θ, η) are DAG dependent and atypical isoforms (aPKC) (ζ, λ, μ), which are independent of Ca^{2+} and DAG.
Protein kinase C consists of a single polypeptide chain. The regulatory domain is located at the amino terminus and the catalytic domain is located at the carboxy terminus. The regulatory domain contains besides an autoinhibitory domain different domains referred to as C1-C2, which differentiate (due to their binding affinity) PKCs in the mentioned three subgroups.

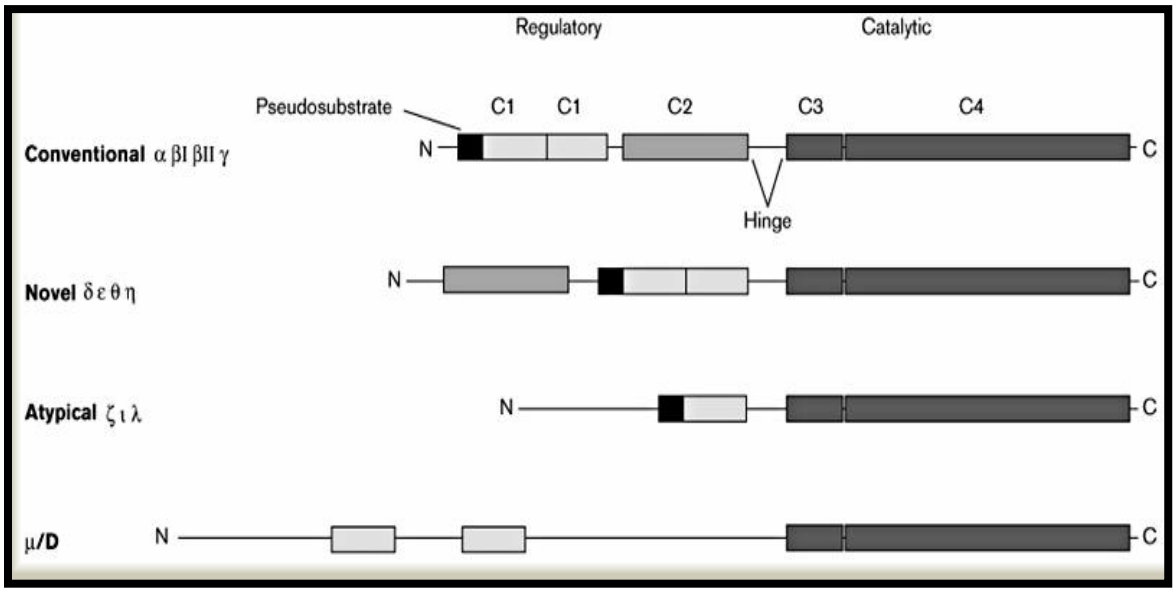

Figure 1.2.4 Schematic presentation of PKC isoforms. Pseudosubstrate (autoinhibitory domain) is indicated black. C1 domain (mostly tandem repeat) binds diacylglycerol or phorbol esters (with exception to atypical isoforms). C2 domain binds Ca^{2+}. C3 and C4 represent ATP-binding and substrate-binding domains. N, amino terminus, C, carboxy terminus. From (Newton 1997).

PKC activation involves their redistribution from the cytosol to the plasma membrane (Newton 1997), (Mosthaf, Kellerer, et al. 1996), (Yamada, Avignon, et al. 1995).
PKCs have been implicated in regulation of insulin secretion (Jones & Persaud 1998) and insulin signal transduction (Haring, Tippmer, et al. 1996), (Mosthaf, Kellerer, et al. 1996), (Bandyopadhyay, Standaert, et al. 1997).
PKC activation increased glucose transport (Cooper, Watson, et al. 1999), (Etgen, Valasek, et al. 1999), (Ishizuka, Kajita, et al. 1999), (Hansen, Corbett, et al. 1997) and induced glucose transporter translocation to the plasma membrane (Standaert, Bandyopadhyay, et al. 1999), (Lawrence, Hiken, et al. 1990) (Holman, Kozka, et al. 1990).

Furthermore, the Pleckstrin homology domain of PKB has been shown to interact with protein kinase isoform PKCζ, suggesting that this PKC might be involved in regulation of PKB (Konishi, Kuroda, et al. 1994) and in vitro expression of active PKCζ stimulates glucose transport in rat skeletal muscle (Etgen, Valasek, et al. 1999).

Another atypical PKCλ has been reported to be downstream of PI3-K (Akimoto, Takahashi, et al. 1996) activating GLUT4 translocation (Standaert, Bandyopadhyay, et al. 1999).
Taking together, PKCs are potent modulators of insulin signal transduction inducing glucose transporter translocation.
As to insulin stimulation of glucose uptake, glucose transporters terminate the insulin signaling cascade.

1.2.6 Glucose Transport via Facilitative Glucose Transporter Family

All mammals possess transport systems for energy substrates across the plasma membrane. The transport system for glucose employs ion-dependent cotransporters, e.g. epithelial cells in small intestine and proximal tubule in the kidney (Bell, Kayano, et al. 1990), which actively accumulate glucose and simple facilitative uniporters “facilitative glucose transporters” (Mueckler 1994), which are passive carriers transporting the D-enantiomer of glucose energy-dependent down a concentration gradient.
Glucose transporters may involve a net input of glucose into the cell or output from the cell, depending on the type of the cell, e.g. net uptake in muscle, output from liver in post-absorptive or fasting state.
Facilitative glucose transporters (GLUTs) represent a family of highly related transporters, which are products of distinct genes. Six mammalian glucose transporter have been characterized thus far (Gould & Holman 1993). The human genes encoding these proteins are named GLUT1-5 and GLUT7. GLUT6 is a pseudogene, that is not expressed at protein level (Kayano, Burant, et al. 1990). The most characteristic feature of GLUTs is the presence of 12 transmembrane segments (amphipatic helices), which are arranged so that both N- and C-termini are located at the cytoplasmatic surface (see below).
GLUTs show tissue specific distribution and transport glucose and other hexoses with different efficiencies and kinetics (Gould & Holman 1993), the glucose transporter isoform 1 (GLUT1), also called the erythrocyte glucose transporter is the most ubiquitously distributed isoform and is highly conserved with 97-98% sequence identity between analogous of human, rat, mouse, rabbit and pig proteins. GLUT1 is expressed highly in all cell culture lines (Gould & Holman 1993) and in many fetal and adult mammalian cells (Thorens, Charron, et al. 1990), although frequently at low levels and in conjunction with other more tissue restricted transporter isoforms. Examples for cooperative coexistence of two isoforms of glucose transporter occur in the insulin sensitive tissues, muscle and fat. In these tissues, GLUT1 provides with low level of glucose required for basal cellular activity (house-keeping function), its high K_m for glucose and its asymmetry allow the transporter to function as unidirectional transporter, when extracellular glucose is low and cell demand for glucose is high.

GLUT1 is translocated to the cell surface by insulin in cardiac muscle (Rett, Wicklmayr, et al. 1996), (Fischer, Thomas, et al. 1997), (Laybutt, Thompson, et al. 1997), in skeletal muscle (Lund, Flyvbjerg, et al. 1994), in adipocytes (Gould & Holman 1993) and in human fibroblasts (Miele, Formisano, et al. 1997).
Furthermore, intracellular abundance of GLUT1 has been shown in cardiac muscle (Fischer, Thomas, et al. 1997), whereas others reported about restriction of GLUT1 to the cell surface (Zorzano, Munoz, et al. 1996), (Marette, Richardson, et al. 1992), where it was found to be 5-6 fold enriched than in transverse tubule membrane (TT) (Ploug & Ralston 1998). No translocation upon insulin stimulation was reported (Galante, Maerker, et al. 1994). Estimations have been made about the content of GLUT1 in muscle and its relation to GLUT4. GLUT1 shows only 8% of GLUT4 expression in rat soleus muscle and after considering of fibroblasts and endothelial cells contained in muscle tissue, there will be for 30 GLUT4 only 1 GLUT1 (Ploug & Ralston 1998). Taken together, GLUT1 is probably localized to both the plasma membrane and intracellular sites and a modest redistribution to the plasma membrane occurs upon insulin stimulation.
GLUT4 is the major insulin sensitive glucose transporter in fat and muscle of rat and man (Rodnick, Slot, et al. 1992), (Friedman, Dudek, et al. 1991). GLUT3 and GLUT5 were also reported to be expressed at a lower abundance in muscle (Grover, Walsh, et al. 1999), (Hundal, Darakhshan, et al. 1998). In contrast to GLUT1, the major pool(s) of GLUT4 is located subcellularly (Bornemann, Ploug, et al. 1992), (Rodnick, Slot, et al. 1992). Insulin stimulates the translocation of GLUT4 to the plasma membrane (Ramlal, Sarabia, et al. 1988), (Rett, Wicklmayr, et al. 1996), (Zorzano, Munoz, et al. 1996), (Guma, Zierath, et al. 1995) and to the TT membrane (Marette, Burdett, et al. 1992), (Munoz, Rosemblatt, et al. 1995), (Wang, Hansen, et al. 1996), (Munoz, Rosemblatt, et al. 1995). Furthermore, Insulin increases the intrinsic activity of glucose transporter (Zierler 1998). Recently, at least two different intracellular pools of GLUT4 have been identified, which are differently sensitive to insulin (Aledo, Lavoie, et al. 1997) and exercise (Hayashi, Wojtaszewski, et al. 1997).

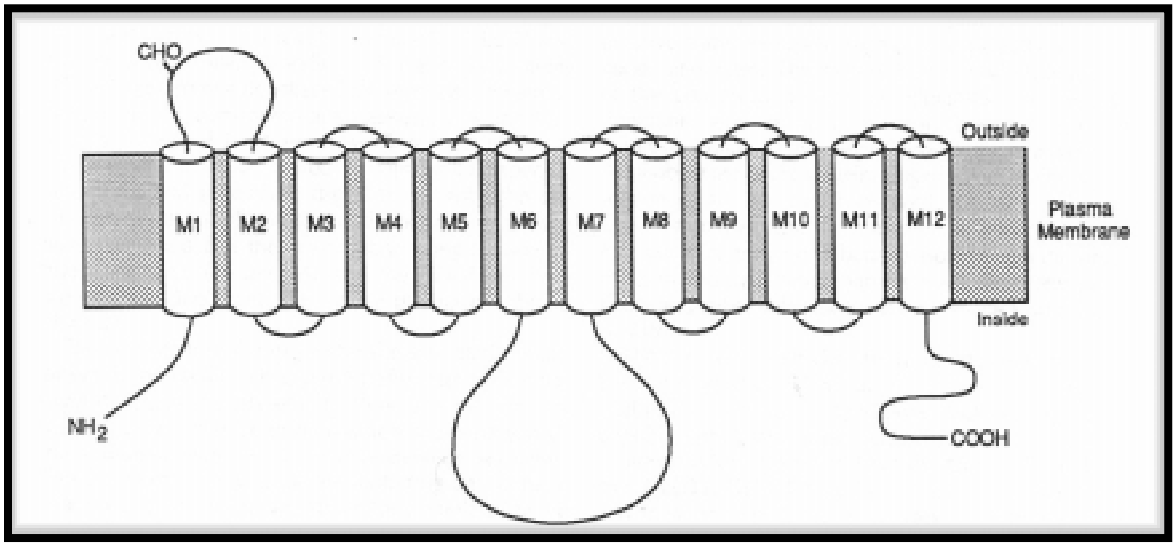

Figure 1.2.5 Schematic presentation of facilitative glucose transporter showing transmembrane domains numbered M1-M12. CHO denotes site of aspargine-linked glycosylation. From (Bell, Kayano, et al. 1990).

1.3 Insulin Signal Transduction in Diabetes

Sensitivity of peripheral tissues for circulating insulin plays a key role in the maintenance of a balanced glucose homeostasis. Skeletal muscle accounts for the majority of whole body glucose uptake (DeFronzo 1988), whereas adipose tissue plays a lesser role in glucose uptake (Garvey 1992). Glucose transport across the plasma membrane is the rate limiting step in the overall glucose uptake process. Insulin-stimulated glucose transport is altered in diabetes (Cline, Petersen, et al. 1999), (Utriainen, Takala, et al. 1998), in obesity (Zaninetti, Greco, et al. 1989), (Miele, Formisano, et al. 1997) and in high fat diet (Han, Hansen, et al. 1997). The mechanism(s) underlying altered glucose transport in diabetes is ill defined.
Total cellular expression of GLUT1 was found to be increased in diabetic mice (Bonini, Colca, et al. 1995), in fibroblasts of NIDDM (Miele, Formisano, et al. 1997) and in muscle of diabetic Zucker rats (Handberg, Kayser, et al. 1994). In contrast, no changes in GLUT1 expression were reported for Zucker rats by (Galante, Maerker, et al. 1994), for diabetic rats (Kahn, Rossetti, et al. 1991), whereas Vogt et al reported decreased cellular GLUT1 expression from NIDDM (Vogt, Muhlbacher, et al. 1992).
GLUT4 cellular expression was reported to be decreased in skeletal muscle of diabetic rats (Dombrowski & Marette 1995), in skeletal muscle of NIDDM subjects (Vogt, Muhlbacher, et al. 1992), in obese rats (Brozinick-JT, Etgen-GJ, et al. 1994), whereas no changes were reported in skeletal muscle of diabetic rats (Kahn, Rossetti, et al. 1991), in hyperinsulinemic hypertensive rats (Bader, Scholz, et al. 1992). Moreover, Sato et al reported an increase in GLUT4 from skeletal muscle of insulin resistant fatty rats (Sato, Man, et al. 1997). Thus changes in total expression of GLUTs may be a site of molecular defects of insulin-stimulated glucose uptake in insulin resistance and in diabetes.
Additionally, decreased translocation of GLUT4 to the plasma membrane and more recently to the transverse tubules membrane was reported for diabetic rats (Kahn, Rossetti, et al. 1991), (Klip, Ramlal, et al. 1990), for streptozotocin rats (Dombrowski, Roy, et al. 1998), (Dombrowski & Marette 1995) and in skeletal muscle of NIDDM (Zierath, He, et al. 1996). Thus altered translocation of glucose transporter seems to be more clearly implicated in altered insulin-stimulated glucose uptake in diabetes.

Moreover, defects in expression and cellular activity of downstreams of insulin receptor towards translocation of glucose transporter have been reported in diabetes. Binding of insulin to its receptor is not changed in diabetes. Even more, binding of insulin to its receptor is not essential for insulin receptor signaling, since anti-insulin receptor antibodies can activate glucose transport (Holman & Kasuga 1997). Insulin binding studies are complicated by the phenomenon of negative cooperation, an observation of accelerated dissociation of insulin from its receptor by excess amount of insulin (Bak 1994).
Total expression of insulin receptor is reduced in adipose tissue of insulin resistant diabetic mice (Bonini, Colca, et al. 1995) and reduced autophosphorylation of IR was reported from skeletal muscle of NIDDM (Obermaier-Kusser, White, et al. 1989), (Maegawa, Shigeta, et al. 1991), whereas others reported no changes in autoactivation of IR in insulin resistant subjects (for review see (Bak 1994)).

Studies with muscle insulin receptor knockout mice (MIRKO) revealed normal glucose homeostasis, (Bruning, Michael, et al. 1998), suggesting a minor role of the insulin receptor in the glucose homeostasis in skeletal muscle. Furthermore, exercise improves glucose uptake in these mice (Wojtaszewski, Higaki, et al. 1999).
Thus post receptor defects may play a role in insulin resistance metabolic states. In fact, insulin-induced phosphorylation of IRS-1 is reduced in skeletal muscle of NIDDM
(Bjornholm, Kawano, et al. 1997) and in diabetic GK rats (Song, Ryder, et al. 1999). PI3-K activity was reduced in NIDDM (Bjornholm, Kawano, et al. 1997) and in GK rats (Song, Ryder, et al. 1999) as well as in high-fat-feeding in mice (Zierath, Houseknecht, et al. 1997). Furthermore, PKB (Krook, Roth, et al. 1998) and PKC activities (Schmitz, Browne, et al. 1997), (Avignon, Yamada, et al. 1996) are altered in diabetes.

1.4 Effects of Hyperglycemia on Insulin Signal Transduction Towards Glucose Transport

Hyperglycemia is a common feature of diabetes mellitus, which is “a group of metabolic diseases characterized by hyperglycemia resulting from defects in insulin secretion, insulin action or both” [1].
Hyperglycemia per se is not only a potent metabolic marker of diabetes, but also a potent regulator of insulin secretion (Leahy, Cooper, et al. 1987), (Ammon 1997) and insulin action (Yki 1992) leading to insulin resistance. A term referring to altered hepatic glucose output (HGO) (Hother & Beck 1991) and insensitivity of peripheral tissues to insulin (Vuorinen, Koivisto, et al. 1992). Inhibition of both insulin secretion and action by hyperglycemia in diabetes is a phenomenon referred to as glucose toxicity. Glucose toxicity is a well-established term involving furthermore the diabetic complications accompanied and/or followed by hyperglycemia (Rossetti, Giaccari, et al. 1990), (King & Brownlee 1996). Skeletal muscle can be protected from diabetic complications due to an adaptation in the insulin stimulated glucose uptake, which limits the glucose flux into this tissue (Yki & Makimattila 1997).
Hyperglycemia, acutely increases glucose uptake in skeletal muscle in a concentration-dependent fashion (glucose mass-action effect) (Yki 1997).
The mass-action effect of glucose implies that the rate of glucose uptake is directly proportional to its plasma glucose concentrations and may compensate for insulin resistance (Vaag, Damsbo, et al. 1992), which is, as mentioned above, evolves to protect insulin sensitive peripheral tissues from glucose oversupply.
In the sum, the absolute rate of whole body glucose uptake in IDDM and NIDDM is not changed from normal subjects, provided that, it is measured under conditions of actual glucose and insulin concentrations found in these patients postprandially (Yki-Jarvinen, Sahlin, et al. 1990), (Henry, Gumbiner, et al. 1990).

[1] Definition extracted from Clinical Practice Recommendations of American Diabetes Association 1998

The mechanism(s), by which hyperglycemia induces glucose uptake was reported to be insulin-independent (Galante, Mosthaf, et al. 1995). Nolte et al. (Nolte, Rincon, et al. 1995) suggested that hyperglycemia activates glucose transport by a Ca^{2+}-dependent mechanism, since activation was blocked by dantrolene. In concomitance, hyperglycemia-induced glucose transport does not appear to employ PI3-K activation (Nolte, Rincon, et al. 1995). Most recently, Kawano et al (Kawano, Rincon, et al. 1999) showed that hyperglycemia-induced glucose uptake in rat skeletal muscle was dependent on activation of PKCβII isoform, since inhibition of PKC blocked the stimulatory effects of hyperglycemia on glucose uptake. In the same approach, it was shown again, that hyperglycemia activates glucose transport in an insulin-independent pathway.

Furthermore, chronic hyperglycemia was reported to induce insulin resistance (Yki 1992), (Yki 1997), (Rossetti, Giaccari, et al. 1990). Insulin-stimulated glucose uptake was lowered after 24h of hyperglycemia in type 1 diabetic patients (Vuorinen, Koivisto, et al. 1992) and insulin resistance was reported from glucose-infused rats for 72h (Hager, Jochen, et al. 1991). Lessons from transgenic animals show that overexpression of GLUT1 in mice leads to decreased insulin-stimulated glucose uptake (Etgen-GJ, Zavadoski, et al. 1999), (Hansen, Wang, et al. 1998). The increased glucose flux in this transgenic animals overexpressing GLUT1 is important for the development of insulin resistance, as further supported by Buse et al (Buse, Robinson, et al. 1996). Furthermore, normalization of glycemia by phlorizin (an inhibitor of proximal glucose reabsorption) reversed the inhibitory effects of hyperglycemia on glucose transport without affecting serum insulin (Dimitrakoudis, Vranic, et al. 1992) suggesting that inhibitory effects of hyperglycemia are located in insulin signaling.

Taken in toto, hyperglycemia may increase glucose flux in insulin sensitive tissues in an insulin-independent fashion and increased glucose flux leads to the development of insulin resistance. The mechanism(s), by which increased glucose flux induces insulin resistance is temporarily a matter of intensive investigations.

One of the plausible mechanisms proposed to underlie hyperglycemia-induced insulin resistance involves the activation of PKCs (Haring, Kellerer, et al. 1994).

Hyperglycemia activates PKC isoforms in fibroblasts (Berti, Mosthaf, et al. 1994), in glomerular cells (Derubertis & Craven 1994), in endothelial cells (Inoguchi, Battan, et al. 1992), in rat fat cells (Muller, Kellerer, et al. 1991), in L6 skeletal muscle cells (Caruso, Miele, et al. 1999), in C_2C_{12} myotubes (Galante, Mosthaf, et al. 1995) and in rat skeletal muscle (Nolte, Rincon, et al. 1995), (Kawano, Rincon, et al. 1999).

PKC stimulates glucose transport (van-de-Werve, Zaninetti, et al. 1987), (Khayat, Tsakiridis, et al. 1998), (Etgen, Valasek, et al. 1999), (Standaert, Bandyopadhyay, et al. 1999), (Lawrence, Hiken, et al. 1990), the translocation of glucose transporter (Holman, Kozka, et al. 1990), (Etgen, Valasek, et al. 1999), (Standaert, Bandyopadhyay, et al. 1999), (Galante, Mosthaf, et al. 1995) by a distinct mechanism of insulin (Hansen, Corbett, et al. 1997) and inhibits insulin-stimulated glucose transport (van-de-Werve, Zaninetti, et al. 1987), (Guma, Camps, et al. 1990), (Filippis, Clark, et al. 1997).

Activated PKC forms a complex with insulin receptor and modulates its tyrosine kinase activity through serine/threonine phosphorylation of the β-subunit of the receptor (Haring, Kellerer, et al. 1994), (Berti, Mosthaf, et al. 1994), (Bossenmaier, Mosthaf, et al. 1997), (Kellerer, Mushack, et al. 1997), (Bollag, Roth, et al. 1986). PKC overexpression, chronic exposure to TPA (PKC activator) downregulates IRS-1 expression and leads to insulin resistance (deVente, Carey, et al. 1996). Furthermore, our laboratory showed that the involvement of IRS-1 in the inhibitory effects of PKCs on insulin receptor function, may be through serine/threonine phosphorylation of IRS-1 (Kellerer, Mushack, et al. 1998). Moreover, inhibitory effects of hyperglycemia and of PKC on the insulin receptor autophosphorylation can be reversed by PKC inhibitor (Muller, Kellerer, et al. 1991), (Berti, Mosthaf, et al. 1994) and hyperglycemia-induced diabetic complications can be nullified by an oral PKC-inhibitor (Koya, Jirousek, et al. 1997). Thus, PKC activation by hyperglycemia and the attenuation of insulin signaling by PKC represents an attractive hypothesis to explain the mechanism of hyperglycemia-induced insulin resistance.

An alternative hypothesis for hyperglycemia-induced insulin resistance suggests increased flux of glucose through the hexosamine biosynthesis pathway (Robinson, Weinstein, et al. 1995), (Yki 1997), (Marshall, Bacote, et al. 1991), (Crook, Zhou, et al. 1995).
In this pathway, under physiological circumstances, 2-3% of phosphorylated glucose (Glc-6-P) is converted to fructose-6-phosphate, which is in turn converted by glutamine:fructose-6-phosphate amidotransferase (GFAT) to glucosamine-6-phosphate (GlcN-6-P). Glc-6-P is metabolized to UDP-N-acetylglucosamine (UDP-GlcNAc) and UDP-N-acetylgalactosmine (UDP-GalNAc). Both of the latter are precursors for synthesis of glycoproteins, proteoglycans and glycolipids (Marshall, Bacote, et al. 1991).

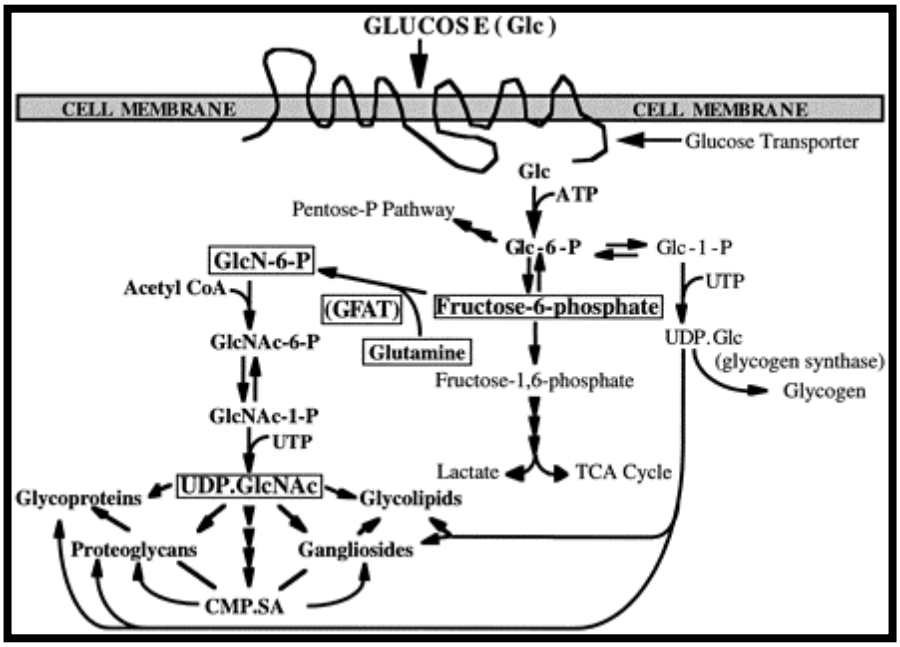

Figure 1.4.1 Schematic presentation of hexosamine biosynthetic pathway. From (Buse, Robinson, et al. 1996).

UDP-GlcNAc is covalently coupled to serine or threonine residues on cytosolic and nuclear proteins (intracellular O-linked glycosylation) (Yki & Makimattila 1997). This step is catalyzed by UDP-GlcNAc β-N-acetylglucosaminyltransferase (O-GlcNAc transferase) (Yki, Vogt, et al. 1997) and interacts with phosphorylation /dephosphorylation state of cellular proteins (Hart 1992). Added on, GlcNAc is coupled to aspargine residues on secreted and surface proteins (N-linked glycosylation) (Dinter & Berger 1995), (Kandror & Pilch 1994).
GFAT activates the rate limiting step in hexosamine biosynthetic pathway and its expression was shown in different tissues including skeletal muscle (Nerlich, Sauer, et al. 1998). Recently, a novel subtype designated GFAT2 (GFAT was then called GFAT1) was identified in human and mouse tissues and different tissue distribution between GFAT1 and GFAT2 has been shown (Oki, Yamazaki, et al. 1999). Whether or not GFAT2 is expressed in skeletal muscle and whether GFAT1 or GFAT2 plays a larger role in hyperglycemia-induced insulin resistance in skeletal muscle is subject to further analysis, since antisera produced in our laboratory recognize both GFATs (Nerlich, Sauer, et al. 1998).
Hyperglycemia increases GFAT activity (Daniels, Ciaraldi, et al. 1996) and GFAT activity is increased in hyperglycemic obese mice (Buse, Robinson, et al. 1997) and in hyperglycemic NIDDMs (Yki, Daniels, et al. 1996).
Overexpression of GFAT leads to insulin resistance (Hebert-LF, Daniels, et al. 1996), (Crook, Daniels, et al. 1993), (Crook & McClain 1996), (Crook, Zhou, et al. 1995) and reduced insulin-stimulated translocation of GLUT4 to the plasma membrane (Chen, Ing, et al. 1997), (Cooksey, Hebert-LF, et al. 1999). Additionally, GFAT inhibition by azaserine (a glutamine antagonist) blocks the ability of glucose, insulin and glutamine to interact with glucose transport (Baron, Zhu, et al. 1995).
Tissue concentrations of UDP-GlcNAc are elevated in insulin resistant ob/ob mice (Buse, Robinson, et al. 1997) and elevated UDP-GlcNAc concentrations correlates with impaired insulin action on muscle glucose uptake (Hawkins, Angelov, et al. 1997).
Glucosamine per se, which enters the cell via glucose transporter and catches into the hexosamine pathway distal to GFAT, impairs glucose transport (Baron, Zhu, et al. 1995). It was reported to induce insulin resistance in isolated rat skeletal muscle (Robinson, Sens, et al. 1993), in 3T3-L1 adipocytes (Heart, Choi, et al. 2000) and after in vivo infusion in rats (Virkamaki, Daniels, et al. 1997) by affecting GLUT4 translocation (Baron, Zhu, et al. 1995). Glucosamine impaired insulin autophosphorylation, IRS-1 phosphorylation (Hresko, Heimberg, et al. 1998) and IRS-1 associated PI 3-K activity (Hresko, Heimberg, et al. 1998), (Hawkins, Hu, et al. 1999). Glucosamine depleted intracellular ATP, which in turn inhibits translocation of GLUT1 and GLUT4 (Hresko, Heimberg, et al. 1998), (Sofue, Yoshimura, et al. 1993). Furthermore, glucosamine impaired insulin-stimulated PKB activation (Heart, Choi, et al. 2000).
Patti et al (Patti, Virkamaki, et al. 1999) confirmed the role of glucosamine-induced O-linked glycosylation in the interaction with insulin signaling cascade.

The impairment of IR, IRS-1 and PI 3-K activity by glucosamine was challenged by the work of (Heart, Choi, et al. 2000) and another group showed that troglitazone (an insulin sensitizer) was able to prevent hyperglycemia-induced but not glucosamine-induced insulin resistance suggesting that hexosamine biosynthetic is not a major mechanism for hyperglycemia-induced insulin resistance (Miles, Higo, et al. 1998). Maegawa et al., (Maegawa, Ide, et al. 1995) showed a normalization of protein-tyrosine phosphatase activities by thiazolidine, which they reported to be higher in hyperglycemia. The latter approach might explain the results reported by Miles et al.

Mechanisms of hyperglycemia-induced insulin resistance merged together, as Kolm et al. reported that glucosamine activates the translocation of PKC isoforms in mesangial cells (Kolm, Tippmer, et al. 1998). Fillipis et al (Filippis, Clark, et al. 1997) have furthermore shown that PKC inhibition can reverse glucosamine effects on glucose transport.
Thus, with the goal of discovery of new remedies in diabetes, the elucidation of the “sinister scenario” of hyperglycemia to positively or negatively alter glucose uptake will be of highest interest to diabetic research.

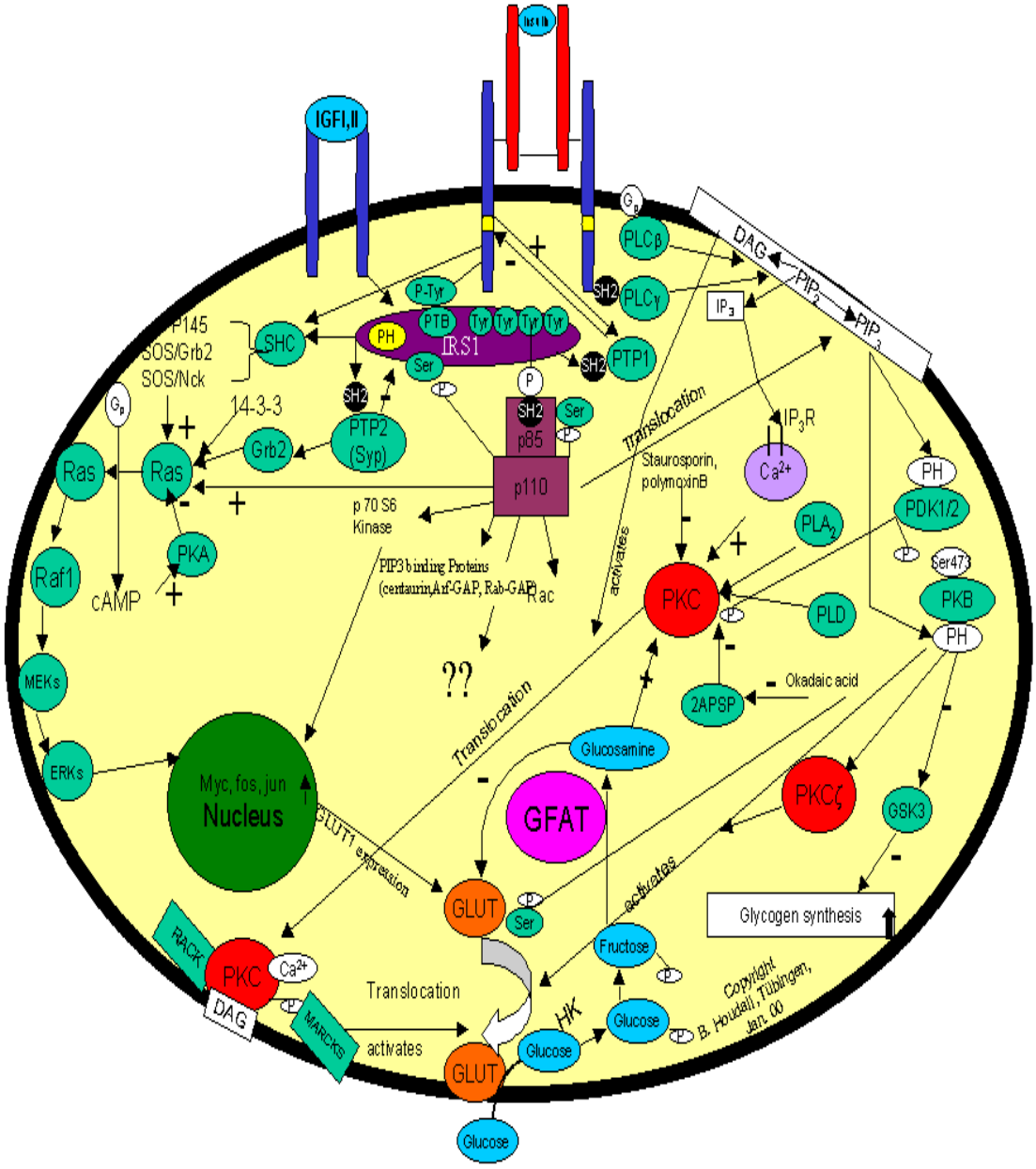

Figure 1.4.2 Shows potential mechanisms involved in insulin signaling cascade.

2 AIM

The aim of this thesis was to elucidate pathological effects of prolonged glucose infusion on insulin signal transduction and glucose transport in normal conscious rats. In our experimental design, we set up an in vivo animal model that has never been described before as to the period of glucose infusion and the simultaneous investigation of effects of glucose infusion on insulin secretion (thesis was performed in parallel by a colleague) and on insulin signal transduction towards glucose transport in skeletal muscle.

The central hypothesis is that infused glucose interacts with its own metabolism in skeletal muscle and propagates its uptake in an insulin-independent fashion leading to insulin resistance.
In particular, the following questions have been addressed:

- Does infused glucose influence insulin signaling and glucose transporter translocation to the plasma membrane?

- Does infused glucose activate PKC isoforms?

- Is the hexosamine pathway involved in effects of infused glucose on its own uptake in skeletal muscle?

3 METHODS

3.1 Materials

Chemicals, solvents and other reagents were purchased from Sigma (Deisenhofen, Germany), Roth (Karlsruhe, Germany), Fluka (Neu-Ulm, Germany) as well as from Boehringer Mannheim / Roche Molecular Diagnostics (Mannheim, Germany).
Exceptions well be specified in context.

3.2 Instruments

Perfusor syringe pump:	B.Braun, Melsungen, Germany.
Micro-Dismembrator s:	B.Braun, Melsungen, Germany.
Potter s:	B.Braun, Melsungen, Germany.
Spectrophotometer:	Genesys 5 (Spectronic, Runcorn, Cheshire, England). GeneQuant II (Pharmacia, Freiburg, Germany).
Centrifuges:	Optima Max (Beckman, München, Germany) Biofuge fresco (Heraeus, Osterode, Germany). Hettich (Universal 30 RF, Tuttlingen, Germany).
Gel electrophoresis Cell:	Protean II 20 cm (Bio-Rad, München, Germany). MWG Biotech (München, Germany).
Semi-Dry-Blotting apparatus:	(Harnischmecher, Arnsberg, Germany).
Film Handling:	Sterling Diagnostic Imaging (Du Pont de Nemours, Bad Homburg, Germany).
Capillary electrophoresis:	BioFocus 3000 (Bio-Rad, München, Germany). ABI PRISM 310 (Perkin-Elmer, Überlingen, Germany)
SpeedVac Concentrator:	Savant (Bachofer, Reutlingen, Germany).
PCR-Cycler:	Perkin-Elmer-PCR-System 9700 Mastercycler Gradient, (Eppendorf-Netheler, Hamburg, Germany). Light-Cycler (Boehringer, Mannheim, Germany).
Scales:	BL 1500 (Sartorius, Göttingen, Germany). AB 104 (Mettler-Toledo, Gießen, Germany).
Gel documentary:	Mididoc (Herolab, Wiesloch, Germany).
Glucose analyzer:	YSI 2300 STAT Plus (Kraienbaum, Langenfeld, Germany).

Water specification:	prepared using Milli-Q plus (Millipore, Bedford, Massachusetts, USA) or Fi-Stream (Fison, Beverly, Massachusetts, USA.
Scanner:	Sharp scanner JX-330, software from ScionImage, (www.scioncorp.com/)

3.3 Prolonged Glucose Infusion into Conscious Rats

3.3.1 Animals

Female Wistar rats weighing 250-350 g were purchased from Charles River, Sulzfeld Germany and were kept at 22 °C with a 12h light-darkness cycle and a relative humidity of 55-60% during the whole experimental period. The rats were given free access to water and standard chow pellet diet (Altromin 1324, Altromin-Futterwerk, Lage, Germany).

3.3.2 Glucose Infusion Procedure

Glucose infusion was performed as previously described (Ammon, Bacher, et al. 1998). Briefly, each rat was anesthetized with an intraperitoneal injection of a mixture of ketamine (Ketanest, Parke-Davis, Freiburg, Germany) and Rompun (Bayer, Leverkusen, Germany) at 45 mg/kg and 12 mg/Kg, respectively.
2-3 drops of atropine sulfate solution (1 mg/ml) were added to 1 ml of the mixture mentioned above.
As anesthesia deepens, the paw reflex of the rat becomes reduced or abolished. Depth of anesthesia was then continuously monitored by this reflex.
Surgery was performed at semisterile conditions, whereas sterile instruments were used.
A 1 cm long incision was made between sternum and mandibula, right external jugular vein was exposed by blunt dissection and was dissected free of the surrounding connective tissue. The jugular vein was ligated cranially and the vein was incised distal to the ligature.
Catheters were constructed in our work group and were made of silicone rubber (Silastic, Dow corning, Midland, MI, USA) and Polyethylene tube and catheter fleece.
The catheter were filled with 50 I.U. heparin (Liquemine, Roche, Grenzach, Switzerland) in 0.9% saline and introduced into the vein so that its tip lays just before the right atrium. Catheter placement was confirmed by aspiration. The catheter was then anchored by double ligature.
The free end of the catheter was then routed dorsally subcutaneously to the back of the neck. A second incision was then made and the catheter was externalized and fixed using a teflon anchoring device.
The incision was then sutured. Externalized catheter was routed through a flexible spring tether to a swivel (ZAK-Medizintechnik, München, Germany) and connected via an oscillating arm to a Perfusor syringe pump (Braun, Melsungen, Germany).

The rats were housed singly in a cylindrical Plexiglas metabolic cage and allowed to recover for 48h, after which glucose infusion (50% glucose, Fresenius, Bad Homburg, Germany) at a rate of 2 ml/h (GIR) versus 0.45% saline infusion at 2 ml/h (Control or SIR) was started. Usually, a glucose and a saline infusion were carried out at a time.
Animals were allowed to water and chow pellet *ad libitum.*

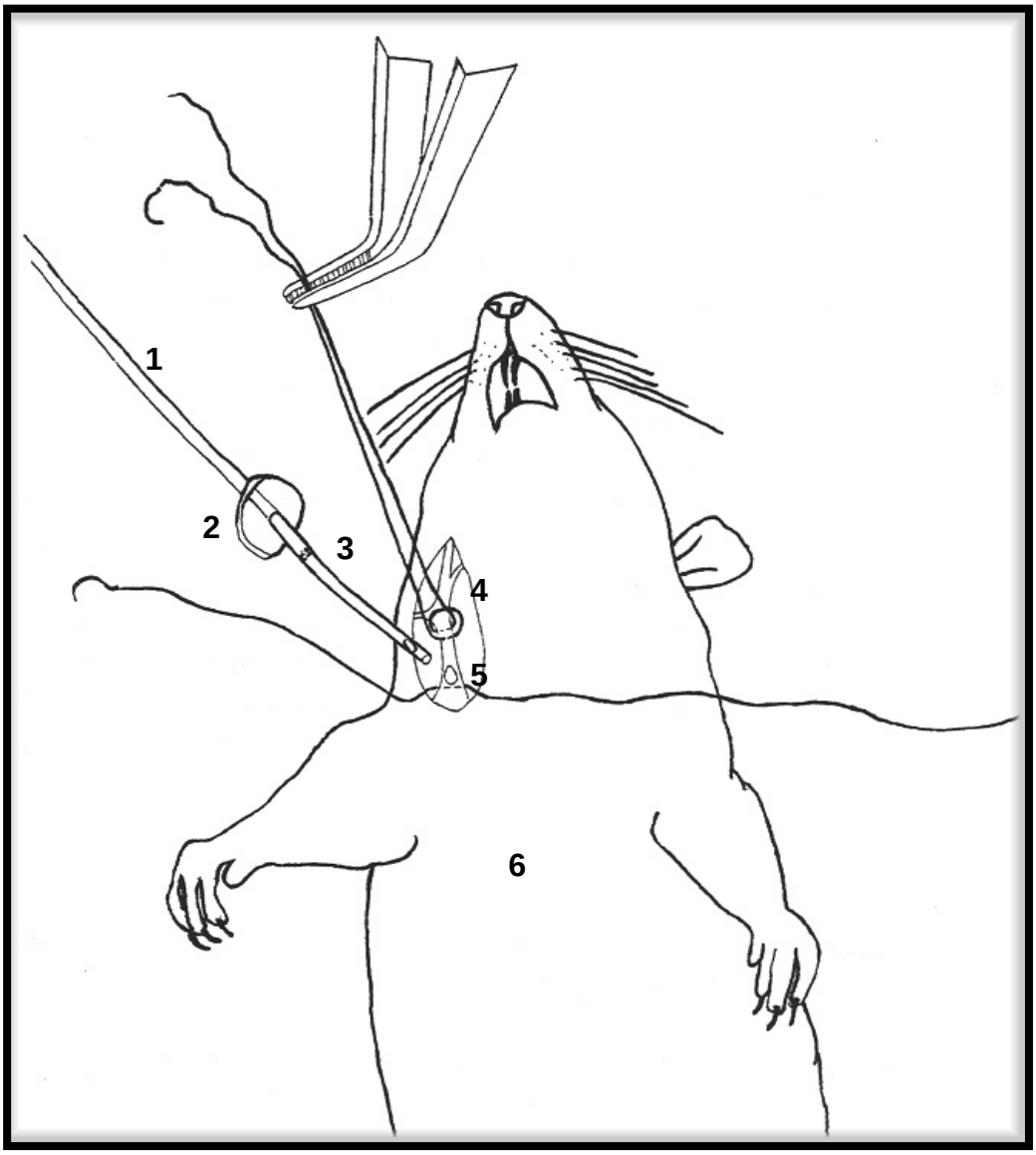

Figure 3.3.1 Implantation of a catheter system for long-term intravenous infusion in unrestrained rats:
1 refers to PE-part of the catheter
2 represents silicone fleece to cover the incision of the vein
3 silastic part of the catheter inserted into jugular vein
4 cranial ligature of the jugular vein
5 incision of jugular vein for the insertion of catheters
6 anesthetized rat
Modified from Brändle, dissertation from the department of Pharmacology at the university of Tübingen, Germany, 1995.

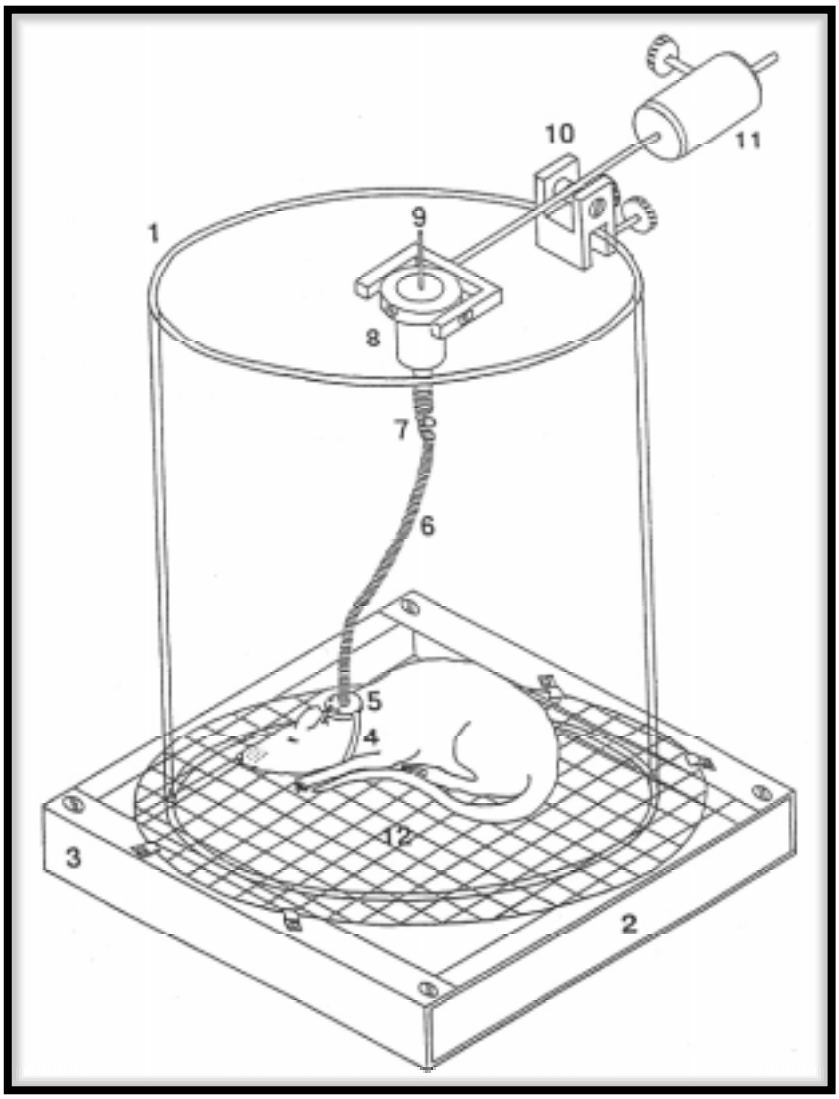

Figure 3.3.2 Free moving system constructed in our work group for single housing of rats during the experimental period:
1 Plexiglas metabolic cage
2 Drawer for disposable sawdust
3 cage gound
4 necklace
5 teflon anchoring device
6 flexible spring tether
7 lower catheter-swivel connection
8 swivel
9 upper swivel- Perfusor syringe pump connection
10 oscillating arm
11 balancing weight
12 lattice
From Brändle, dissertation from the department of Pharmacology at the university of Tübingen, Germany, 1995.

3.3.3 Monitoring of Plasma Glucose and Insulin Concentrations During the Experimental Period

Blood samples were withdrawn from the tail vein and glucose and insulin concentrations were determined as previously described (Ammon, Bacher, et al. 1998).

3.3.4 Sacrificing of Animals and Excision of Hind Limb Muscle

After 48h (2d) or 120h (5d) of continuous glucose or saline infusion, experiments were terminated by disconnecting the syringe pump. Animals were then immediately removed from the Plexiglas cage and sacrificed by placement in a container saturated with Diethylether (Ether). Hind (pelvic) limb muscles were then quickly excised; hind limb were firstly amputated, skin was then excised and mixed hind limb muscles, e.g. soleus, gastrocnemius, flexor and adductor digitorum groups, adductor group, gracilis, vastus lateralis and gluteus were dissected free of connective tissue and fat and were chopped in small pieces. This step was carried out on ice.
Chopped muscles were immediately frozen in liquid nitrogen and subsequently stored at -80 °C until further preparation. Thoracic limbs were not excised.
In the meanwhile of muscles excision, the pancreas was excised by a colleague for the investigation of insulin secretion parameters.

3.4 Preparation of Muscle Extracts for SDS-PAGE and Western-Blotting

For characterization of intracellular proteins, their extraction in a harmless method is a prerequisite. A variety of homogenization techniques has been developed.
Non of the developed methods can be considered as universally applicable.
In the following, a combination of chopping and forcing the tissue through a narrow opening (potter, liquid shear) was chosen.
Although the potter method is a standard technique for smooth tissues (liver) and is considered to be inefficient for skeletal muscle, the method efficiency should be sufficient if muscles were grounded beforehand.
The liquid shear or potter method was the standard technique used for homogenization in this work, since the resulting homogenate can be further centrifuged per differential pelleting and isopycnic centrifugation techniques.
Aliquots of excised muscles were weighted, grounded in a liquid nitrogen cooled Porcelain mortar using a Porcelain pistil. Muscles were subsequently placed in liquid nitrogen cooled Dismembrator (B. Braun, Melsungen, Germany) and powdered at setting 2000 rpm for 1 min.
Powdered muscles were placed in ice-cold buffer A (10 mM $NaHCO_3$ pH=7, 0.25 M sucrose, 5 mM NaN_3, freshly added protease inhibitor cocktail (Sigma, P8340) and 100 µM PMSF). Further homogenization was carried out with a motor-driven Potter-Elvehjem Teflon-glass tissue grinder at setting 1500 rpm for 1 min and approximately 10 ups-and-downs.

The resulting homogenates were taken for protein concentration determination. Equal amounts of protein were introduced into the wells of gel ranging from 50-200 µg per lane, separated on 7.5-10% SDS-PAGE and used for the study of:

1) Insulin receptor total protein expression and its tyrosine phosphorylation. S. 4.2.
2) IRS-1 total protein expression and its tyrosine phosphorylation. S. 4.3.
3) PI3-K total protein expression. S. 4.4.A.
4) PKB total protein expression and its serine phosphorylation. S. 4.5.
5) Total protein expression of PKC isoforms. S. 4.6.
6) GFAT total protein expression. S. 4.7.1.
7) O-GlcNAc-glycosylation. S. 4.9.
8) GLUT4 total protein expression. S. 4.10.1.
9) GLUT1 total protein expression. S. 4.11.1.

3.5 Protein Concentration Determination

Protein concentrations were determined using the dye-based Bradford assay. This assay is also referred to as Bio-Rad assay after the company which sells the kit.
Aliquots of samples (ranging from 1-5 µl) were diluted in water to 800 µl and 200 µl of the Bio-Rad-Kit (Biorad, München, Germany) was added.
Extinction of the contained Serva Blue G dye was then measured after 20-30 min at 595 nm in a Genesys 5 spectrophotometer (Spectronic, Runcorn, Cheshire, England).
A standard curve with samples of known protein concentration was prepared in parallel to assess the unknown protein concentrations.
Bovine serum albumin, BSA, (Boehringer, Mannheim, Germany) was used as a standard and the following dilutions were usually used for the standard curve:

Standard	Protein/µg	µl BSA(200 µg/ml)
1	0	0
2	4	20
3	8	40
4	12	60
5	16	60
6	20	100

Table 3.5.1 Known protein concentrations used for the standard curve

Extinction was measured in plastic cuvettes and polynomic regression was used for the calculation of unknown protein concentration of the sample.

3.6 Membrane-Cytosol Fractionation for the Assessment of Subcellular Distribution of PKCs

Many papers have dealt with PKC subcellular redistribution from cytosolic fraction to the total membrane fraction (Avignon, Standaert, et al. 1995), (Mosthaf, Kellerer, et al. 1996), (Standaert, Bandyopadhyay, et al. 1999), (Schmitz, Browne, et al. 1996), (Berti, Mosthaf, et al. 1994). Considering only papers dealing with skeletal muscle, e.g. (Avignon, Standaert, et al. 1995), (Schmitz, Browne, et al. 1996), (Schmitz, Browne, et al. 1997), (Khayat, Tsakiridis, et al. 1998), (Kawano, Rincon, et al. 1999), there still a big variety in fractionation media and centrifugation conditions.
In this work total homogenate was obtained as described in 3. 4.
Total homogenate was then spun at 186000 g for 1h using TLA 55-eppendorf cups rotor (Beckman, München, Germany) and Optima Max centrifuge (Beckman, München, Germany). Supernatant was referred to as cytosolic fraction, whereas pellet contained total membrane fraction. The latter was resuspended in buffer A containing 1% Triton X-100, solubilized and centrifuged again at 10000 g in MLA 80 rotor (Beckman, München, Germany) for 10 min. The supernatant was retained and referred to as total membrane fraction. All steps were carried out at 4 °C.
This method was applied for the study of PKC translocation. S. 4.6.

3.7 Subcellular Fractionation of Rat Skeletal Muscle

The first prerequisite for the establishment of a method for subcellular fractionation is the knowledge of the ultrastructure of the tissue type being dealt with.
The homogenization media and homogenization method must take the ultrastructure of the material being homogenized into consideration. Homogenization methods like nitrogen cavitation (French pressure cell) will result in small vesicles with similar sizes from both endosomal compartment and plasma membrane, besides it might cause damage to cell organelles separated. Thus one would prefer liquid shear method like potter, in spite of relatively poor reproducibility, if cell organelle damage is to be avoided.
It should be stressed that damage to a part of cell organelles is obvious in each homogenization method.
Successful homogenization combined maximal retention of cell organelle nature and maximal cell lysis and plasma membrane disruption.
To meet this requirements, a homogenization method as in 3.4 was again used for subcellular fractionation of rat skeletal muscle.
5 g of mixed hind muscles were homogenized as in 3.4. The powdered muscle was placed in buffer A (5g/75 ml buffer A) and pottered as described in 3.4. In this crude homogenate four classes of structure will be encountered:
First, the relatively compact cell organelles, nuclei, mitochondria, microbodies, lysosomes and secretion granula, which will survive the homogenization procedure intact.
A second class of structure is membrane systems of the plasma membrane, the endoplasmatic reticulum as well as the Golgi apparatus. The endoplasmatic compartment will form small vesicles. Plasma membrane and Golgi apparatus will partially stay intact, provided that mild homogenization was used.

Fragmentation of the plasma membrane to small vesicles will be encountered, where either “right side out” or “inside out” vesicles are formed. Sheets of plasma membrane will form, only where strong junctional complexes are available.
Attention must be paid to the latter, since a lot of centrifugation works of skeletal muscle do not consider the low spin pellet for further analysis, albeit this pellet will be enriched in sheets of plasma membrane important for evaluation of translocation studies, e.g. of glucose transporter.
The third class of structures is the cytoskeletal elements. Usually, no big attention has to be paid for cytoskeletal elements in subcellular fractionation.
The fourth class encountered is the proteins and small vesicles of the cytosol. Usually, they do not interfere with cell organelle separation because of their small size (they remain in the supernatant of the 190000 g centrifugation).

A typical subcellular centrifugation involves two different centrifugal methods for the separation of the cell organelles:
First, differential pelleting, where the difference in particle size is used for separation. In this technique, a suspension of particles is placed into a centrifuge and centrifuged to pellet the largest group of particles. The supernatant is then poured off and recentrifuged to collect the next fraction and so on.
The first fraction yielded is usually referred to as Low spin pellet or fraction N (nuclear fraction). It is enriched in unbroken, partially broken cells and large sheets of the plasma membrane as well as Transversal-tubules region and contains ~ 40% of total GLUT4 and > 50% of sarcoplasmatic reticulum (Rodnick, Slot, et al. 1992). Repeated wash of this pellet reveals no more than 20-30% of the surface membranes (Rodnick, Slot, et al. 1992).
In this work, the Nuclear pellet was resuspended in LiBr-containing buffer B (50 mM Tris-HCl, 0,5M LiBr) and freshly added protease inhibitor cocktail (Sigma) and stirred at 4 °C for 4h. LiBr was added to break actin-myosin bond and liberates GLUT4-enriched internal membranes as described in (Burdett, Beeler, et al. 1987), (Dombrowski, Roy, et al. 1996).
Washing of the low speed pellet is important to minimize the loss of the small organelles. The combined supernatants were then centrifuged at 9000 g for 10 min. The resulting pellet is usually referred to as M-fraction (mitochondria fraction), large particulate fraction or high density membrane fraction (HDM). This fraction contains the majority of intact organelles.
Finally, microsomes (small vesicles of all kind of membranes) were pelleted by centrifugation at 190000 g for 1h. The supernatant is referred to as cytosolic fraction and the pellet represents total membranes fraction or low density membrane fraction (LDM). Microsomal fraction contains small size vesicles of different origins that can not be further separated by differential pelleting.
Further separation is performed depending on density. In this case, resuspended microsomal fraction was topped on a sucrose step gradient and centrifuged for 7h. During this time, microsomes sediments until they reach a region of their own density and stops there. This is referred to as isopycnic or buoyant density banding (isopycnic centrifugation).
Interphases from the gradient were then collected, diluted with sucrose free buffer A and repelleted at 444000 g for 1h.

Further centrifugation steps are outlined in fig. 3.7.1.
Pellets were re-suspended in appropriate volume of buffer A and protein concentration was determined.

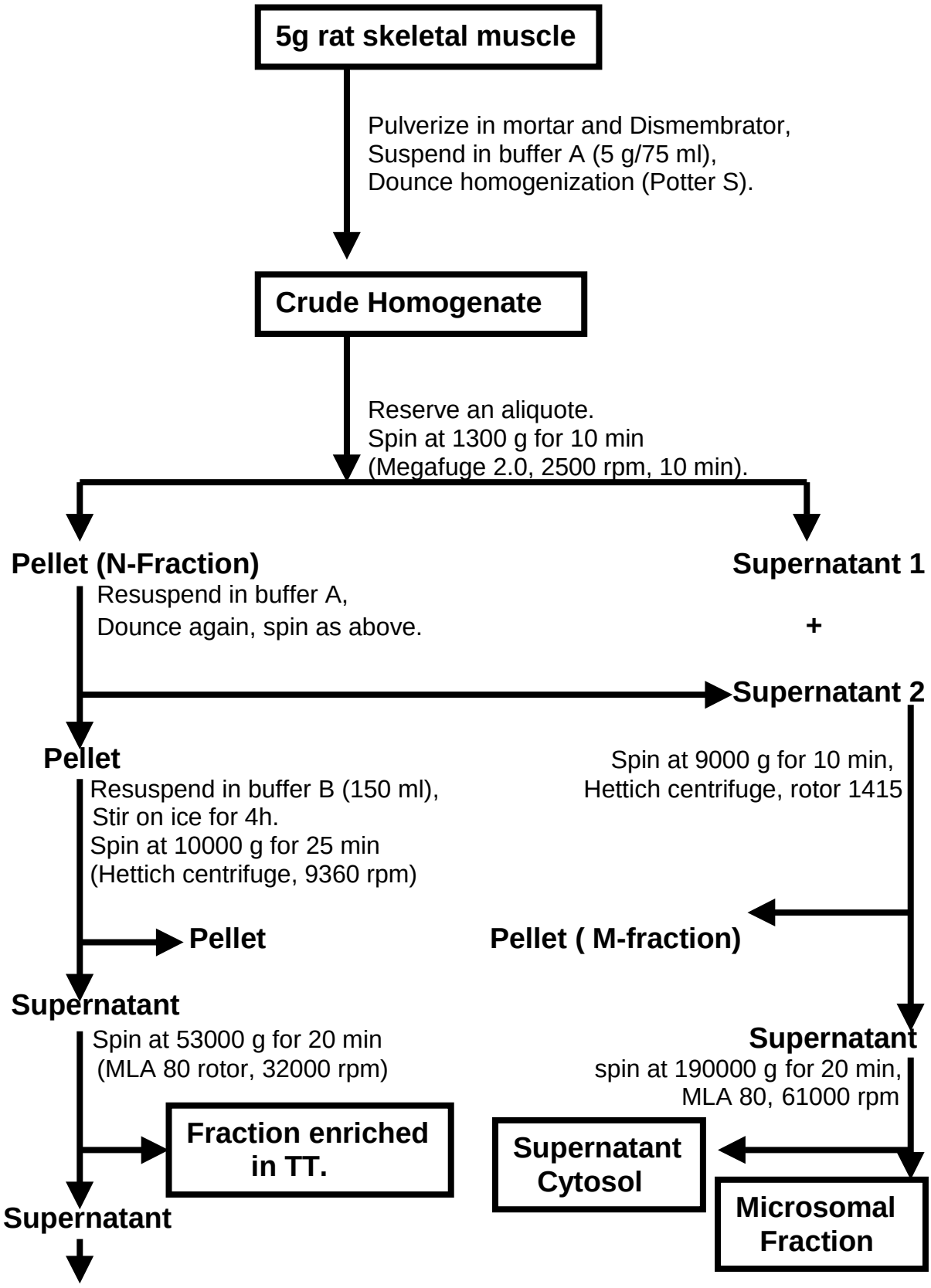

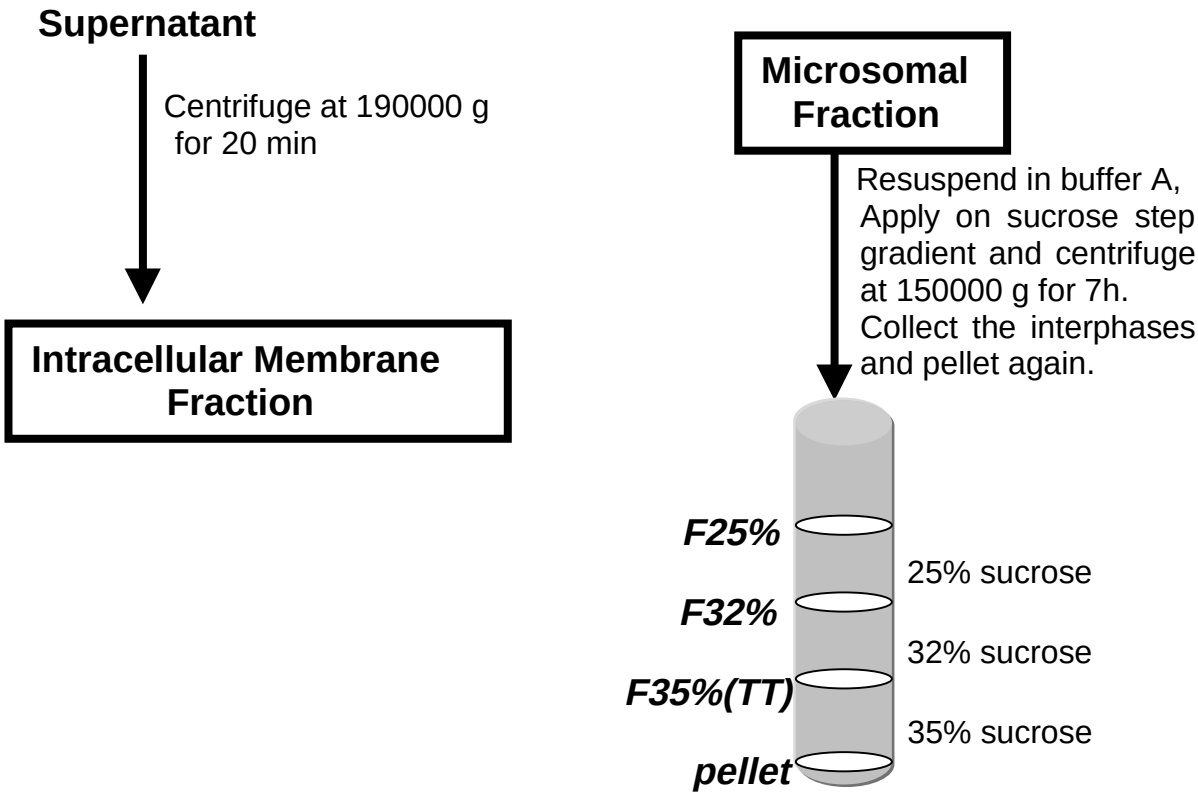

Figure 3.7.1 Schematic presentation of subcellular fractionation method.

3.8 Identification and Purity Assessment of Separated Fractions

Marker enzymes were used to identify the separated fractions.
Na^+/K^+-ATPase is found only in the plasma membrane. Methods for the measurement of the activity of this enzyme were developed to identify cardiac sarcolemma (Bers 1979), (Bers, Philipson, et al. 1980), (Pierce & Dhalla 1983). Lately, Western-Blot was employed to identify the expression of the α1 and α2 subunits of Na^+/K^+-ATPase in the plasma membrane (Hundal, Marette, et al. 1992). Insulin does not affect the expression of the α1 subunit, whereas it induces the translocation of the α2 and β1 subunits (Hundal, Marette, et al. 1992), (Marette, Krischer, et al. 1993). In this work, Western-Blot analysis of insulin independent α1 subunit was used to identify plasma membrane fractions.
For the characterization of fractions enriched in transversal tubules, the dihydropyridine receptor α1 subunit was employed in Western-Blot as described (Munoz, Rosemblatt, et al. 1995), (Horgan & Kuypers 1988).

3.9 Immunoprecipitation

Immunoprecipitation allows the concentration of isolated proteins by the use of a protein-specific antibody. The procedure consists of three steps. First, the specific antibody is added to the extract and allowed to bind specifically to the protein of interest. Second, purified protein A (or alternatively protein G) coupled to beads of Sepharose is added. Protein A is a bacterial protein with high affinity to the F_c portion of immunoglobulins. It binds to the antibody-antigen complex and provides a mass necessary for precipitation from solution. Antigen-antibody-protein complex is subsequently pelleted. Finally, the pellet is thoroughly washed to remove unprecipitated material.
The immunoprecipitaion procedure was used in this work for the isolation of the insulin receptor and the insulin receptor substrate 1 as well as for the measurement of IRS-1 associated PI3K activity (Wang, Bilan, et al. 1998), (Smith, Elmendorf, et al. 1997).
Immunoprecipitaion was performed as follows:

Immunoprecipitation of IR/IRS-1 from Rat Skeletal Muscle:

200 mg mixed muscle of hind limb

1.) Pulverize in a mortar, Dismembrator for 1 min 2000 rpm,
both steps liquid nitrogen cooled.
2.) Suspend in buffer at 1.5 ml / 200 mg muscle
(buffer IP with 1% Triton X-100 (m/V) and freshly added Na_3VO_4 and 20 µl Protease Inhibitor Cocktail Sigma)
or in IP-1 with NP-40 1% instead of Triton X-100 and 1 mM $CaCl_2$ for PI3-K Assay.
3.) Potter in motor-driven Potter-Elvehjem, ice-cooled.
4.) Incubate for 5 min on ice.

Crude Homogenate

Spin at 10000 g for 10 min and discard pellet.

Supernatant

Spin again at 10000 g for 10 min and discard pellet.

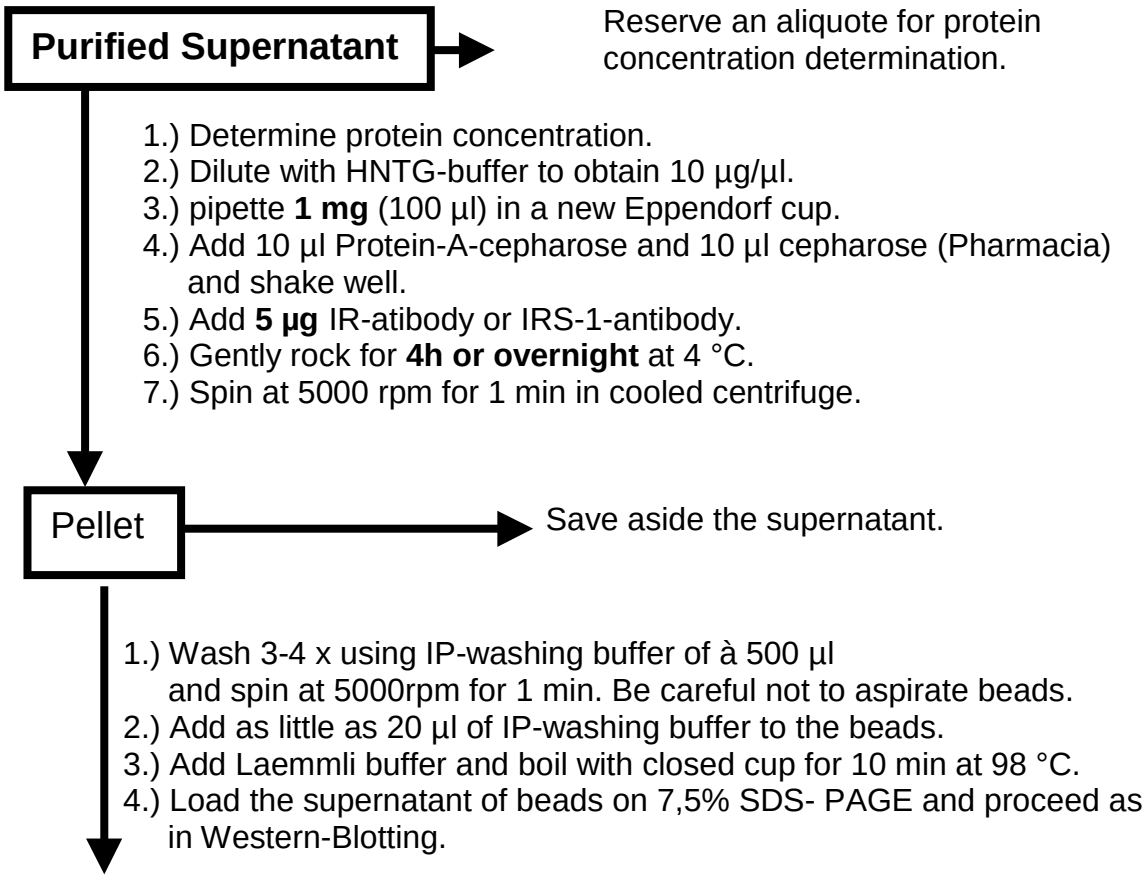

Figure 9.3.1 Schematic presentation of the used immunoprecipitation method.

IP-buffer:

50 mM HEPES pH 7.5
150 mM NaCl
1.5 mM $MgCl_2$
1 mM EGTA
10% Glycerol
1% (m/V) Triton X-100 (use NP-40 for PI3-K assay)
100 mM NaF
10 mM $Na_4P_2O_7$

Add freshly
1 mM PMSF
20 µl/1.5 ml buffer Protease inhibitor cocktail
400 mMNa_3VO_4

Washing-buffer for IP:

50 mM HEPES pH 7.5
150 mM NaCl
0,1%(m/V) Triton X-100
10% Glycerol
100 mM NaF
2 mM Na_3VO_4 to be added freshly

3.10 Sodium Dedecyl Sulfate - Polyacrylamide Gel Electrophoresis (SDS-PAGE)

SDS-PAGE is a rapid qualifying and quantifiying method for proteins. The method separates proteins based on their molecular weights (Laemmli 1970).
SDS binds to hydrophobic domains of proteins and disrupts their folded structure allowing them to exist stable in solution. The resulting SDS-protein complex is proportional to the molecular weight of the protein. SDS-protein complexes have all a negative charge and can be size-separated; SDS-treatment masks individual charge differences of proteins. During separation, SDS-protein complexes are attracted to the anode and separated by enforcement through the porous acrylamide gel.
Usually, proteins are first concentrated on a stacking gel and later separated on a separating gel.
In this work, a separating gel of 7,5-10% acrylamide was used.
Protein samples were combined with 5x Laemmli-buffer and heated at 95 °C for 10 min.

5x Laemmli buffer: 1 M Tris-HCl pH 6.8, 10% SDS, 50% glycerol, 0.1% bromophenol blue, 50% 2-mercaptoethanol.

Samples and weight marker (cat. No.1495922, Boehringer, Mannheim, Germany) were introduced into wells of stacking gel using Hamilton syringe (Exmire Microsyringe, Roth, Karlsruhe, Germany). Gel apparatus (Protean II Cell, Bio-Rad, München, Germany) was assembled. Power supply was attached and separation was performed overnight.

Separating gel:
12.5 ml Acrylamide solution (Rotiphorese gel 30, Roth, Karlsruhe, Germany)
12.5 ml Lower buffer (1,5 M Tris-HCl pH 8.8, 2% SDS)
25 ml Aqua dest.
0.33 ml Ammonium persulfate 10% solution.
80 µl N,N,N',N',- Tetramethylethylendiamine (TEMED).

Stacking gel:
1.8 ml Acrylamide solution (Rotiphorese gel 30, Roth)
3.5 ml Upper buffer (1,5 M Tris-HCl pH 6.8, 2% SDS)
9.4 ml Aqua dest.
0.15 ml Ammonium persulfate 10% solution.
20 µl N,N,N',N',- Tetramethylethylendiamine (TEMED).

Electrophoresis buffer:
248 mM Tris-base
1918 mM Glycin
1% SDS

Usually four 1.5 mm thick gels of each 15 wells were separated at a time. Electrophoresis was terminated, after the bromophenol blue dye front had passed through the majority of the separating gel. Thereafter, Immunoblots were performed.

3.11 Immunoblotting (Electrotransfer and Immunodetection)

In immunoblotting or also called Western-blotting, SDS-PAGE separated proteins are transferred and immobilized on a matrix. Thereafter, monoclonal or polyclonal primary antibodies are added. Binding of primary antibodies to the antigen is visualized using horseradish peroxidase bound second antibodies. The limit of detection of this method is reported to be about 10 pg.
In this work, semi-dry blotting was performed using nitrocellulose membranes (Protran 0.45 µm, Schleicher & Schuell, Dassel, Germany).

Semi-dry transfer buffer (10x Stock):
480 mM Tris-HCl pH 7.5
390 mM Glycin
400 ppm SDS
100 ml of the 10x transfer buffer was freshly diluted with 200 ml methanol and made up to 1 L with water.

Transfer was performed at 0.8 mA/cm^2 for 2h at room temperature. The transfer efficiency was verified by Ponceau staining of the nitrocellulose membranes (Fractosan staining solution, Olympus, Hamburg).
Nitrocellulose membranes were subsequently soaked with blocking agent (NET-G) in a plastic container. This step was repeated 3x a 15 min.
After the membrane was blocked, so that primary antibodies can not bind to the membrane nonspecifically, solution of the primary antibody or also called first antibody in NET-G was added and gently rocked for 2h at room temperature or overnight at 4 °C.
Membranes were subsequently washed in NET-G 2 x a 15 min (first antibody wash) and a dilution of the appropriate second antibody was added and incubated at room temperature for 1h.
The second antibody recognizes the F_c portion of the first antibody and was purchased as horseradish peroxidase-conjucated. Second antibody wash was performed (2 x a 15 min.). Antibody detection was performed using a chemiluminescent detection reagent (Amersham, England). Emitted light was detected by Hyperfilm ECL films (Amersham, England). Films were developed using a Sterling Diagnostic Imaging apparatus (Du Pont de Nemours, Bad Homburg Germany) and measured by scanning densitometry using Sharp Scanner JX-330.
Membrane were reblotted, if indicated, using Strip-buffer at 50 °C for 30 min in a water bath, blocked and incubated with a new antibody as described.
Membranes were stored after use in heat-sealed plastic bags at 4 °C.

NET-G:
150 mM NaCl
5 mM EDTA
50 mM Tris-HCl pH 7.5
0.05 Triton X-100
0.255 Gelatin (microbiology grade, Merck, Darmstadt, Germany)

Strip-buffer:
66 mM Tris-HCl pH 6.8
0.55 2-mercaptoethanol
2% SDS

In tables 3.11.1 and 3.11.2 used first and second antibodies, their working dilutions and commercial supplier are summarized

Antibody against	Supplier	Dilution	Species
IRβ subunit	Sc-711	1:500	Rabbit polyclonal
p-Tyrosine(PY99)	Sc- 7020	1:500	Mouse monoclonal
IRS-1	Sc-560 UBI- 06248	1:500 1:500	Rabbit polyclonal Rabbit polyclonal
p85 PI3K	UBI-06195	1:500	Rabbit polyclonal
PKB or Akt1	Sc-7126	1:500	Rabbit polyclonal
p-Akt1(Ser473)	UBI-06801	1:500	Rabbit polyclonal
PKCα	Sc-208	1:500	Rabbit polyclonal
PKCβI	Sc-209	1:500	Rabbit polyclonal
PKCβII	Sc-210	1:500	Rabbit polyclonal
PKCθ	Sc-212-G	1:500	Goat polyclonal
PKCδ	Sc-213	1:500	Rabbit polyclonal
PKCε	Sc-214	1:500	Rabbit polyclonal
PKCζ	Sc-7262	1:500	Goat polyclonal
PKCλ	Sc-1091	1:500	Goat polyclonal
GFAT	Donated by Prof. Schleicher	1:500	Rabbit polyclonal
O-GlucNAc	MA1-072	1:1000	Mouse monoclonal
GLUT4	Sc-1608	1:800	Goat polyclonal
GLUT1	Sc-1605	1:400	Goat polyclonal
Na/K-ATPase α1	UBI-06-520	1:500	Rabbit polyclonal
DHPRα1	Sc-8160 MA3-920	1:500 1:500	Goat polyclonal Mouse monoclonal

Table 3.11.1 Summary of used primary antibodies in Western-Blot.

Second antibody	Supplier	Dilution
Anti-goat IgG-HRP	Sc-3020	1:2500
Anti-rabbit IgG-HRP	Sc-2004	1:10000-1:20000
Anti-mouse IgG-HRP	Sc-2005	1:2000

Table 3.11.2 Summary of used second antibodies in Western-Blot.

Abbreviations of providers: Sc: Santa Cruz, UBI: Upstate Biotechnology,
MA: antibody from Affinity Bioreagents.

3.12 Phosphatidylinositol 3-Kinase Activity Assay

Activity of IRS-1 associated PI3-kinase was assayed as previously described (Mosthaf, Kellerer, et al. 1996) with some modifications.
Immunoprecipitaion was performed as described in 3.9 using NP-40 as a detergent.
Collected immunoprecipitate were washed with freshly prepared buffers as follows:

- Immunoprecipitates were washed three times with Phosphate buffered saline pH 7.5 containing 1% NP-40 and 100 µM Na_3VO_4.
- Immunoprecipitates were then washed three times with 100 mM Tris-HCl pH 7.5, 500 mM LiCl and 100 µM Na_3VO_4.
- Thereafter, twice washed with 10 mM Tris-HCl pH 7.5, 100 mM NaCl, 1 mM EDTA and 100 µM Na_3VO_4.
- The last wash was completely removed and beads were stored in 50 µl of 10 mM Tris-HCl pH 7.5, 100 mM NaCl, 1 mM EDTA and 100 µM Na_3VO_4 at -80 °C until assay was performed.
- Phosphoinositol (PI) (Avanti, Albaster, USA) was prepared by removing the organic solvent under nitrogen stream and resuspending the PI pellet in 10 mM Tris-HCl pH 7.5, 1 mM EGTA by sonication in ice bath at setting 7 (2µg/µl).
- 20 µg of PI and 10 µl of 100 µM $MgCl_2$ were added to each tube of beads.
- Phosphorylation was started by the addition of γ-[^{32}P]ATP and $MgCl_2$ at final concentrations of 20 µCi and 5 mM, respectively.
- Mixture was incubated for 10 min at 22 °C.
- Reaction was stopped by adding 20 µl of 8 N HCl.
- Lipids were extracted by addition of 160 µl of $CHCl_3$: MeOH [1:1].
- Organic phase was separated by centrifugation for 3 min.
- 50 µl of the lower organic phase was spotted on TLC Plates (Merck 5735, Darmstadt, Germany).
- TLC plate was developed by chromatography in $CHCl_3$:MeOH:H_2O:NH_4OH [60:47:11.3:2].
- Plates were then dried and spots were detected by autoradiography.

3.13 Quantitative Analysis of Nucleotid-linked Hexoses and Hexosamines by Capillary Zone Electrophoresis

Capillary electrophoresis represents one of the most efficient and easy-to-use techniques in separation of peptides, proteins, glycoproteins and oligonucleotides (Lehmann, Voelter, et al. 1997), (Landers, Oda, et al. 1992), (Rickard, Strohl, et al. 1991). In capillary electrophoresis, charged molecules migrate to the electrode of opposite charge and are separated depending on their electrophoretic mobility. The latter is dependent on charge and size of molecules being separated and will be influenced by type, concentration and pH of the used puffer as well as by temperature and field strength. In capillary zone electrophoresis (CZE) a homogeneous buffer system is used over the whole separation time to ensure a constant pH. Separation is performed in a fused silica capillary of 20-30 cm and an internal diameter of 25-100 µm. the capillary is immersed at both ends in buffer. High voltage power supply is needed for field strengths up to 30000 V. The capillary is usually cooled.
Separation times are relatively short as capillary wash and conditioning times between runs are. Detection is typically carried out by UV/Vis at 260-280 nm.

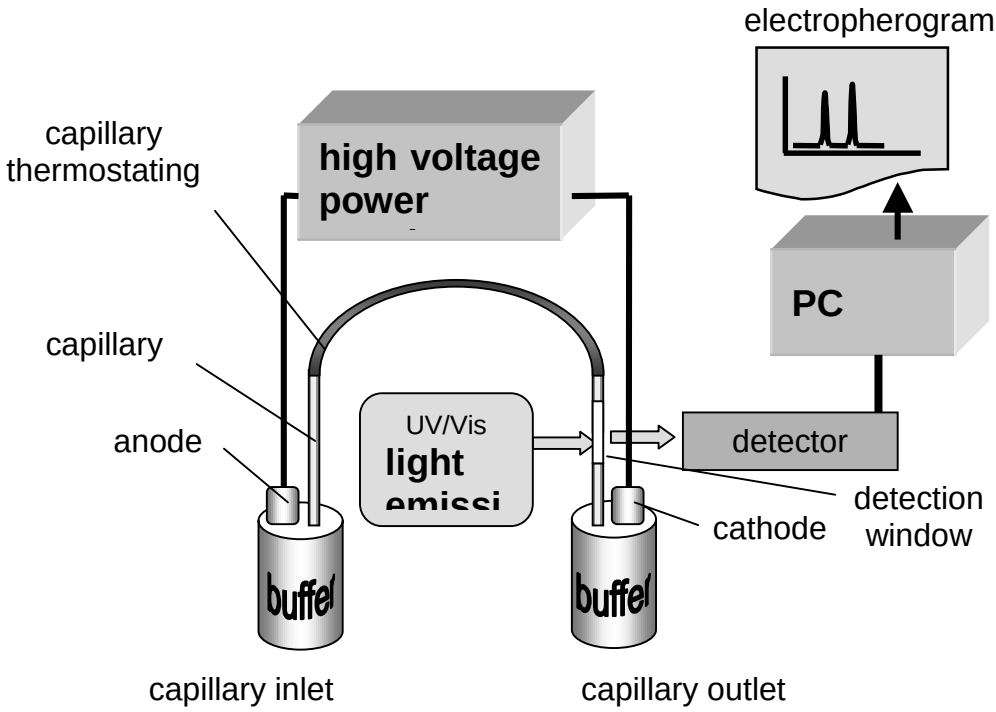

Figure 3.13.1 Instrumentation used for capillary electrophoresis.

In this work, optimal results were obtained with 90 mM borate buffer pH 9.0 at 18 °C and 15.5 kV in an uncoated fused silica capillary (Grom, Herrenberg, Germany) of 50 cm length and an internal diameter of 50 µm. UV-detection was carried out at λ = 262 nm. The method was evaluated in our group for the measurement of UDP-sugars in different systems like mesangial cells and leukocytes and was eventually evaluated for rat skeletal muscle.

3.13.1 Sample Preparation

Rat skeletal muscle was prepared as described by (Lehmann et al. 2000). Briefly, 100 mg of frozen muscle tissue were powdered in a Dismembrator. Powdered muscle was suspended in 0.6 ml phosphate buffered saline (PBS) pH 7.3 containing 0.5% Triton X-100 and 10 µm 8-bromoguanosine (Sigma) as internal standard.
Extracts were subsequently sonicated at lowest setting and centrifuged in a cooled microcenrifuge (15000 rpm for 2 min). Supernatant was deproteinized with acetonitrile (at final concentration of 66%). Supernatants were dried in SpeedVac concentrator and reconstituted in 40 µl H_2O for CZE analysis.
Run conditions were exactly as described (Lehmann et al, 2000).
In the following, there will be a presentation of migration times identification of UDP-sugars.

3.13.2 Identification of UDP-sugars in Rat Skeletal Muscle Extracts

Standards of UDP-sugars were added separately to a sample and spiked samples were analyzed. Migration times were identified by integration of peak areas.

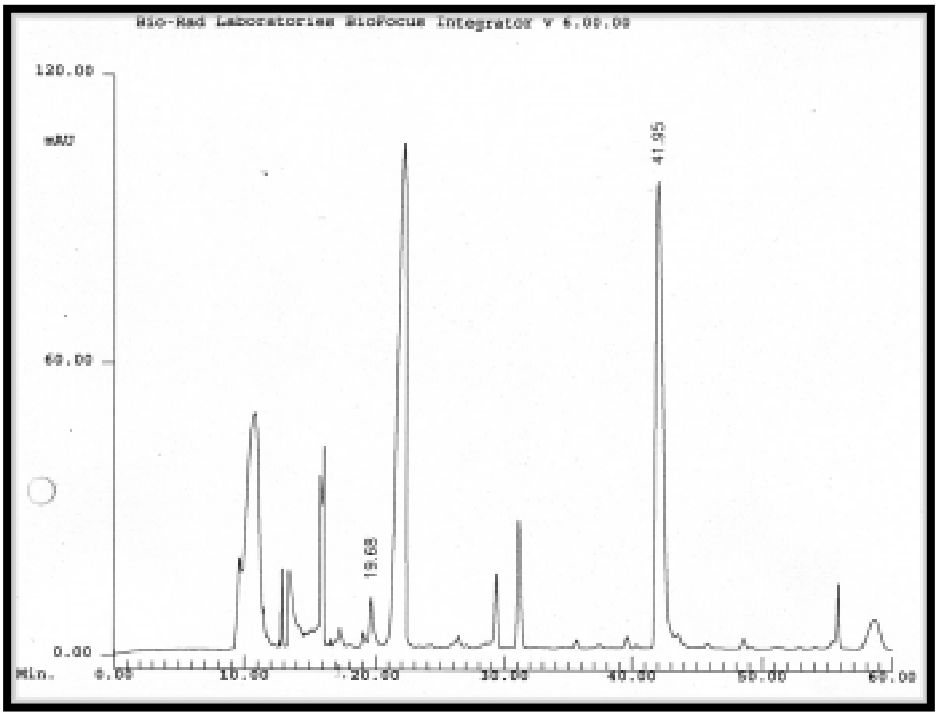

Figure 3.13.2 Electropherogram of sample of rat skeletal muscle extract spiked with UDP-Glc-NAc. UDP-Glc-NAc migration time 41.95 min.

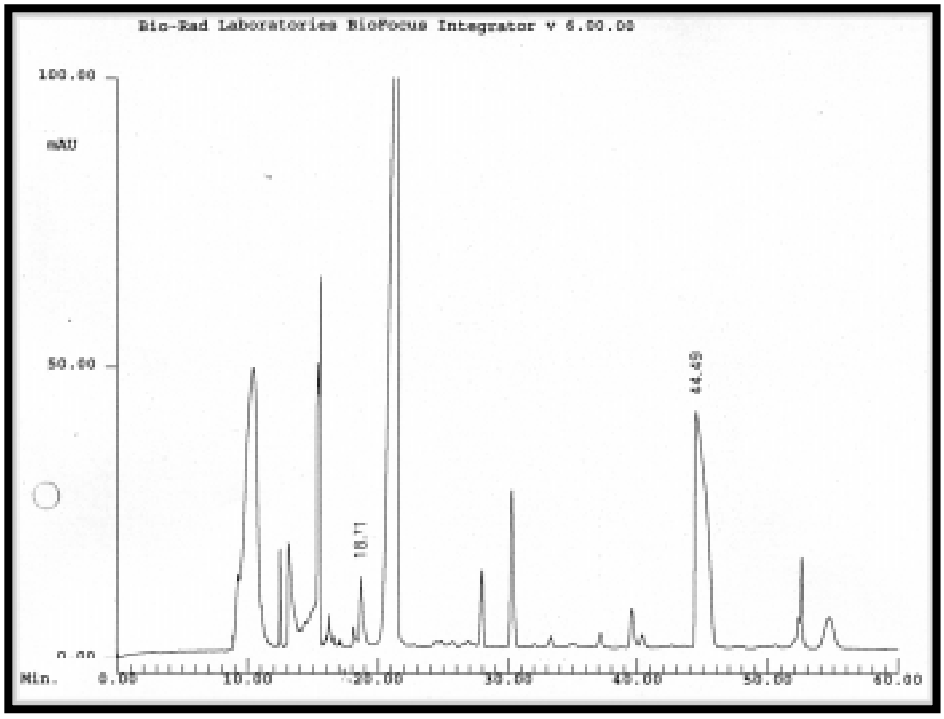

Figure 3.13.3 Electropherogram of sample of rat skeletal muscle extract spiked with UDP-Gal-NAc. UDP-Gal-NAc migration time 44.49 min.

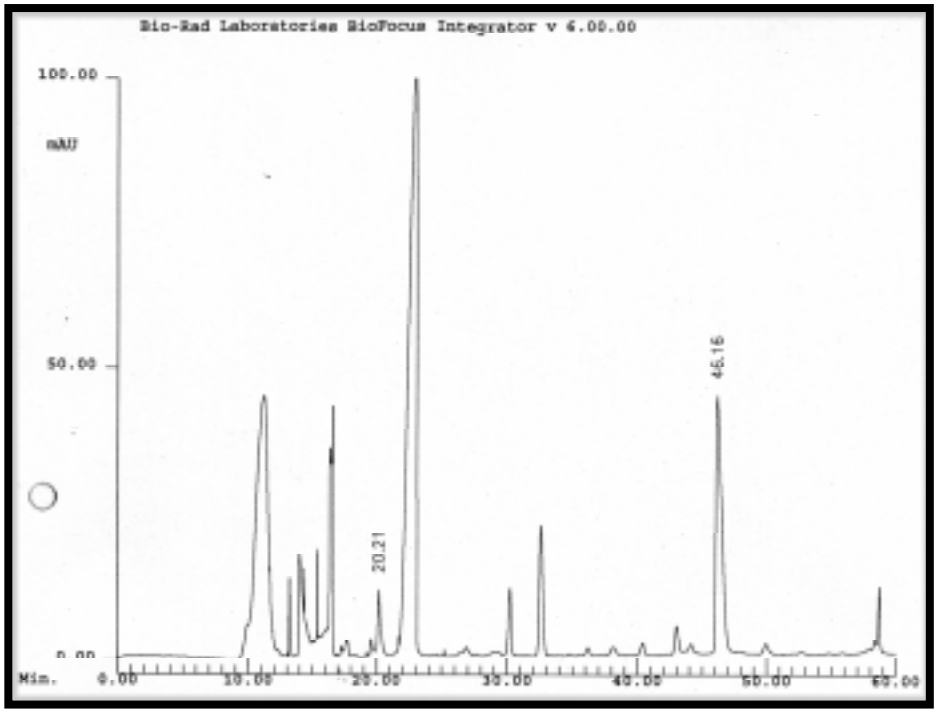

Figure 3.13.4 Electropherogram of sample of rat skeletal muscle extract spiked with UDP-Glc. UDP-Glc migration time 46.16 min.

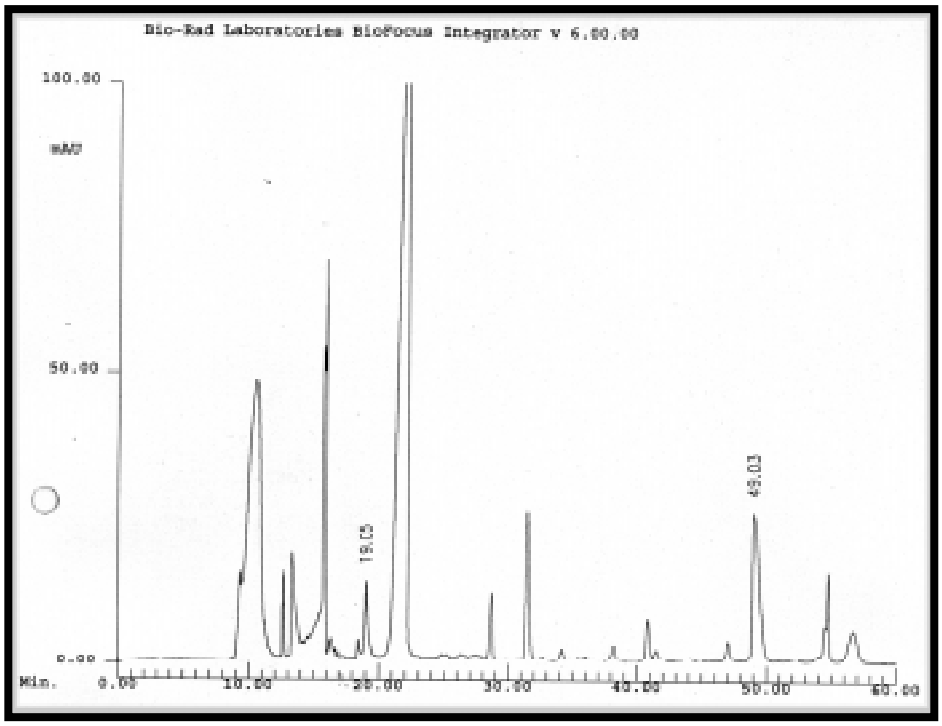

Figure 3.13.5 Electropherogram of sample of rat skeletal muscle extract spiked with UDP-Gal. UDP-Gal migration time 49.03 min.

Time shifts between different runs were corrected using relative migration to the internal standard (8-bromoguanosine).
Quantification was made by analyzing the peak levels and plotting them against the added amount of the standard. Procedure was repeated individually for each UDP-sugar. Sample's content was then calculated from the intercept and the slope of the line.

3.14 Preparation of Total RNA from Rat Skeletal Muscle

Analysis of RNA levels is a method for gene expression studies. Isolation of total RNA of full-length is the first and may be the most critical step in analyzing RNA levels. Total RNA from eukaryotic RNA contains primarily ribosomal RNA (rRNA) and transfer RNA (rRNA) and in a much lesser amount messenger RNA (mRNA).
The quanidinium-isothicyanate method represents a powerful means for total RNA preparation (Laville, Auboeuf, et al. 1996), (Auboeuf & Vidal 1997), (Kohout & Rogers 1993). In this work, an optimized one step Guaninidinium isothiocyanat / Phenol method was used for isolation of total RNA (peqGOLD TriFast, peqLab Biotechnology, Erlangen, Germany). In this method, simultaneous extraction of RNA, DNA and proteins is performed. Isolation was performed according to manufacturer's instructions with minor modifications. Briefly,

- 1 ml of peqGOLD reagent was added to 100 mg rat skeletal muscle. The suspension was well mixed using Vortex Genie, subsequently forced through a 12-gauge needle and further homogenized using ice-cooled motor driven Potter S (Braun, Melsungen, Germany) at setting 2000 rpm for 1 min.
- Samples were incubated at room temperature for 1h.
- 0.2 ml chloroform was added, well mixed again and incubated for 10 min at room temperature.
- Separation of the organic phase from the aqueous was then performed by centrifugation at 12000 g for 5 min.
- RNA was retained in the aqueous phase, whereas DNA and protein were yielded in the organic phase and the interphase.
- RNA precipitaion was performed by adding 0.5 ml isopropanol to the separated aqueous phase.
- Samples were incubated at room temperature for 10 min and centrifuged at 13000 g for 10 min.
- Supernatant was removed and the RNA-pellet was washed twice with 75% ethanol and centrifuged at 13000 g for 10 min.
- RNA was then dried and reconstituted in 75 µl ribonuclease-free water (RNAse free H_2O).
- Quantification of RNA was made using absorption at 260 nm (GeneQuant II, Pharmacia, Freiburg, Germany).

3.15 Reverse Transcription of mRNA in Complementary DNA (cDNA)

Reverse transcription was performed using a 1^{st} Strand cDNA synthesis Kit for RT-PCR with AMV (*avian myeloblastis virus*) as reverse transcriptase (Boehringer, Mannheim, Germany) and Random primer $p(dN)_6$. A larger amount of a master mix was prepared and aliquots were added to each sample reaction tube.

For 20 µl total volume, the following volumes were pipetted:

2 µl 10x reaction buffer
4 µl 25 mM $MgCl_2$ (final concentration 5 mM)
2 µl Desoxynucleotide mix (dNTPs) (final concentration 1 mM)
2 µl random primer (final concentration 0.08 A_{260} units)
1 µl RNase inhibitor (final concentration 50 units)
0.8 µl AMV reserve transcriptase (final concentration more than 20 units)
0.2 µl gelatin (final concentration 0.01 mg/ml)
1 µg total RNA
Sterile water ad 20 µl
Reverse transcription was performed in Perkin-Elmer-PCR-System 9700 (Überlingen, Germany). RNA was preincubated at 65 °C for 15 min and reverse transcription was performed with the following cycling-program:
10 min at 25 °C / 60 min at 42 °C / 5 min at 95 °C.

3.16 Primer Design and Annealing Temperature Determination Using a Gradient Cycler

Primer design was made from a gene sequence of a discrete DNA segment, which was extracted from the GenBank (www.genome.ad.jp/dbget/dbget.links.html).
The software program "Primer" was used and primer sequence alignment to gene sequence was then verified by using BLAST (www.ncbi.nlm.nih.gov/BLAST/html).

Primers	Primer sequence	Product length, bp
IR		
Forward	5´-CTG GAT TAC GTG GAG GAC AA-3´	381
Reverse	5´-GTG AAG GTC TTG GCA GAA GC-3´	
IRS-1		
Forward	5´-CAA GGA GGT CTG GCA GGT TA-3´	356
Reverse	5´-GGT TGG AGC AAC TGG ATG AA-3´	
PI3-K		
Forward	5´-TTC TTC CAG GCA AGT CAG GT-3´	355
Reverse	5´-GCC AGT GGA TGA CGG AGT TA-3	
PKC α		
Forward	5´-TCA ACT TCC TCA TGG TGC TG-3´	393
Reverse	5´-TGA CGT TGT CCA GCT TCA GA-3´	
PKC βI		
Forward	5´-CAG CAG GAA TGA CTT CAT GG-3´	373
Reverse	5´-CTT CAG GAT CTT CAC GGC AT-3´	
PKC δ		
Forward	5´-GTG GTG TTG ATC GAC GAT GA-3´	315
Reverse	5´-CTT GAT GTG GCC ATC CTT GT-3´	

Table 3.16.1 Summarizes primer sequence and base pair of the corresponding PCR product .

Primers	Primer sequence	Product length, bp
PKC ε		
Forward	5´-GTG GTG TTG ATC GAC GAT GA-3´	315
Reverse	5´-CTT GAT GTG GCC ATC CTT GT-3´	
PKC ζ		
Forward	5´-GAC GAA GTG CTC ATC ATC CA-3´	309
Reverse	5´-GGA AGG CAT GAC AGA ATC CA-3´	
PKC λ		
Forward	5´-CGG GAA GGT CTC CAT TTG AT-3´	168
Reverse	5´-GTT CCT TTG GGT CCT TGT TG-3´	
GFAT		
Forward	5´-CAG TTC GTG TCC CTT GTG ATG-3´	239
Reverse	5´-ATA TAT GTA ATC TCC TTG-3´	
GLUT1		
Forward	5´-CTT CCA ACT CAA CCA ACC AC-3´	191
Reverse	5´-GAG TGT CCG TGT CTT CAG CA-3´	

Table 3.16.1 Summarizes primer sequence and base pair of the corresponding PCR product, continue.

The approximate primer annealing temperature was estimated with the “Primer” software and exact annealing temperature was obtained using a gradient cycler (Mastercycler gradient, Eppendorf-Netheler, Hamburg, Germany).

3.17 Polymerase Chain Reaction (PCR) using the Light-Cycler-System

The PCR is a rapid procedure for the in vitro amplification of a specific segments of DNA of as little as several nanomols. A segment of DNA is amplificated using specific two single-stranded oligonucleotides (primers). Furthermore, a DNA polymerase, deoxyribonucleoside triphosphate (dNTPs) and a buffer system are needed. Denaturation (melting the DNA to single strands), annealing (flanking of single-stranded DNA by primers) and synthesis (amplification of complementary strands to produce double-stranded DNA) are the three components of ”PCR amplification cycle”. Usually 30 cycles are performed resulting in a 2^{28}-fold amplification of a discrete product.
The Light-Cycler-System (Roche Diagnostics, Mannheim, Germany) is a novel fast thermocycler (30 cycles can be run in less than 30 min) with integrated fluorimeter and specially developed fluorescent dyes. Data are monitored online in a real time kinetics and quantification software replaces conventional post PCR processing.
(s. manufacturer’s homepage in the world wide web and manufacturer released information).
In this work, the SYBR Green I dye (Roche Diagnostics, Mannheim, Germany) was used for DNA detection. This stable fluorescent dye binds to minor groove of the DNA double helix. This in turn enhances fluorescence of the dye. Fluorescence is measured at the end of synthesis step of each cycle. In post run analysis, the product can be easily identified and quantification can be performed.

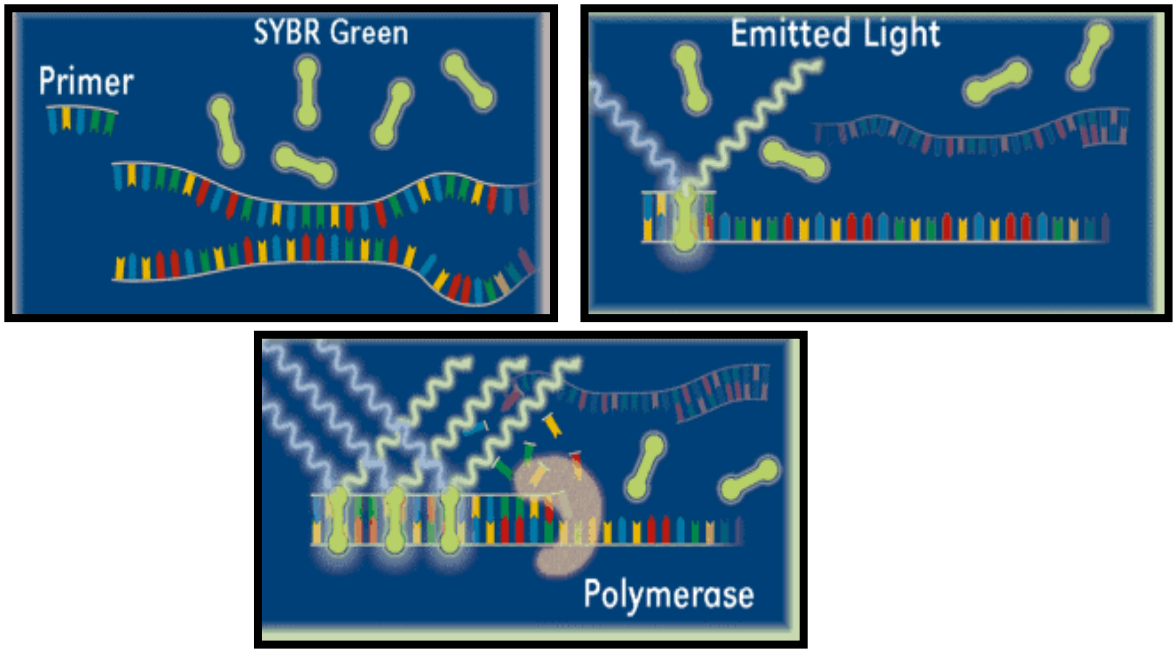

Figure 3.17.1 Illustrates the principle of DNA detection using the SYBR Green dye.
Upper left panel: in a mixture of denatured DNA, primers and SYBR Green dye, unbound dye molecules weakly fluoresce, producing a background fluorescence signal which is subtracted in post run analysis.
Upper right panel: after annealing of primers, SYBR Green can bind to double-stranded DNA and a dramatic increase in light emission upon exicitation can be monitored.
Lower panel: gradually, more and more SYBR Green can bind to synthesized DNA and a continuous increase in fluorescence can be monitored. Denaturation of DNA in the following cycle release the dye molecules, the fluorescence signal decays. Figures were extracted from (http://biochem.boehringer.com/lightcycler/monito01.htm)**.**

β-Globin was used as external standard for quantification, known amounts of β-Globin were simultaneously run with samples and quantification was performed using the Light-Cycler-software version 3.0. Control animals were set at 100 % per definition and comparison was made to the corresponding treated animals.
PCR product sizes expected were additionally verified in a conventional way using 2% agarose gel electrophoresis. Agarose was dissolved in TAE-buffer by microwave heating, poured into electrophoresis apparatus and allowed to cool a little before ethidium bromide (Roth, Karlsruhe, Germany) was added. PCR products were recovered from the Light-Cycler capillaries by short centrifugation in upside down position and were mixed with sample-indicator (10% bromphenol blue-glycerol). Samples were subsequently introduced into gel wells and electrophoresis was run at 10 V/cm for 60-90 min. Gel was then placed on a UV-transilluminator (Stratagene transilluminator 400) and photographed using Mididoc gel documentation system (Herolab, Wiesloch, Germany).

50x TAE-buffer: 2.0 M Tris-HCl pH 8.0, 1.0 acetic acid, 50 mM EDTA.
To be diluted with water.

3.18 DNA Sequencing of PCR Product of GFAT

The PCR product of GFAT was sequenced using an automated fluorescent DNA sequencer (ABI-PRISM 310 Gene analyzer, Perkin-Elmer, Überlingen, Germany) according to manufacturer's instructions. Briefly, the PCR product was purified using a Qiagen Purification kit (PCR purification kit) and purity was verified using agarose-electrophoresis. 2 µl of Pre-Mix (DNA sequencing kit bigdye, Perkin-Elmer, Überlingen, Germany) and 0.5 µl of specific Primer solution (20 µM) were added to 1µl of PCR porduct and made up to 10 µl with water. Amplification was then carried out after incubation for 1 min at 96 °C using the following cycling-program:
10 s at 96 °C / 10 s at 50 ° C / 4 min at 60 °C for 25x cycles. Fluorescent reaction mixture was subsequently purified on CENTRI-SEP columns (Princenton, Adelphia, New Jersey, USA), 5 µl were mixed with 20 µl template suppression Reagent (TSR) to avoid damage to the capillary, placed into special sequencing cups and analyzed using capillary electrophoresis. Data evaluation was made with sequencing analysis software provided.
Sequence comparison was made with BLAST (www.ncbi.nim.nih.gov/BLAST/)

3.19 Quantitative Assay of Muscle Tissue Glycogen

Glycogen values assay from rat skeletal muscle was performed as described in (Carr & Neff 1984). Briefly, ca 100 mg of pulverized mixed hind limb muscle were weighted. 0.75 ml of preheated (40 °C) citrate buffer (100 mM sodium citrate, pH 5.0 adjusted with citric acid) were added, mixed well and homogenized using Potter S at 1500 rpm for 30 s. Two sets of aliquots of each 200 µl were made from each sample. One of the sets was incubated with 0.5% amyloglucosidase in citrate buffer at 55 °C for 150 min with periodical agitation (amyloglucosidase from aspergillus niger, A7420, Sigma, München, Germany). Samples were then centrifuged at 28000 rpm in TLA 55 rotor (Beckman, München, Germany) for 30 min. Supernatants were measured using YSI analyzer (YSI 2300 STAT Plus, Kraienbaum, Langenfeld, Germany). Observed and expected glucose readings of 0.1% glycogen standard (Type III from rat liver, Sigma) were processed for quantification.
In preliminary experiments, different concentrations of glucose were measured in citrate buffer pH 5.0. Regression analysis revealed a correlation coefficient of r^2=0.9995.

3.20 Statistical analysis

All data are expressed as means ± SEM. Data were analyzed using SPSS software. The one-tailed student's unpaired test was used for comparison of mean values. Statistical significance was accepted at $p < 0.05$.

4 RESULTS

4.1.1 Effects of Continuous Glucose Infusion on Plasma Glucose and Insulin Concentrations in Rats

To characterize the metabolic state reached after glucose infusion (2d vs. 5d), plasma glucose and insulin concentrations were monitored from blood samples taken from the tail vein of saline-infused rats (SIR) and glucose-infused rats (GIR).
Plasma glucose concentrations peaked after 24h of glucose infusion and decreased continuously to reach normoglycemia after 5d of infusion.
Extended glucose infusion up to 7d showed, that GIRs were able to maintain reached normoglycemia despite ongoing glucose infusion:

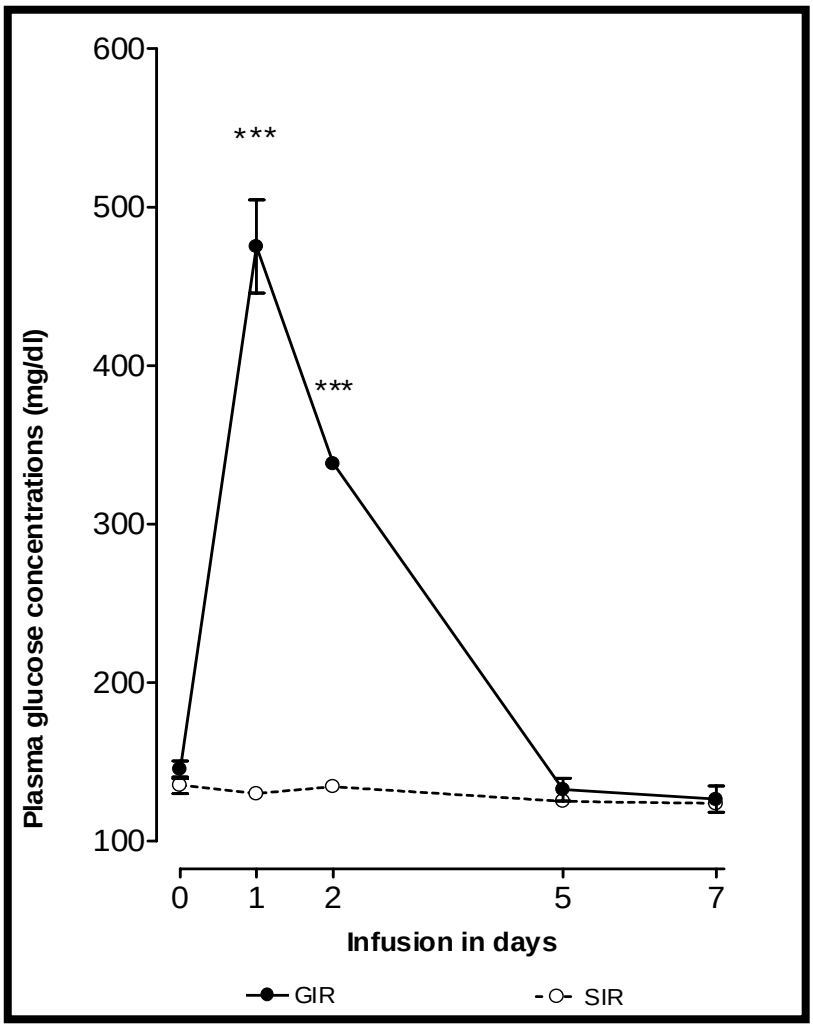

Figure 4.1.1.1 Plasma glucose concentrations reached during glucose infusion, *** p<0.001.

Serum insulin concentrations followed a similar pattern. Hyperinsulinemia sustained, albeit rats were normoglycemic. Hyperinsulinemia monitored after 5d of infusion was “mild” when compared with hyperinsulinemia after 2d of glucose infusion.

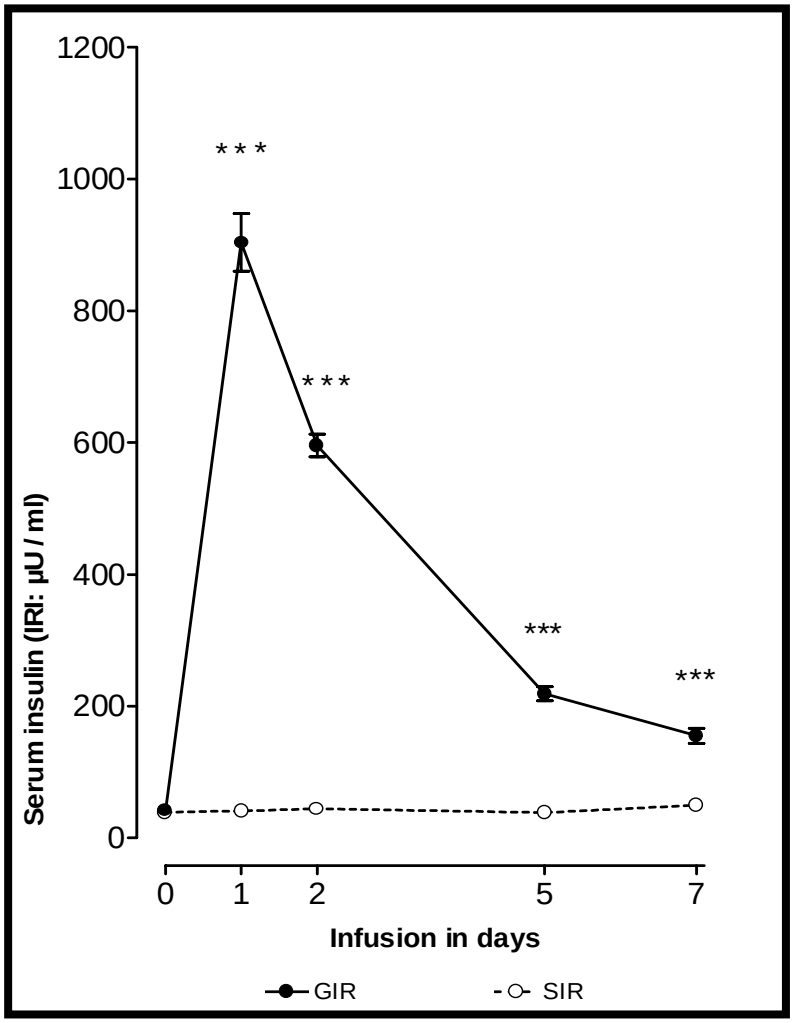

Figure 4.1.1.2 Serum insulin concentrations reached during glucose infusion, *** p<0.001.

4.1.2 Effects of Continuous Glucose Infusion on Body weight, Glucosuria and Food Consumption in Rats

Infusion period	2d		5d	
	control	GIR	control	GIR
Glucose infused (g/d)	0	24	0	24
Urine glucose	Negative	Positive	Negative	Negative
Food consumption (g/d)	10 ± 0.3	7.8 ± 0.2	12 ± 0.3	7 ± 0.3
Gained weight (g/d)	1.8 ±0.1	3	1.8 ± 0.1	3.4 ±0.2

Table 4.1.2 Summarizes metabolic data monitored during the infusion period.

4.2 Effects of Glucose Infusion on The Insulin Receptor

To investigate whether early events of insulin signal transduction are altered due to the prolonged glucose infusion period, insulin receptor protein expression, its phosphotyrosine phosphorylation and messenger expression were determined:

A. Insulin Receptor Protein Expression

Insulin receptor protein expression in total extracts of mixed hind limb muscle was determined using immunoprecipitation, SDS-PAGE and Western-Blotting.
Antibodies directed against the β-subunit were used.
Protein expression of the insulin receptor was not significantly changed after 2d of glucose infusion, whereas it was slightly diminished after 5d:

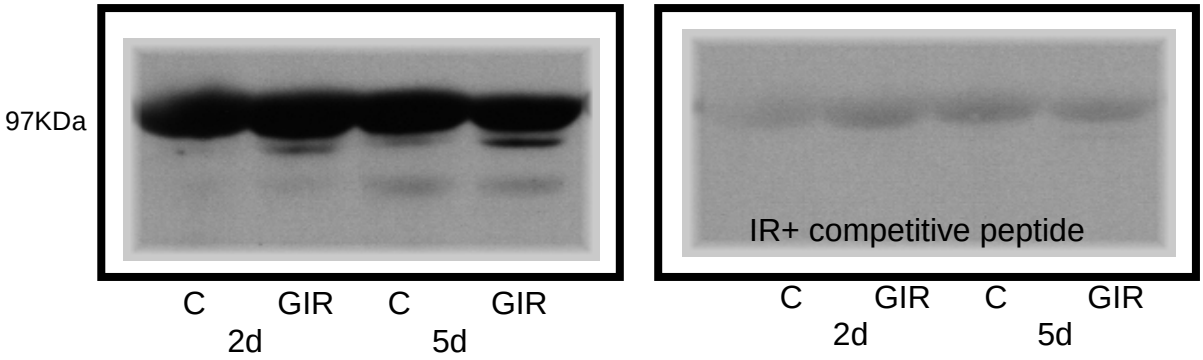

Figure 4.2.1 Western-Blot of IR-β-subunit after 2 and 5d of glucose infusion (left hand-side) and a Western-Blot of the same when specific antibodies were blocked using a competitive peptide (right hand side). C: controls, GIR: glucose-infused rats.

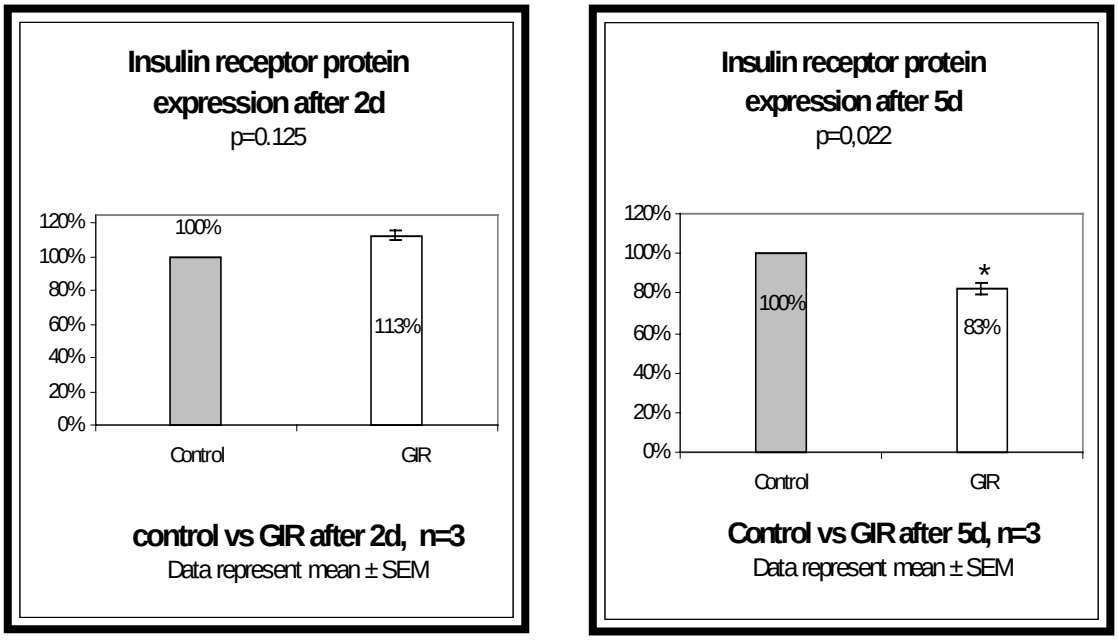

Figure 4.2.2 Shows results of scanning densitometry of Western-Blots of n=3 different experiments, results are expressed relative to control animals.

B. Insulin Receptor Tyrosine Phosphorylation

The phosphorylation of the insulin receptor on tyrosine residues and thus its functional activation was investigated using a non site-specific anti-phosphotyrosine-antibody.
Again no significant change was monitored after 2d of infusion, whereas phosphorylation of the β-subunit was decreased after 5d.
To determine whether this decrease is only due to decreased protein expression, the ratio of phosphorylation of IR / IR protein expression was calculated and resulted at 91.5%. Thus, decreased phosphorylation observed was not only due to decreased protein expression of insulin receptor β-subunit.

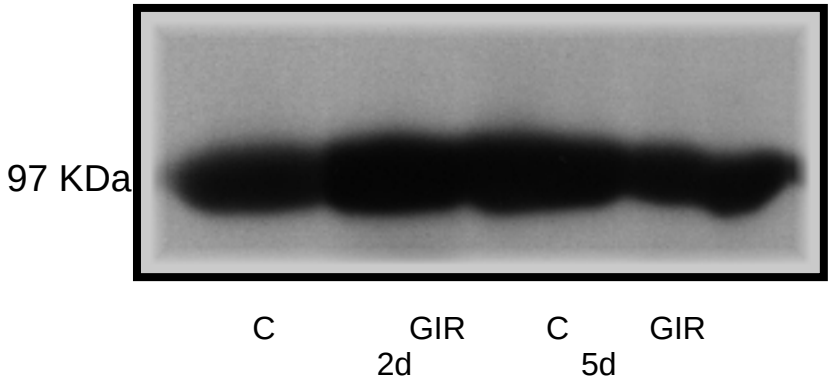

Figure 4.2.3 Western-Blot of p-tyrosine-phosphorylation of the β-subunit of the insulin receptor.

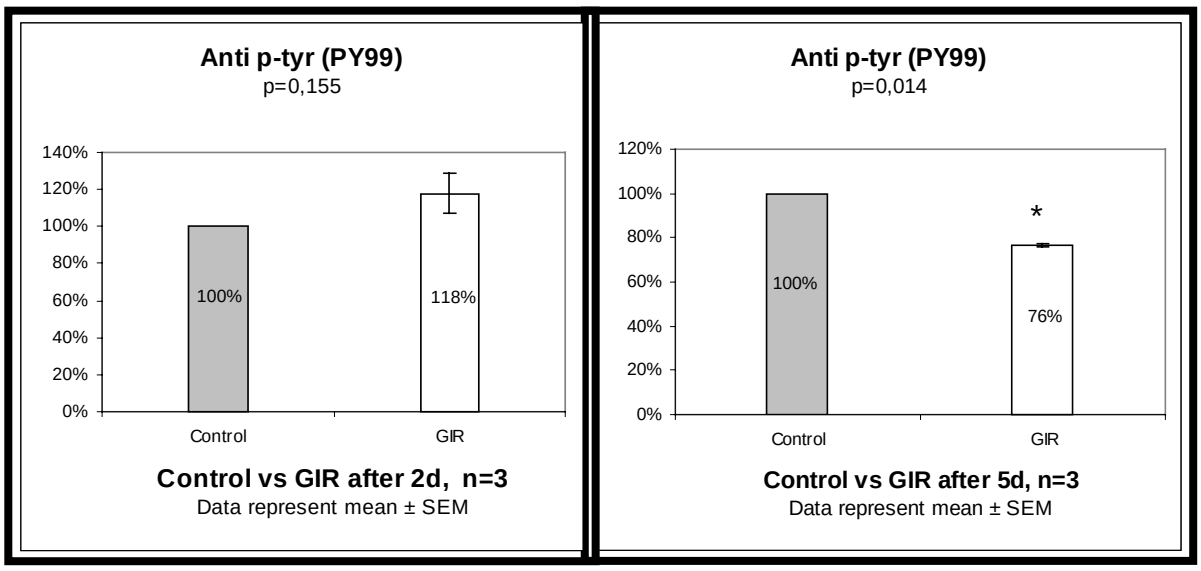

Figure 4.2.4 Shows results of scanning densitometry of Western-Blots of n=3 different experiments, results are expressed relative to control animals.

C. Insulin Receptor mRNA-Expression

The messenger RNA-Expression of the insulin receptor was determined by RT-PCR using the Light-Cycler-System with β-Globin as an external standard.
The mRNA-expression after 2d of infusion was not significantly changed, whereas it decreased after 5d of infusion.

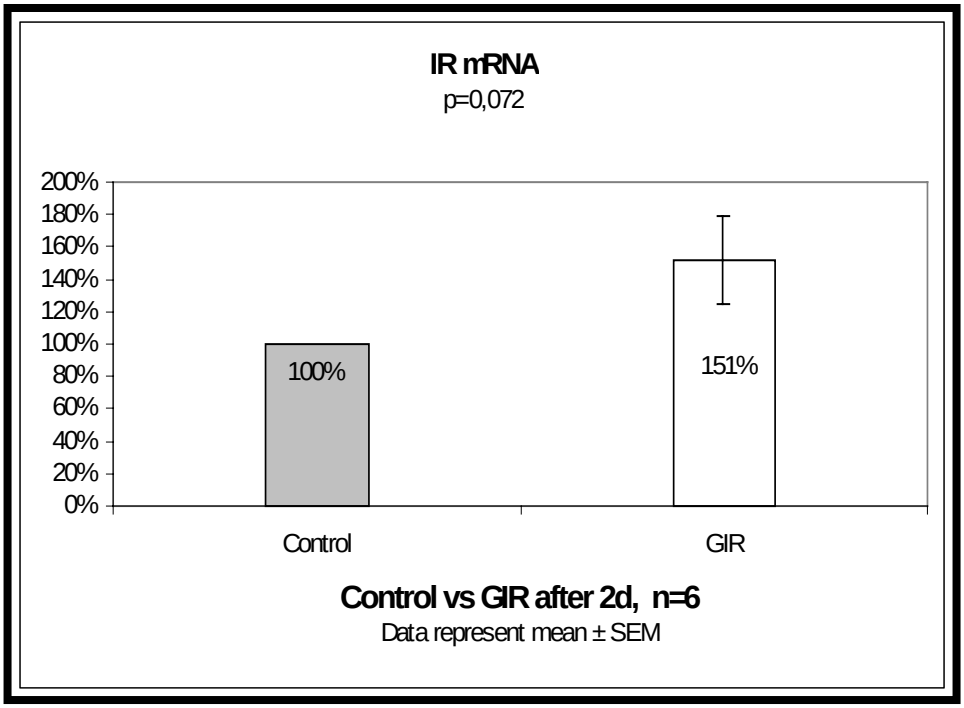

Figure 4.2.5 mRNA-Expression of IR in mixed hind limb muscle after 2d of glucose infusion.

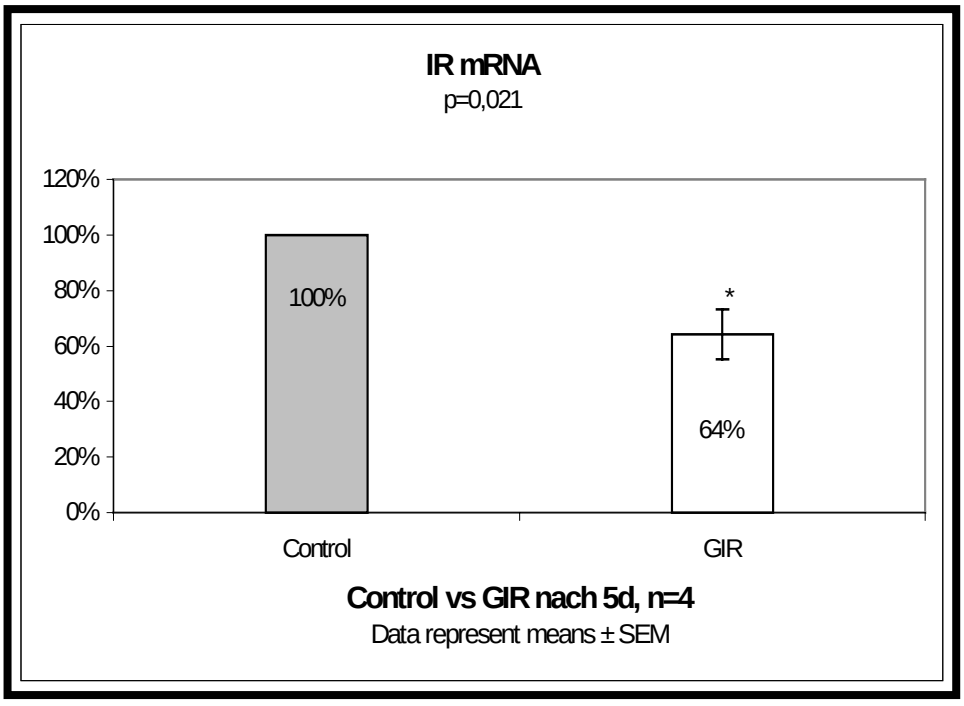

Figure 4.2.6 mRNA-Expression of IR in mixed hind limb muscle after 5d of glucose infusion.

4.3 Effects of Glucose Infusion on Insulin Receptor Substrate 1 (IRS-1)

The major cytosolic substrate of IR, IRS-1, was investigated at protein expression level, p-tyrosine phosphorylation and mRNA-level:

A. IRS-1 Protein Expression

Western-Blot analysis showed no significant change in protein expression of IRS-1:

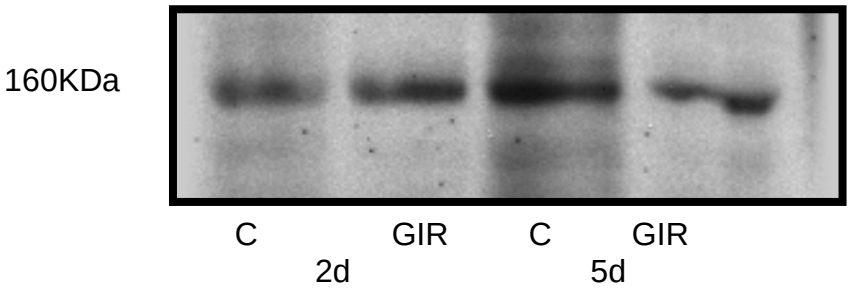

Figure 4.3.1 Representative Western-Blot of IRS-1. N=3 different experiments were performed.

B. IRS-1 Tyrosine Phosphorylation

The tyrosine phosphorylation of IRS-1 was not significantly changed:

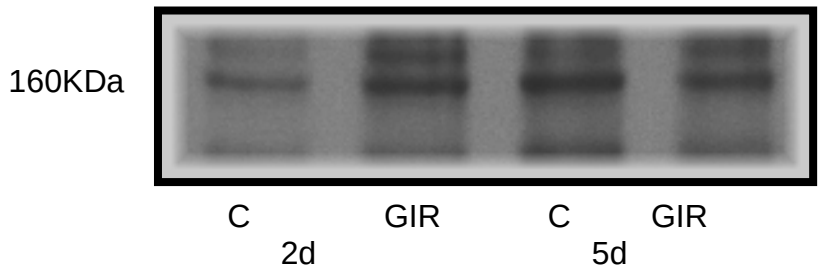

Figure 4.3.2 Representative Western-Blot of IRS-1 P-Tyr-phosphorylation. N=3 different experiments were performed.

C. IRS-1 mRNA-Expression

The mRNA-expression of IRS-1 was determined by RT-PCR using the Light-Cycler-System with β-Globin as an external standard.
The mRNA-expression was not significantly changed during the whole infusion period.

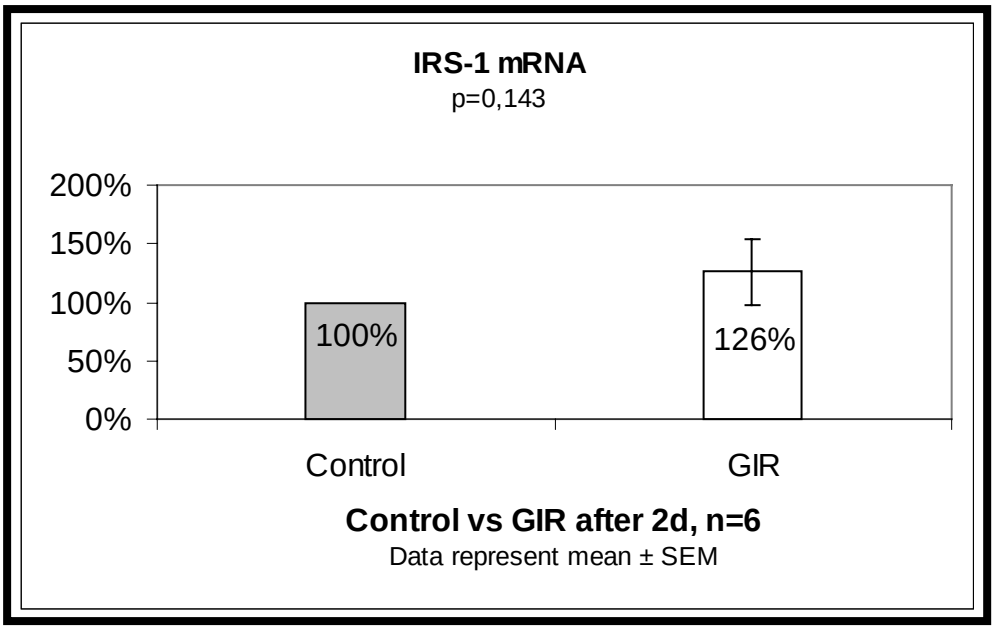

Figure 4.3.3 mRNA-Expression of IRS-1 in mixed hind limb muscle after 2d of glucose infusion.

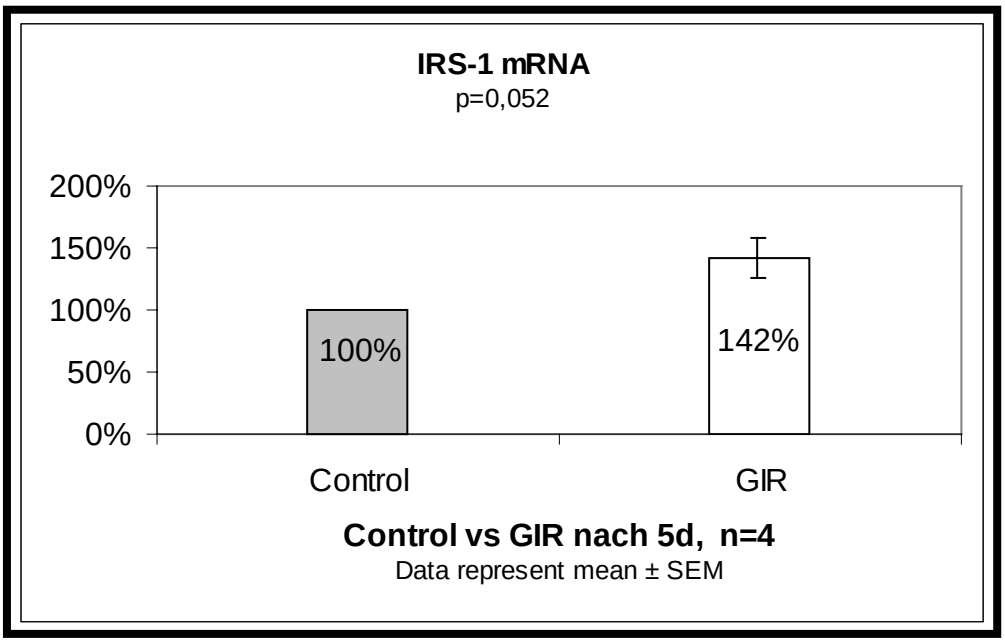

Figure 4.3.4 mRNA-Expression of IRS-1 in mixed hind limb muscle after 5d of glucose infusion.

4.4 Effects of Glucose Infusion on Phosphatidylinositol 3-Kinase (PI3-K)

Protein expression of PI3-K regulatory domain p85, mRNA-expression and enzyme activity of PI3-K were measured:

A. Protein Expression of PI3-K p85-Subunit

p85-subunit expression in total extracts of mixed hind limb muscle was determined using SDS-PAGE and Western-Blotting.
No significant changes in the protein expression of the p85-subunit was detected during the whole infusion period.

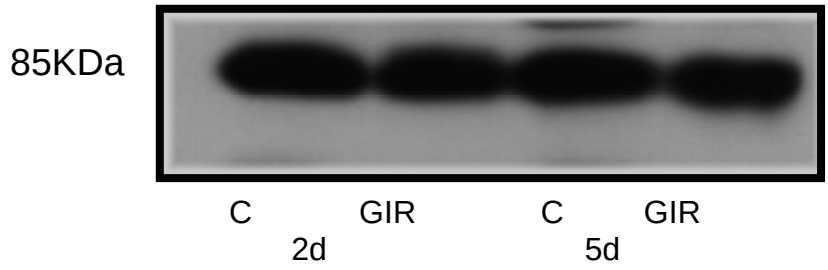

Figure 4.4.1 Representative Blot of PI3-K-p85-subunit. N=3 different experiments were performed.

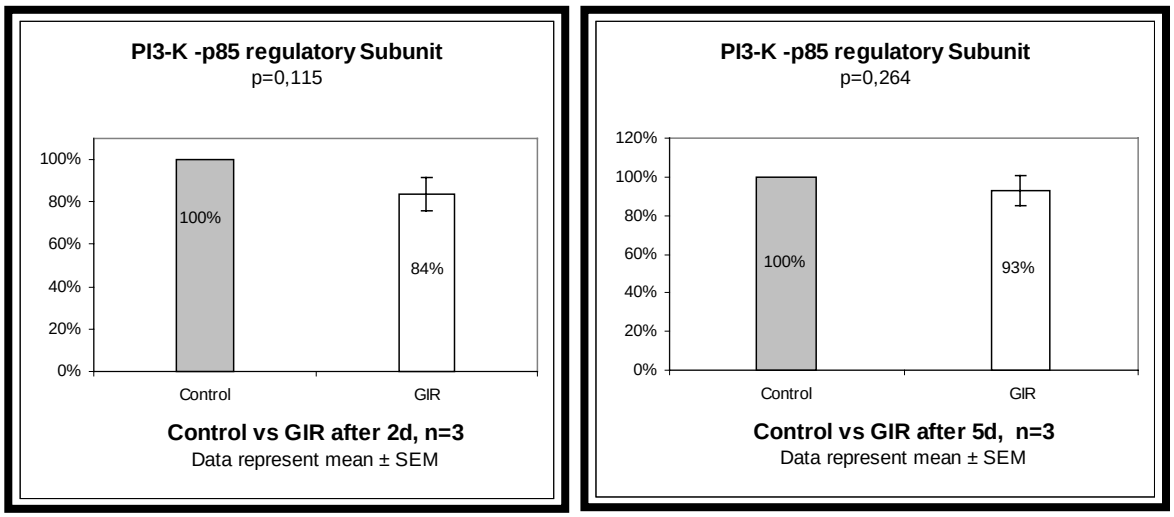

Figure 4.4.2 Results of scanning densitometry of Western-Blots of n=3 different experiments, results are expressed relative to control animals.

B. PI3-K mRNA-Expression

No significant changes in PI3-K mRNA-expression were detected during the whole period of infusion:

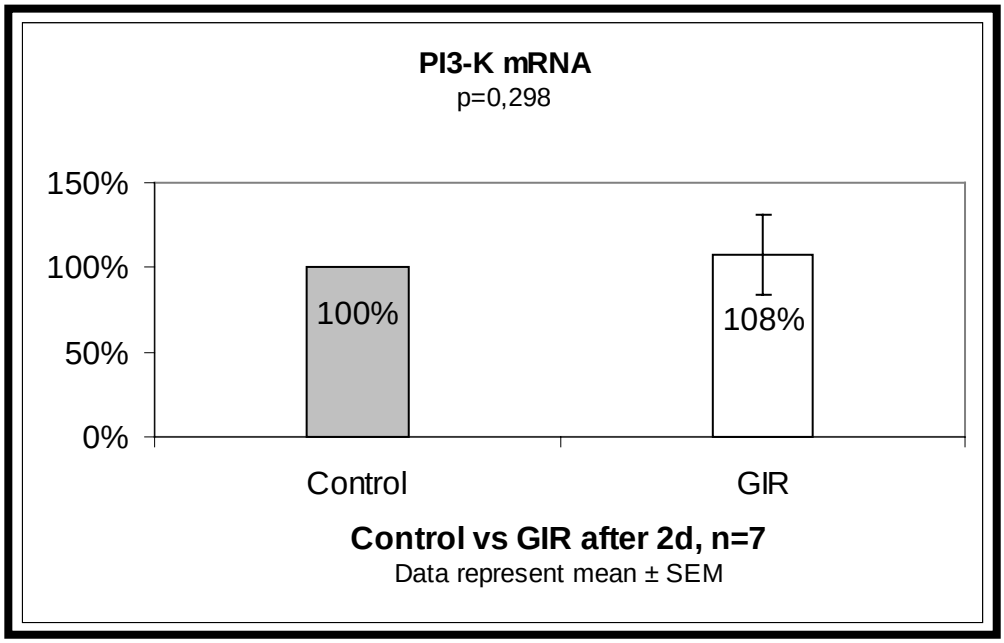

Figure 4.4.3 mRNA-Expression of PI3-K in mixed hind limb muscle after 2d of glucose infusion.

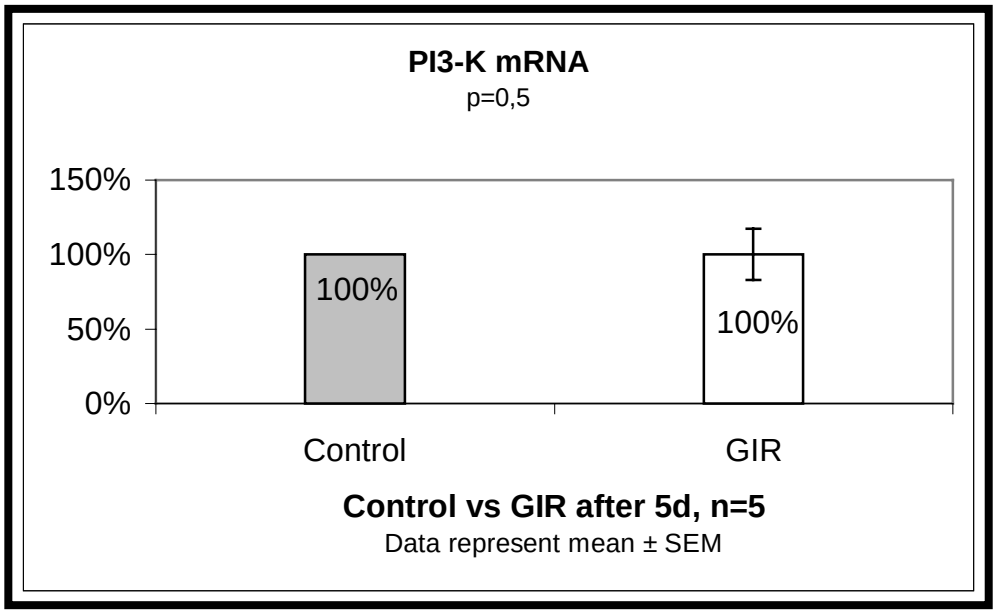

Figure 4.4.4 mRNA-Expression of PI3-K in mixed hind limb muscle after 5d of glucose infusion.

C. IRS-1 Associated Phosphatidylinositol 3-Kinase Activity Assay

The ability of PI3-K to phosphorylate Phosphatidylinositol-4-phosphate PtdIns(4)P and/or Phosphatidyl-4,5-phosphate (PtdIns(4,5)P_2) at position 3 of the inositol ring to Phosphatidylinositol-3,4-phosphate (PtdIns(3,4)P_2) or Phosphatidylinositol-3,4,5-phosphate (PtdIns(3,4,5)P_3) was investigated. No significant changes were seen during the whole infusion period. Wotmannin was used as inhibitor of PI3-K.

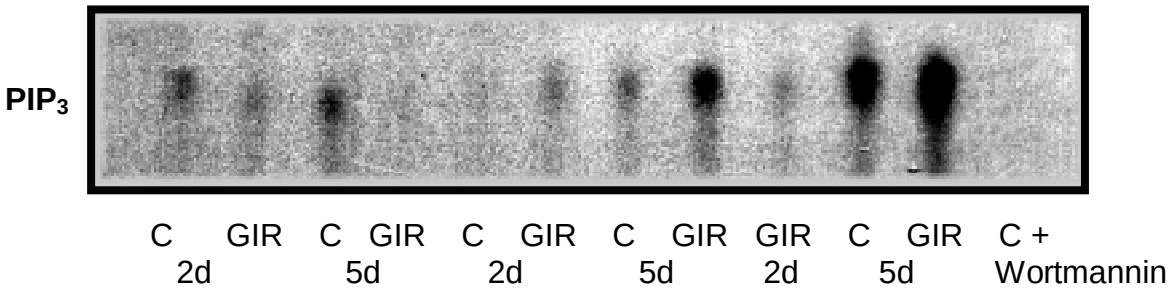

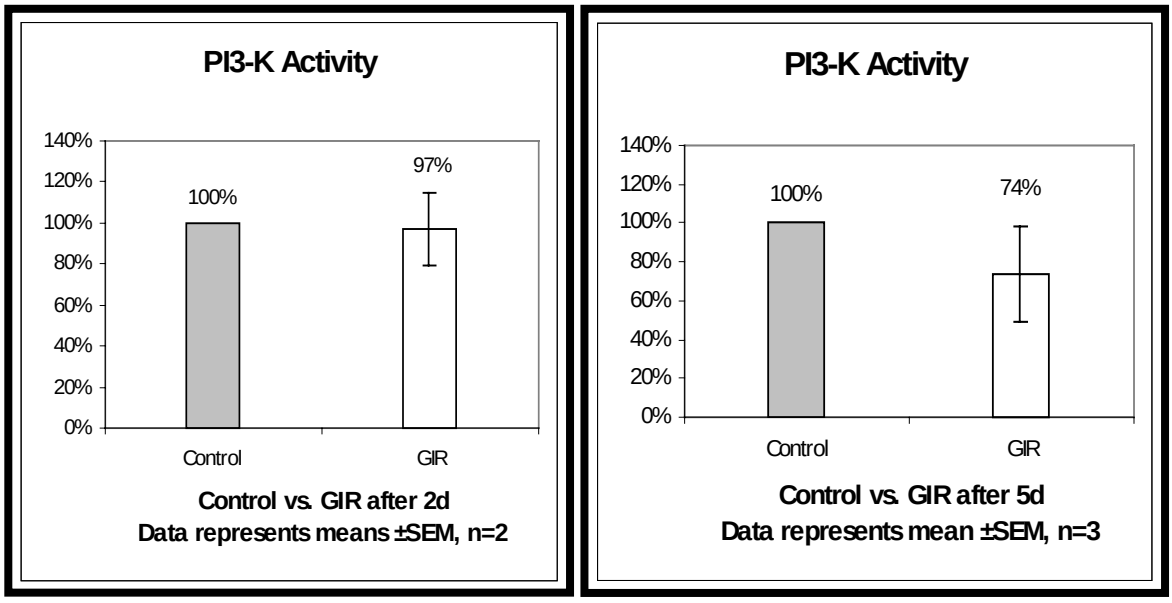

Figure 4.4.5 Effect of glucose infusion on IRS-1 associated PI3-K activity, measured by autoradiography and calculated results. The PI3-K activity is expressed relative to control animals.

4.5 Effects of Glucose Infusion on Protein Kinase B (PKB or AKT1) Expression and its Serine Phosphorylation

A. Protein Expression

Protein expression was determined using a specific antibody against PKB.
No significant changes were seen during the whole period of infusion.

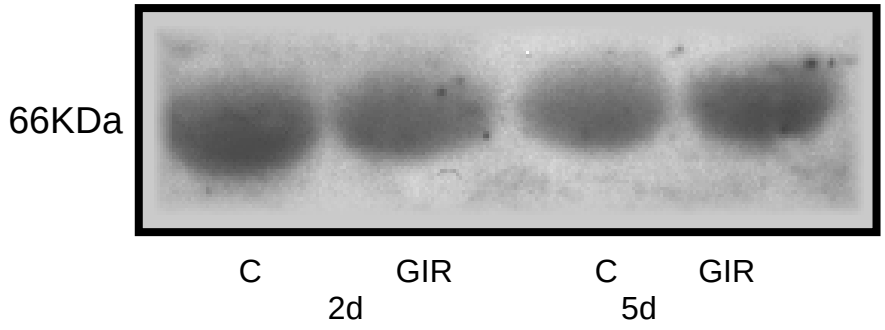

Figure 4.5.1 Representative Western-Blot of PKB. N=3 different experiments were performed.

B. Serine Phosphorylation

Serine phosphorylation on serine 473 of PKB was unchanged during the entire period of infusion.

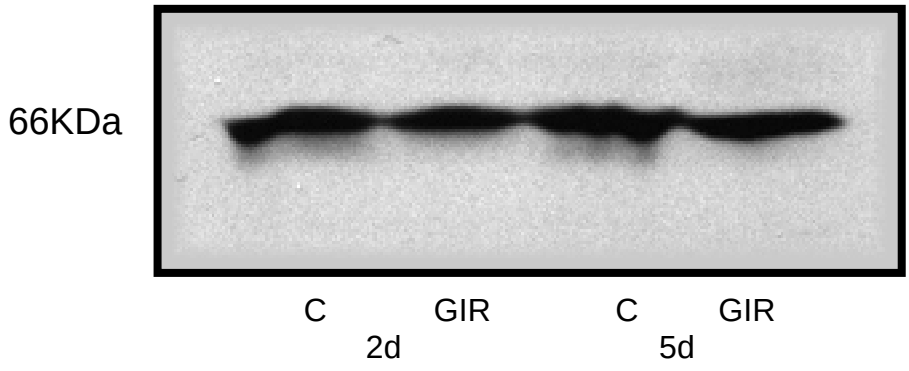

Figure 4.5.2 Representative Western-Blot of PKB-serine 473 -phosphorylation. N=3 different experiments were performed.

4.6 Effects of Glucose Infusion on Protein Kinase C Isoforms (PKC)

Protein expression and cellular distribution of thoroughly all detectable isoforms of PKC were investigated. Translocation and thus activation resulted in redistribution of PKC isoforms from total membrane fraction to cytosolic fraction. In addition, the mRNA-expression was determined, where applicable.

A. Classical PKC Isoforms

Among these, PKCα, βI, βII were investigated.

A.1.1 Effects of Glucose Infusion on Protein Kinase C Isoform α Expression and Translocation (PKCα)

Protein expression of total PKCα increased significantly after 2d, whereas PKCα expression was significantly decreased after 5d.

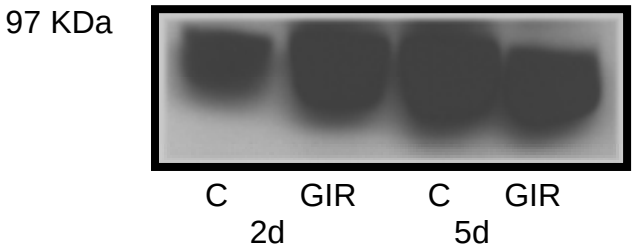

Figure 4.6.1 Representative Western-Blot of total PKCα in mixed hind limb muscle homogenate.

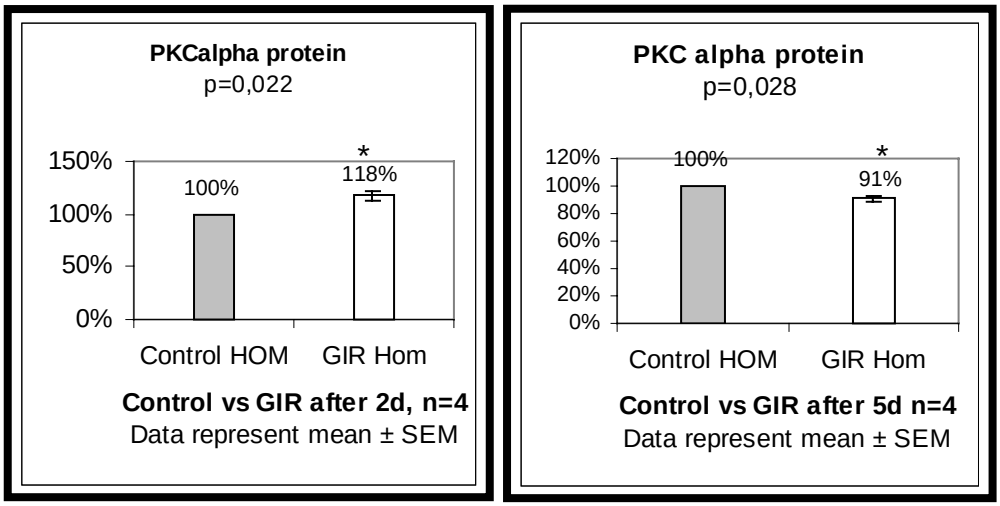

Figure 4.6.2 Results of scanning densitometry of PKCα in mixed hind limb muscle homogenate.

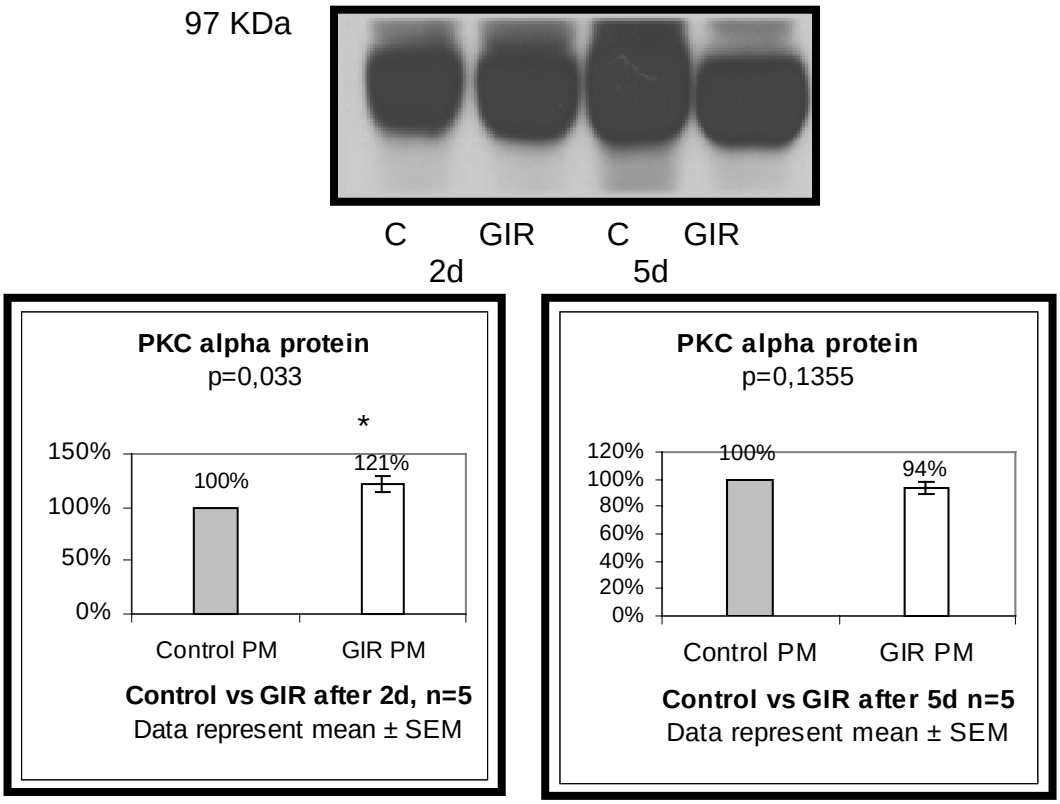

Figure 4.6.3 Representative Western-Blot of PKCα in membrane fraction of mixed hind limb muscle and results of scanning densitometry.

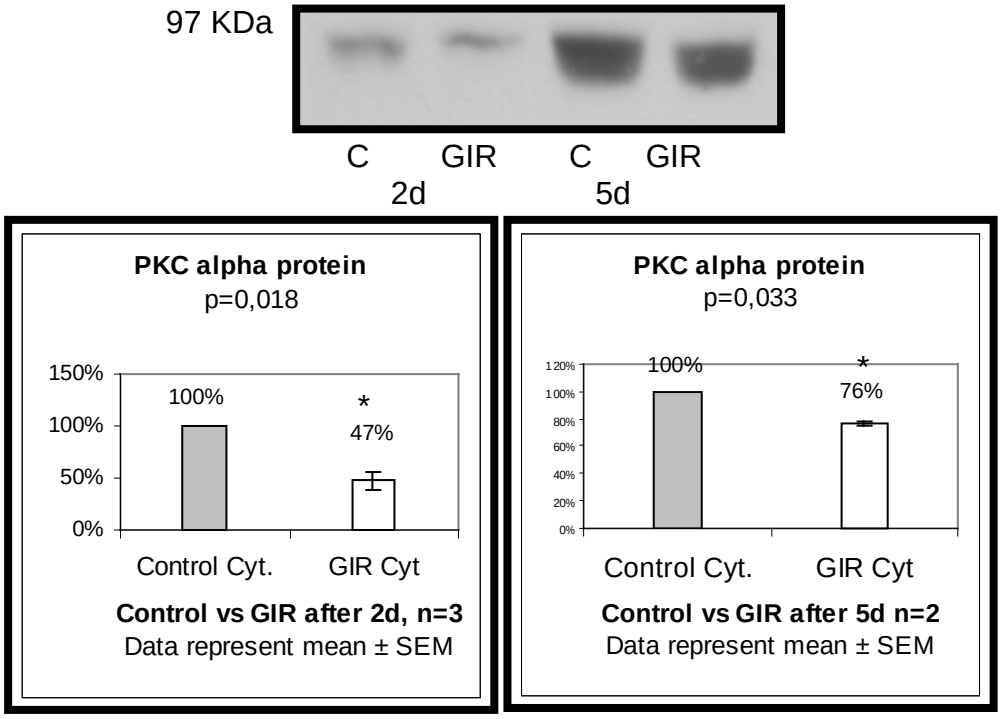

Figure 4.6.4 Representative Western-Blot of PKCα in cytosolic fraction of mixed hind limb muscle and results of scanning densitometry .

A significant translocation can be shown after 2d, whereas after 5d a decrease in both membrane and cytosolic fractions was seen.

A.1.2 Effects of Glucose Infusion on mRNA-Expression of PKCα

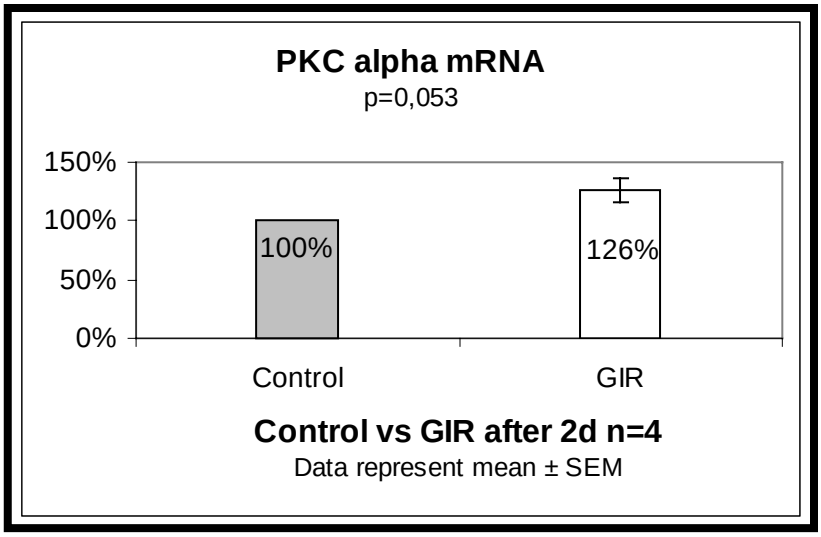

Figure 4.6.5 mRNA-expression of PKCα after 2d of glucose infusion.

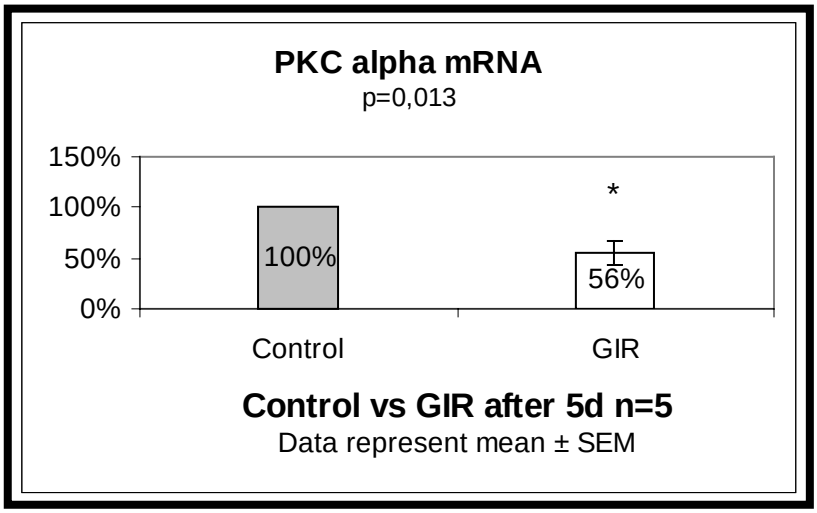

Figure 4.6.6 mRNA-expression of PKCα after 5d of glucose infusion.

The tendency towards an increase in mRNA-expression after 2d just missed statistical significance, whereas a significant decrease can be shown after 5d of infusion.

A.2.1 Effects of Glucose Infusion on Protein Kinase C Isoform βI Expression and Translocation (PKCβI)

Protein expression of PKCβI increased significantly after 2d and was restored to normal levels after 5d of infusion.

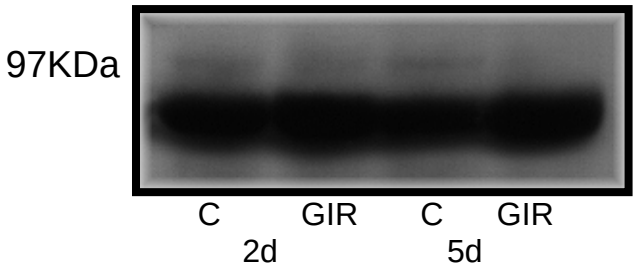

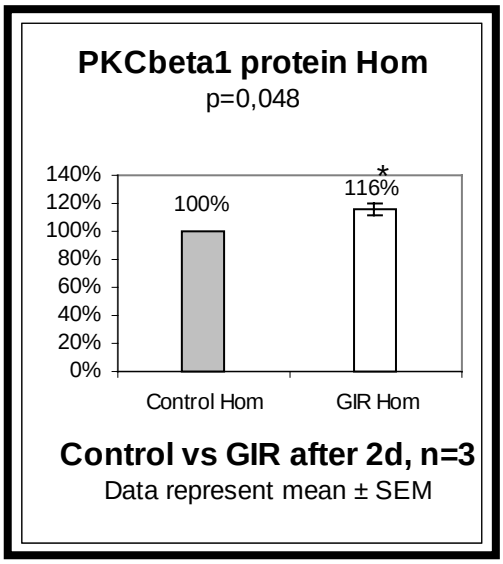

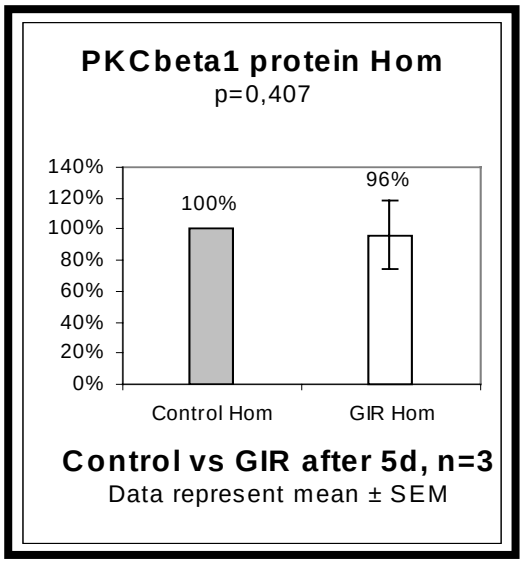

Figure 4.6.7 Representative Western-Blot of PKCβI in mixed hind limb muscle homogenate and results of scanning densitometry.

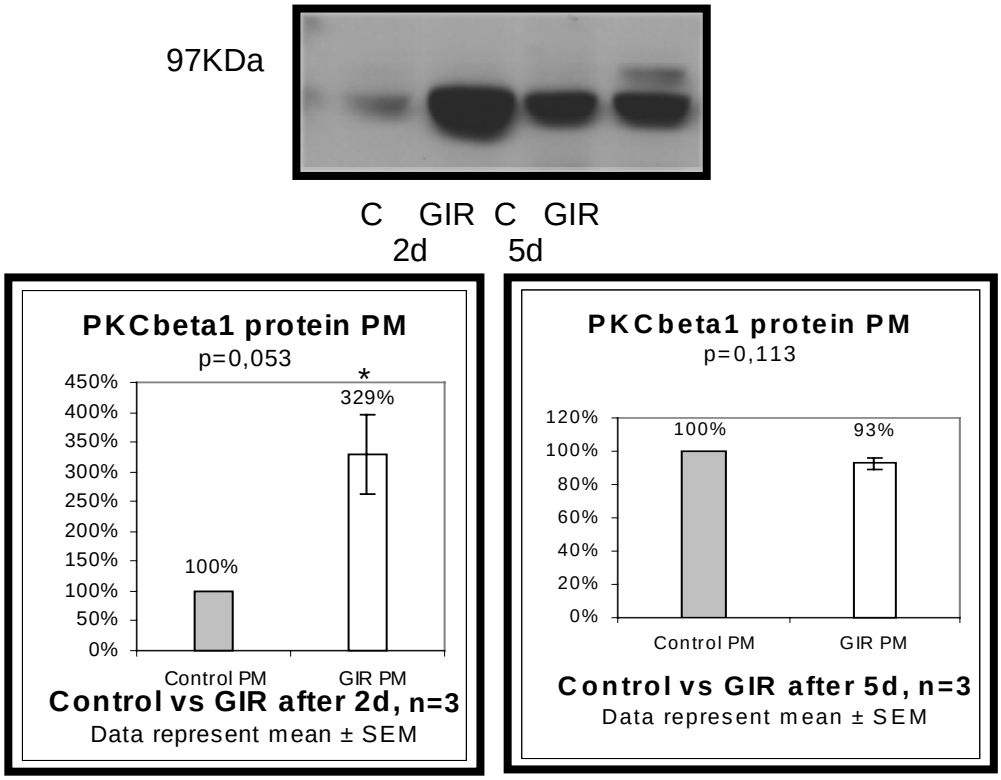

Figure 4.6.8 Representative Western-Blot of PKCβI in membrane fraction of mixed hind limb muscle and results of scanning densitometry.

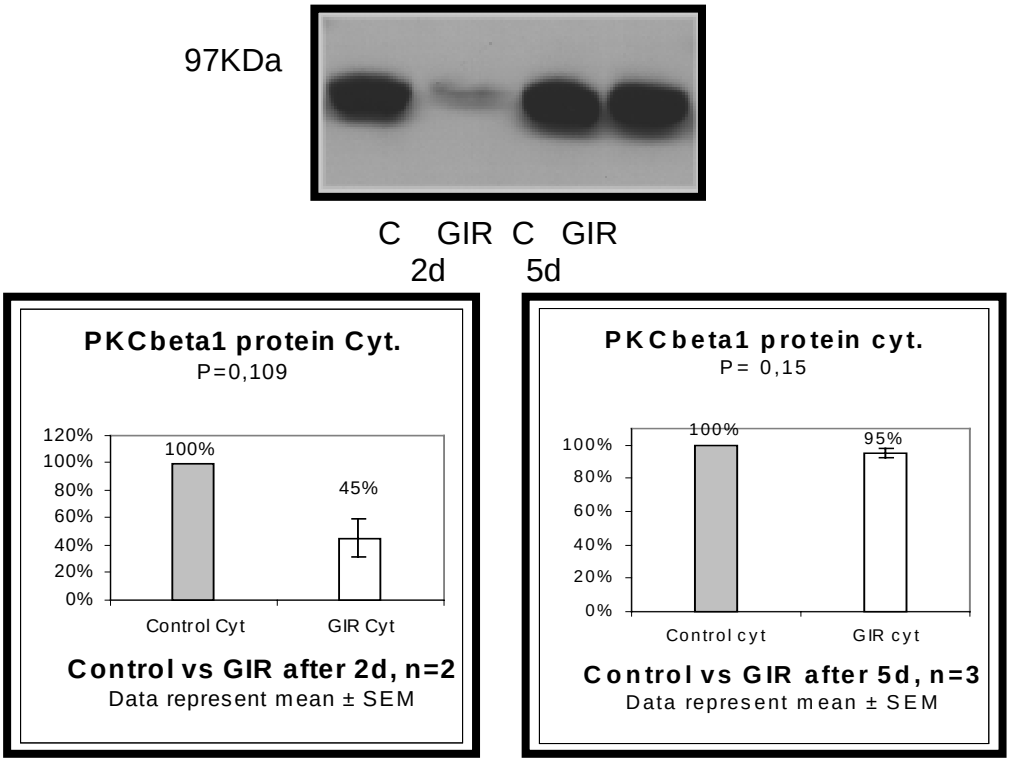

Figure 4.6.9 Representative Western-Blot of PKCβI in cytosolic fraction of mixed hind limb muscle and results of scanning densitometry.

The strong translocation from the plasma membrane fraction to cytosolic fractions after 2d indicates a strong activation of PKCβI during the early hyperglycemic period, whereas translocation was unchanged after 5d of infusion.

A.2.2 Effects of Glucose Infusion on Protein Kinase C Isoform βI mRNA-Expression

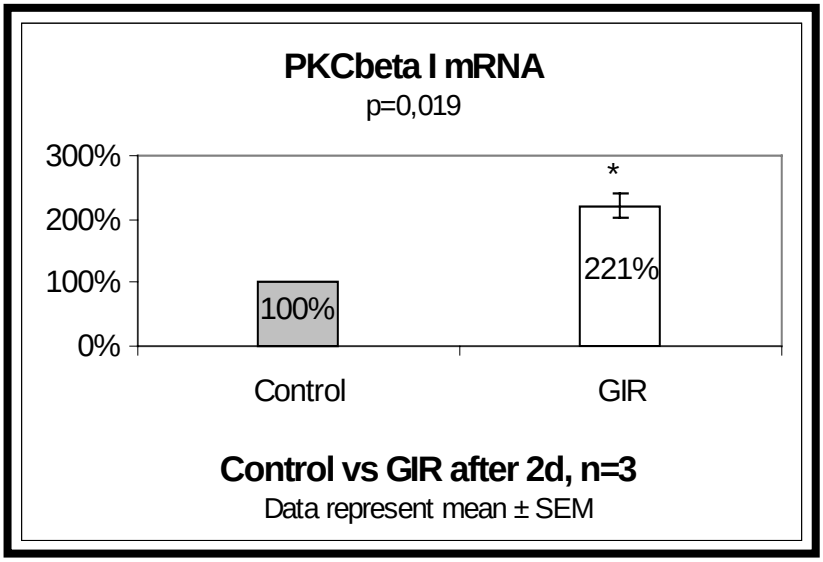

Figure 4.6.10 mRNA-expression of PKCβI after 2d of glucose infusion.

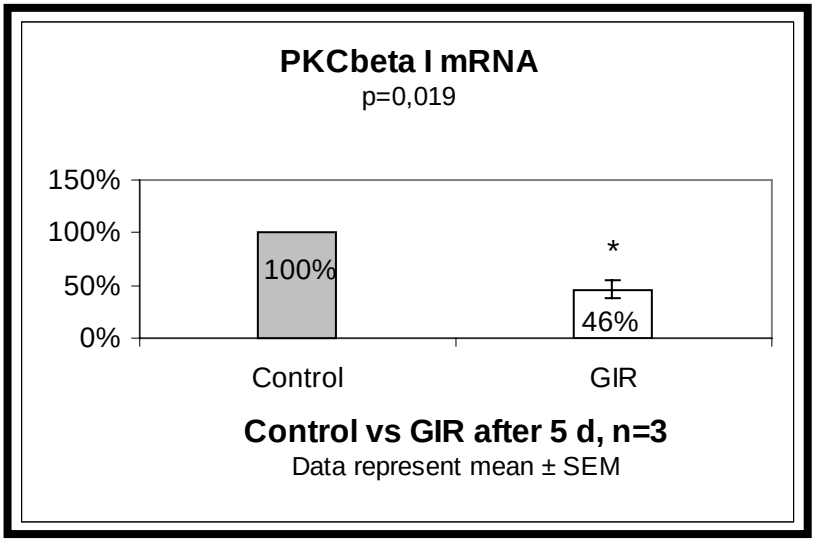

Figure 4.6.11 mRNA-expression of PKCβI after 5d of glucose infusion.

mRNA-expression increased significantly after 2d of infusion and decreased below normal levels after 5d of infusion.

A.3 Effects of Glucose Infusion on Protein Kinase C Isoform βII Expression and Translocation (PKCβII)

Protein expression of PKCβII was not significantly changed after 2d, whereas it was significantly decreased after 5d of infusion.

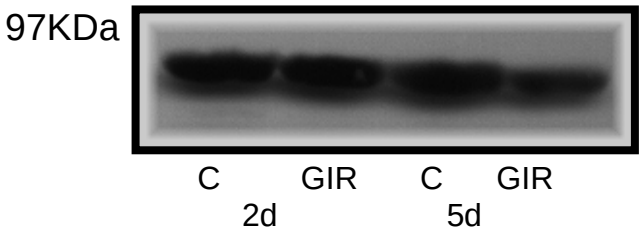

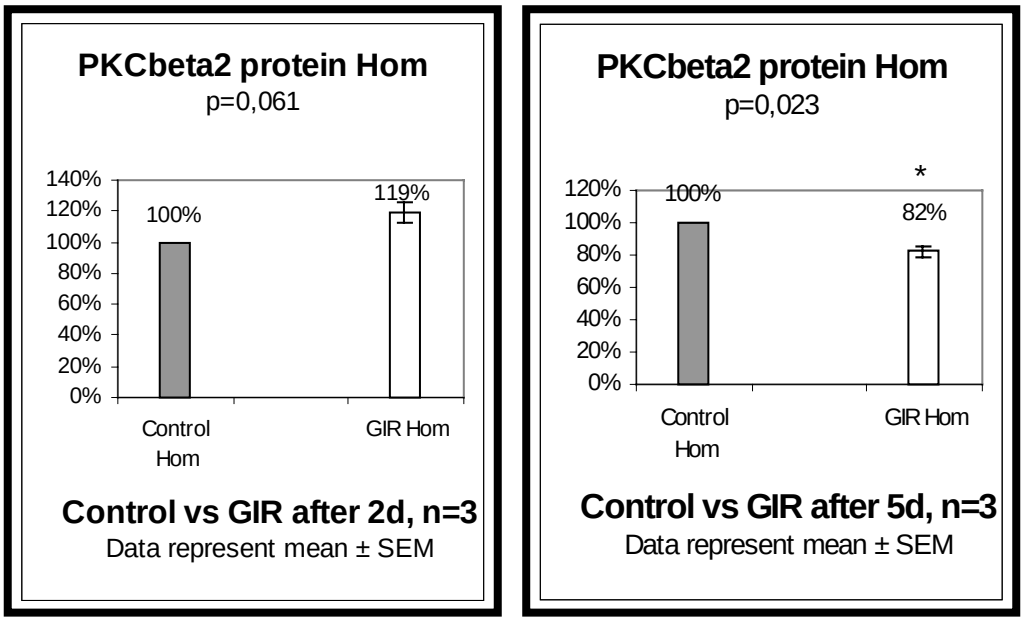

Figure 4.6.12 Representative Western-Blot of PKCβII in mixed hind limb muscle homogenate and results of scanning densitometry.

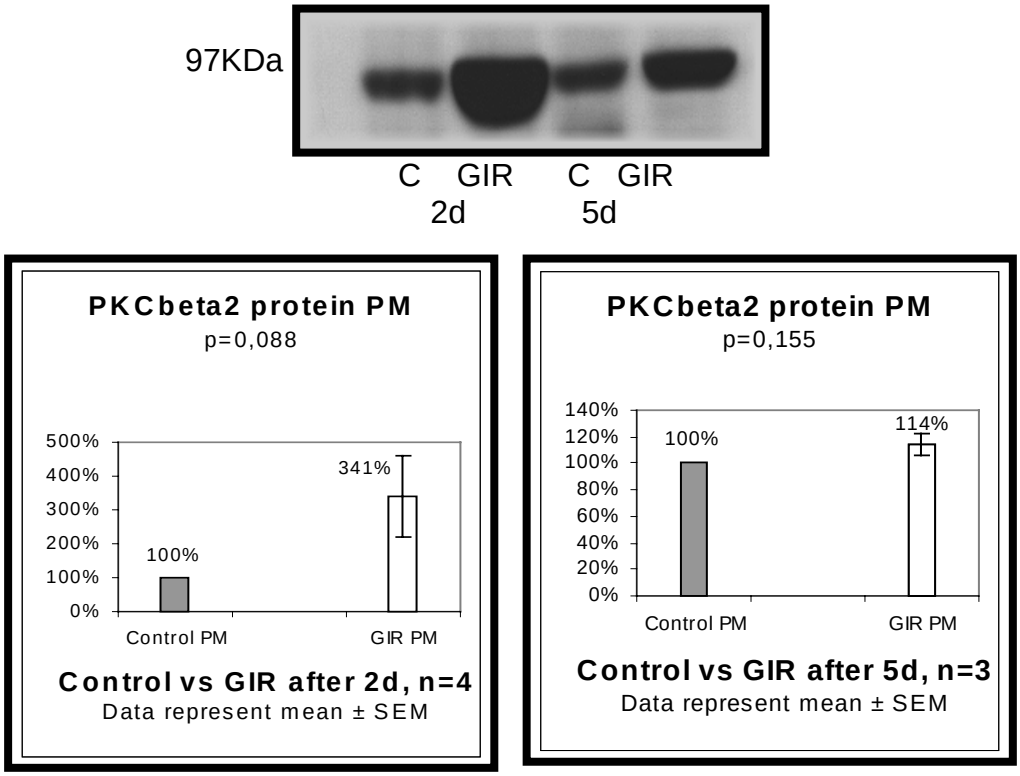

Figure 4.6.13 Representative Western-Blot of PKCβII in total membrane fraction of mixed hind limb muscle and results of scanning densitometry.

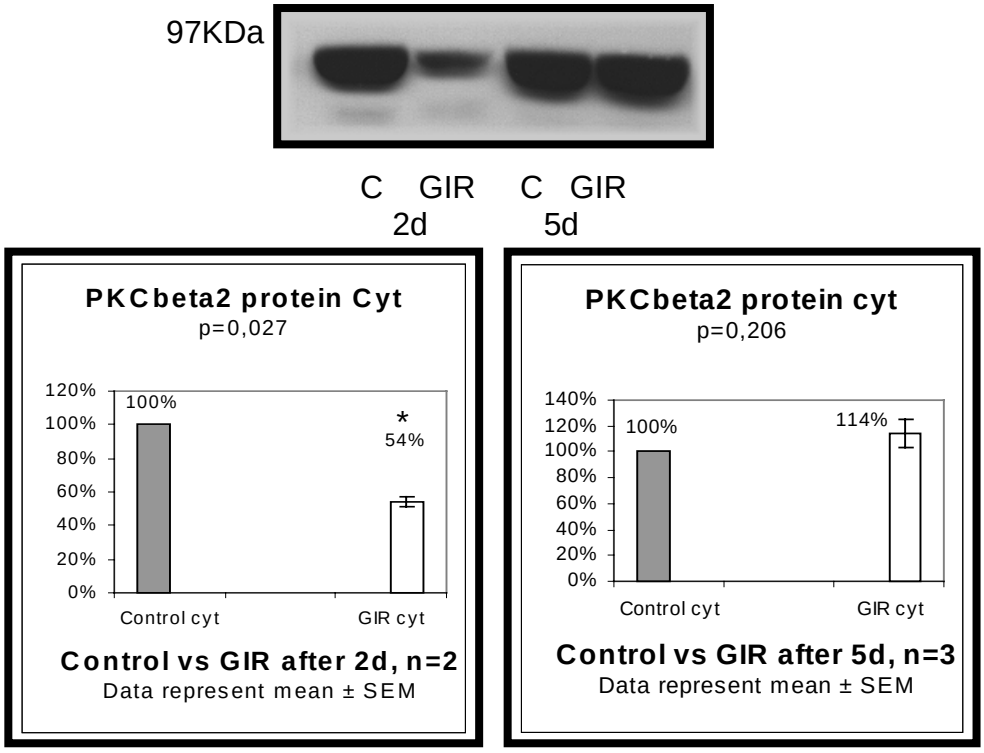

Figure 4.6.14 Representative Western-Blot of PKCβII in cytosolic fraction of mixed hind limb muscle and results of scanning densitometry.

Strong translocation from the cytosolic fraction to the plasma membrane fraction after 2d indicates a strong activation of PKCβII during the early hyperglycemic period, whereas translocation was unchanged after 5d of infusion.

B. New PKC Isoforms

Among these, PKCθ, δ and ε were investigated.

B.1 Effects of Glucose Infusion on Protein Kinase C Isoform θ Expression and Translocation (PKCθ)

Protein expression of PKCθ was signifcantly increased after 2d and after 5d of glucose infusion.

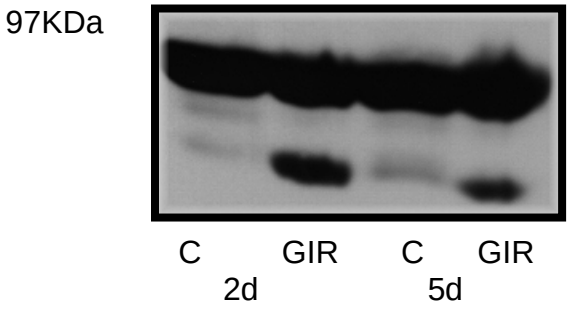

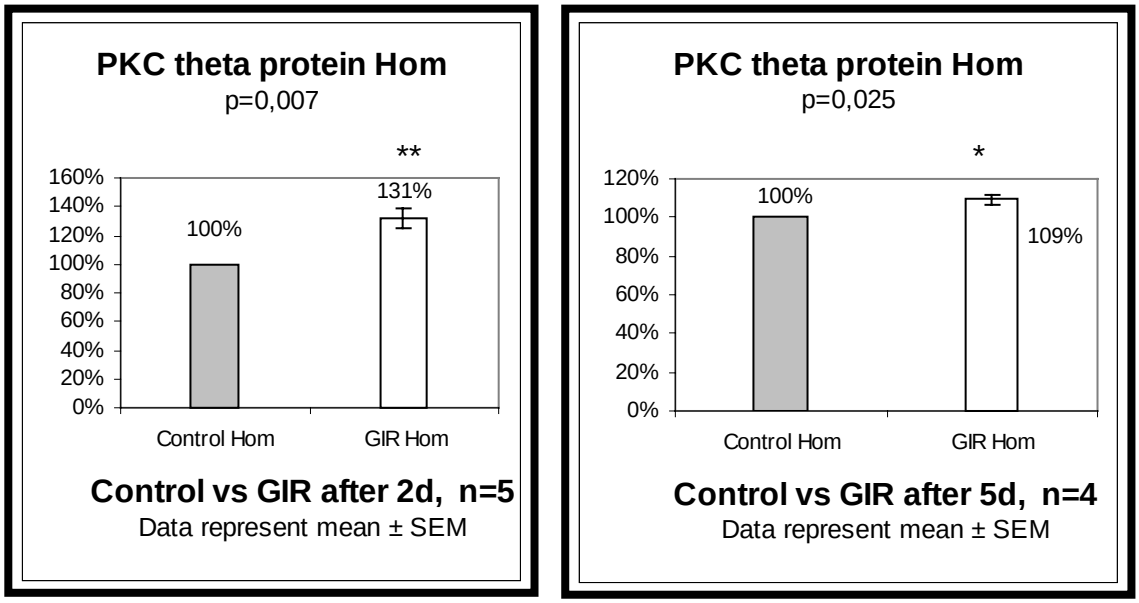

Figure 4.6.15 Representative Western-Blot of PKCθ in mixed hind limb muscle homogenate and results of scanning densitometry.

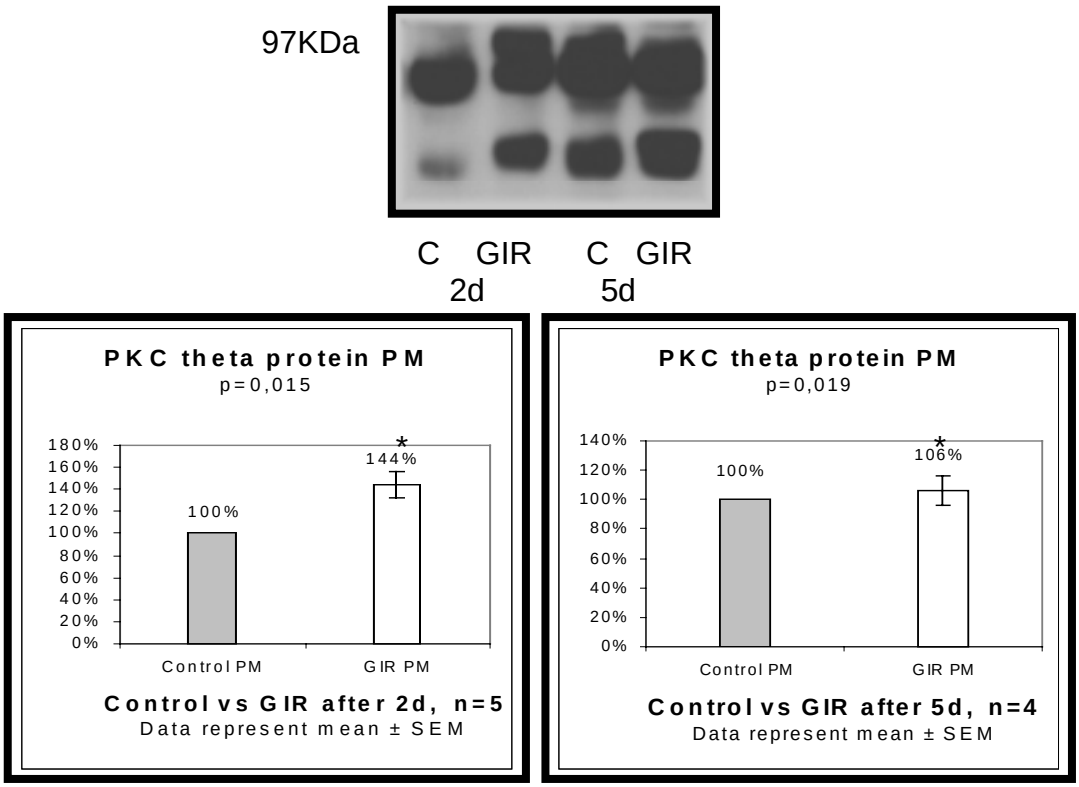

Figure 4.6.16 Representative Western-Blot of PKCθ in total membrane fraction of mixed hind limb muscle and results of scanning densitometry.

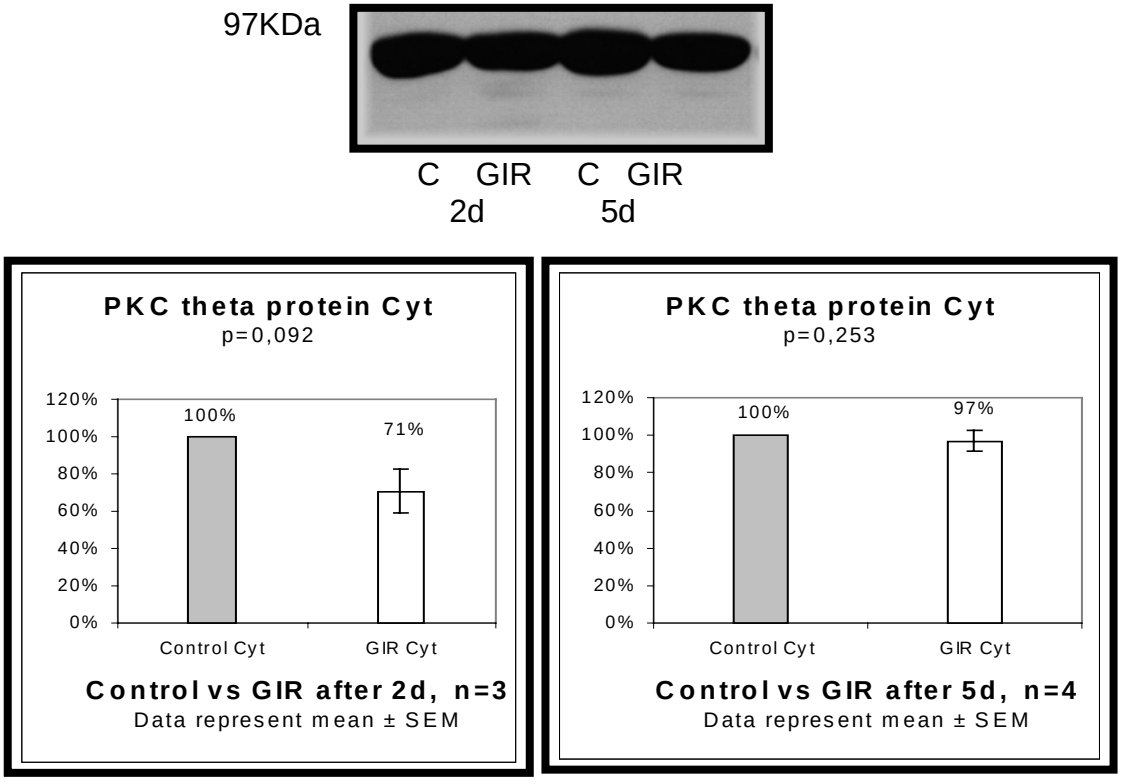

Figure 4.6.17 Representative Western-Blot of PKCθ in cytosolic fraction of mixed hind limb muscle and results of scanning densitometry.

Translocation from the cytosolic fraction to the plasma membrane fraction was shown after 2d, whereas no translocation can be shown after 5d of glucose infusion.

B.2.1 Effects of Glucose Infusion on Protein Kinase C Isoform δ Expression and Translocation (PKCδ)

Protein expression of PKCδ was significantly increased after 2d, whereas no significant changes were seen after 5d.

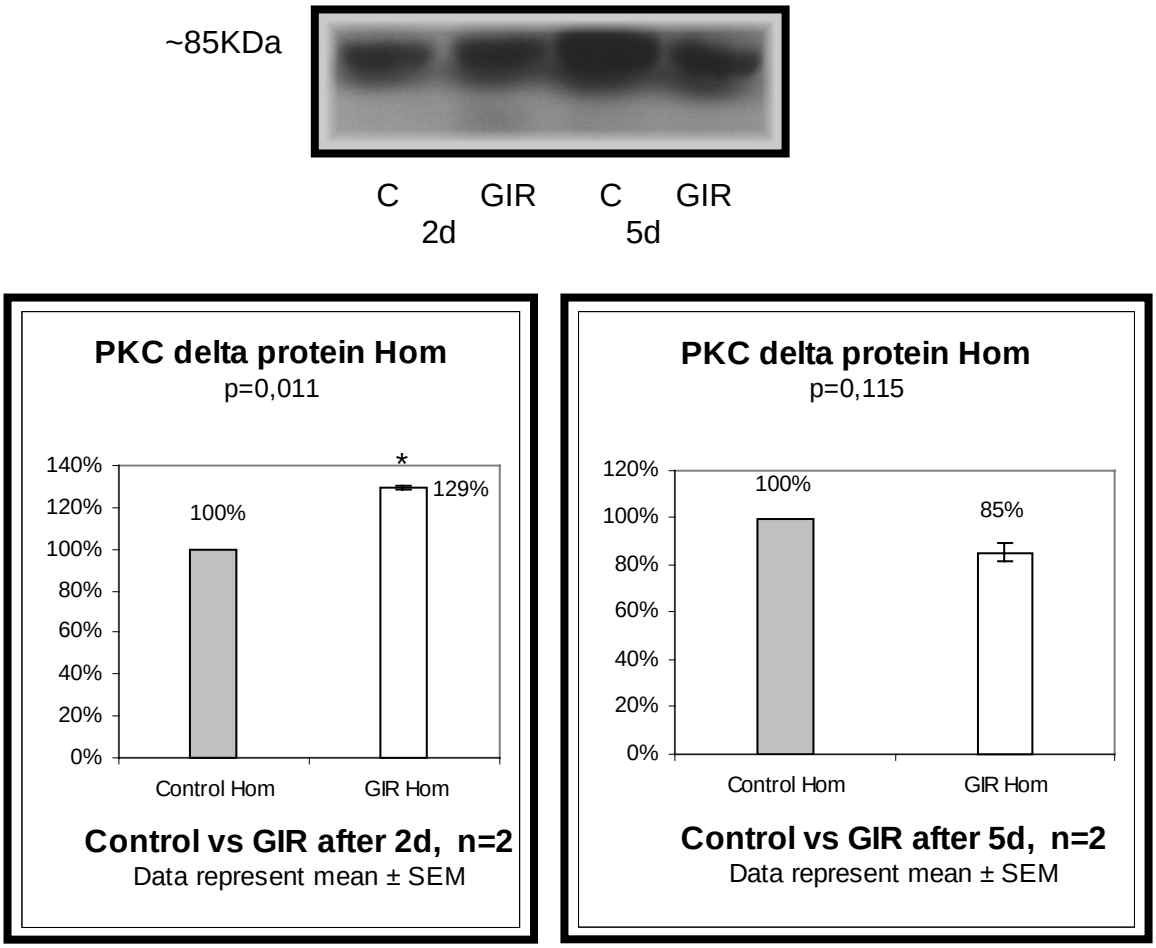

Figure 4.6.18 Representative Western-Blot of PKCδ in mixed hind limb muscle homogenate and results of scanning densitometry.

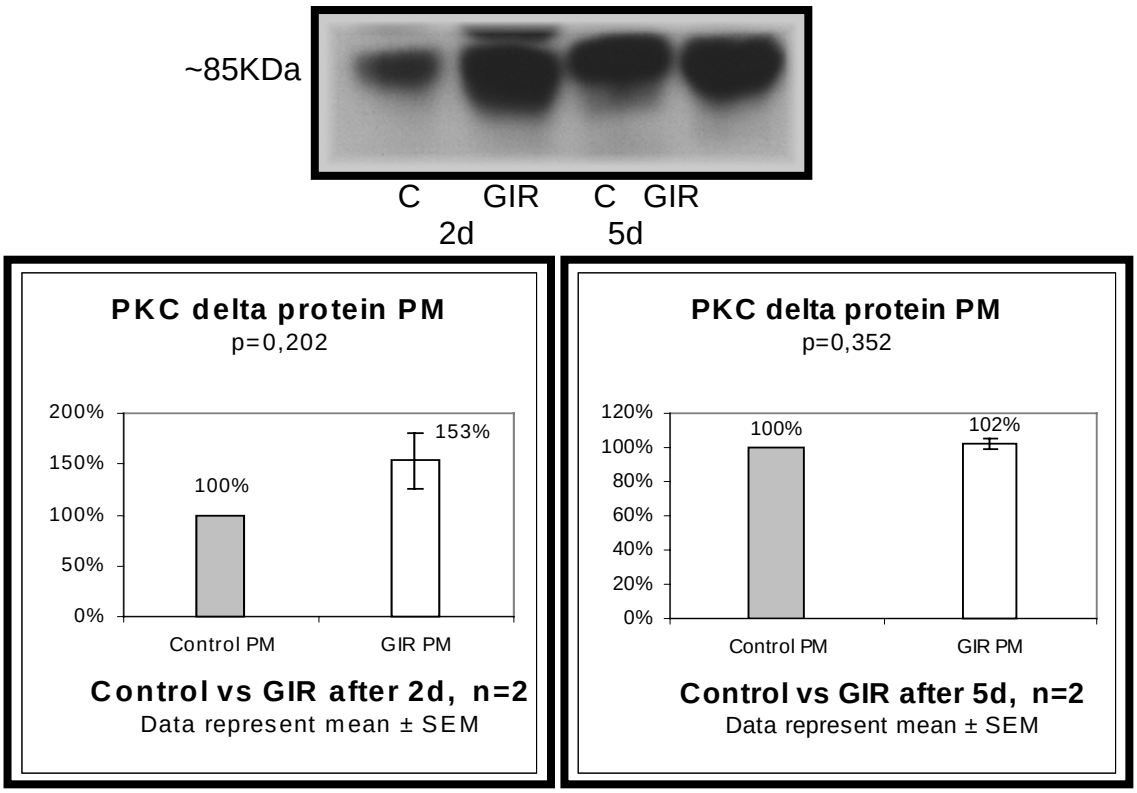

Figure 4.6.19 Representative Western-Blot of PKCδ in total membrane fraction of mixed hind limb muscle and results of scanning densitometry.

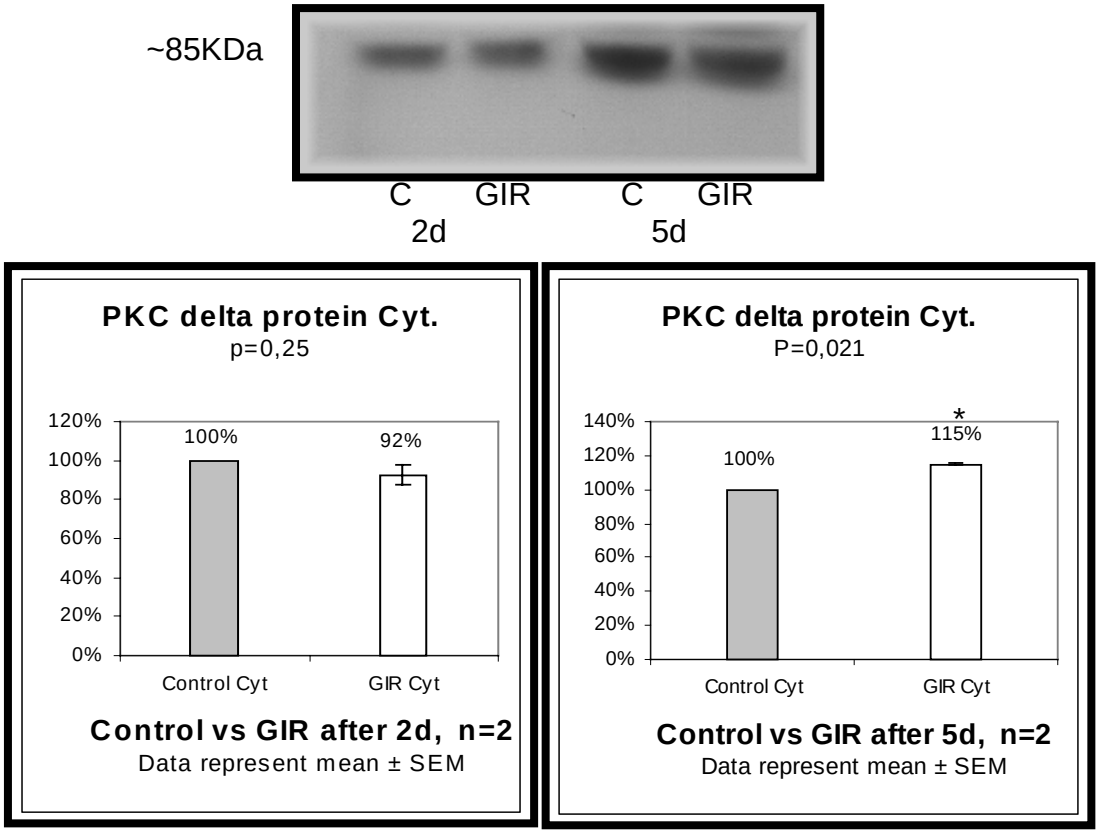

Figure 4.6.20 Representative Western-Blot of PKCδ in cytosolic fraction of mixed hind limb muscle and results of scanning densitometry.

No significant translocation from the cytosolic fraction to the plasma membrane fraction was seen after 2d, nor after 5d.

B.2.2 Effects of Glucose Infusion on Protein Kinase C Isoform δ mRNA-Expression

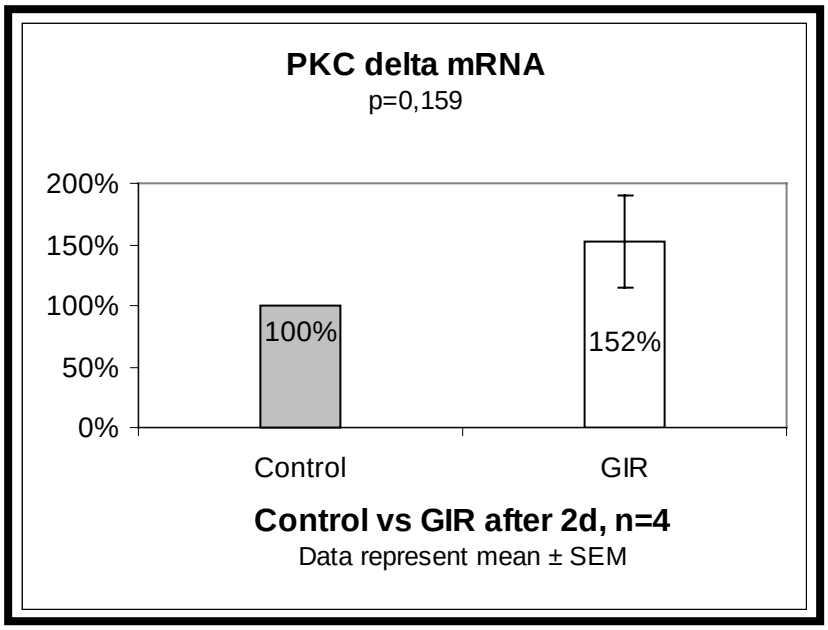

Figure 4.6.21 mRNA-expression of PKC δ after 2d of glucose infusion.

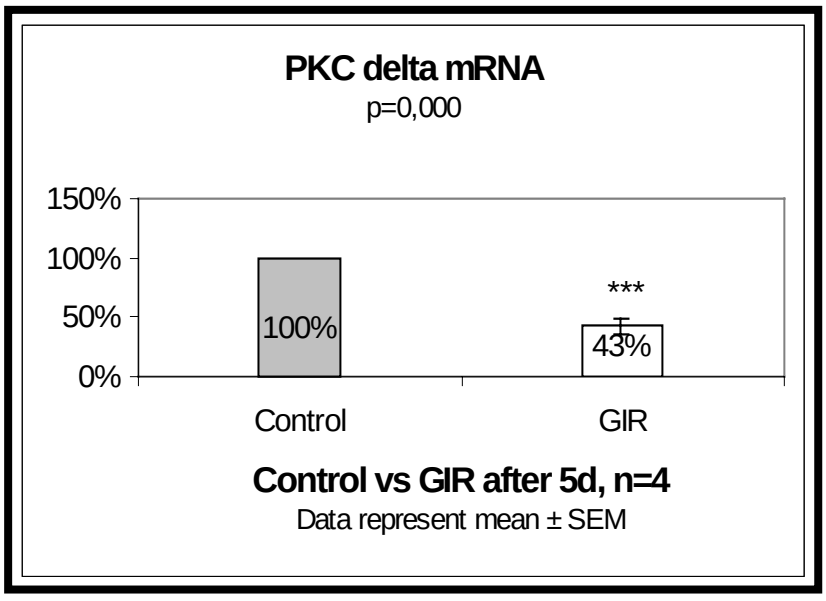

Figure 4.6.22 mRNA-expression of PKCδ after 5d of glucose infusion.

mRNA-expression did not significantly change after 2d of infusion and decreased below normal levels after 5d of infusion.

B.3 Effects of Glucose Infusion on Protein Kinase C Isoform ε Expression (PKCε)

PKCε was not detectable by Western blotting at 100µg/Lane.
The following results are restricted to mRNA-expression.

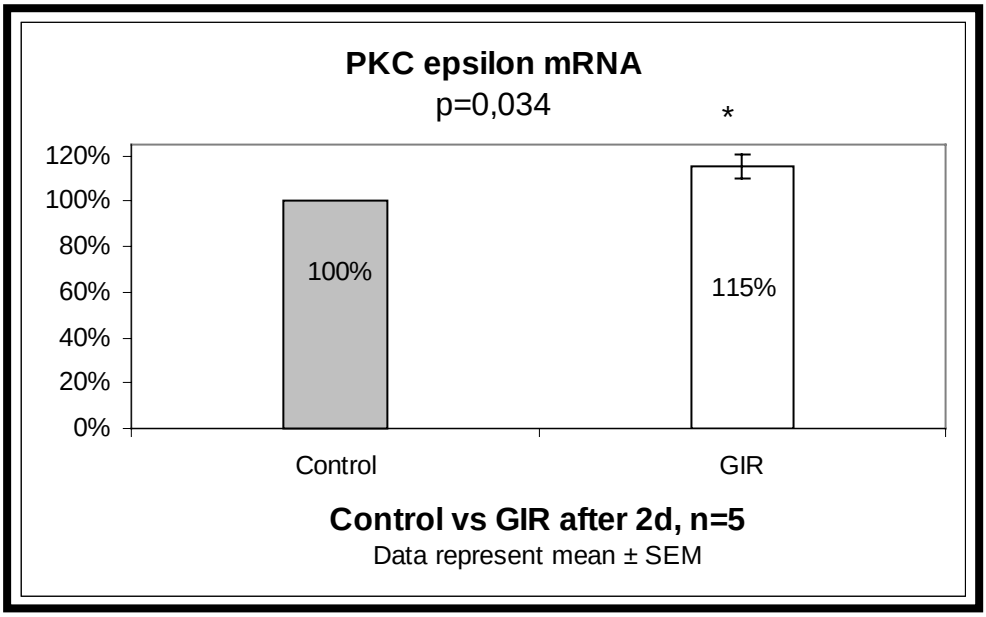

Figure 4.6.23 mRNA-expression of PKC ε after 2d of glucose infusion.

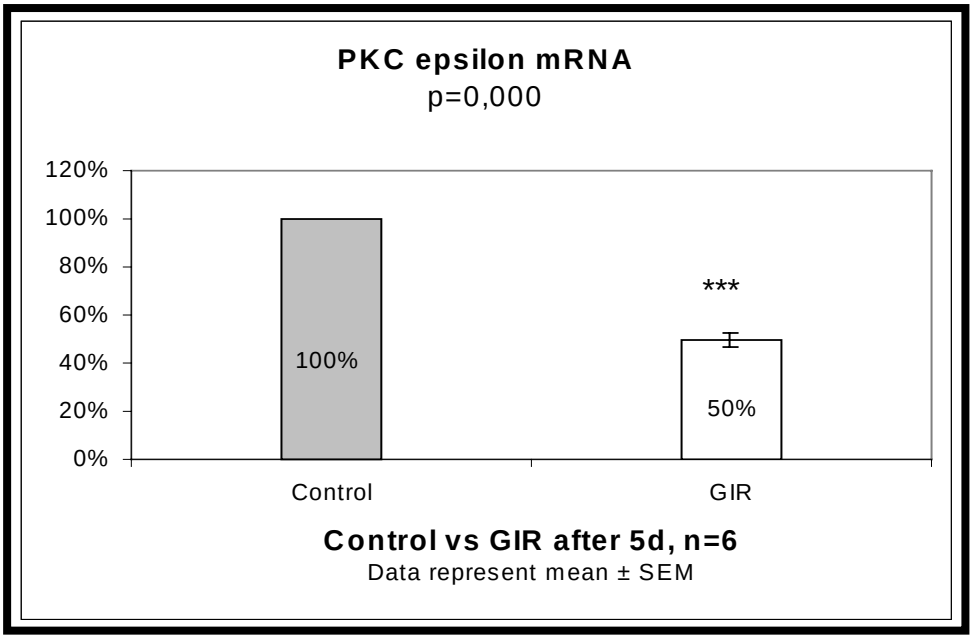

Figure 4.6.24 mRNA-expression of PKC ε after 5d of glucose infusion.

mRNA-expression increased significantly after 2d of infusion and was diminished significantly after 5d of infusion.

C. Atypical PKC Isoforms

PKC ζ, λ were investigated.

C.1.1 Effects of Glucose Infusion on Protein Kinase C Isoform ζ Expression and Translocation (PKCζ)

Protein expression of PKCζ was significantly increased after 2d and decreased significantly after 5d.

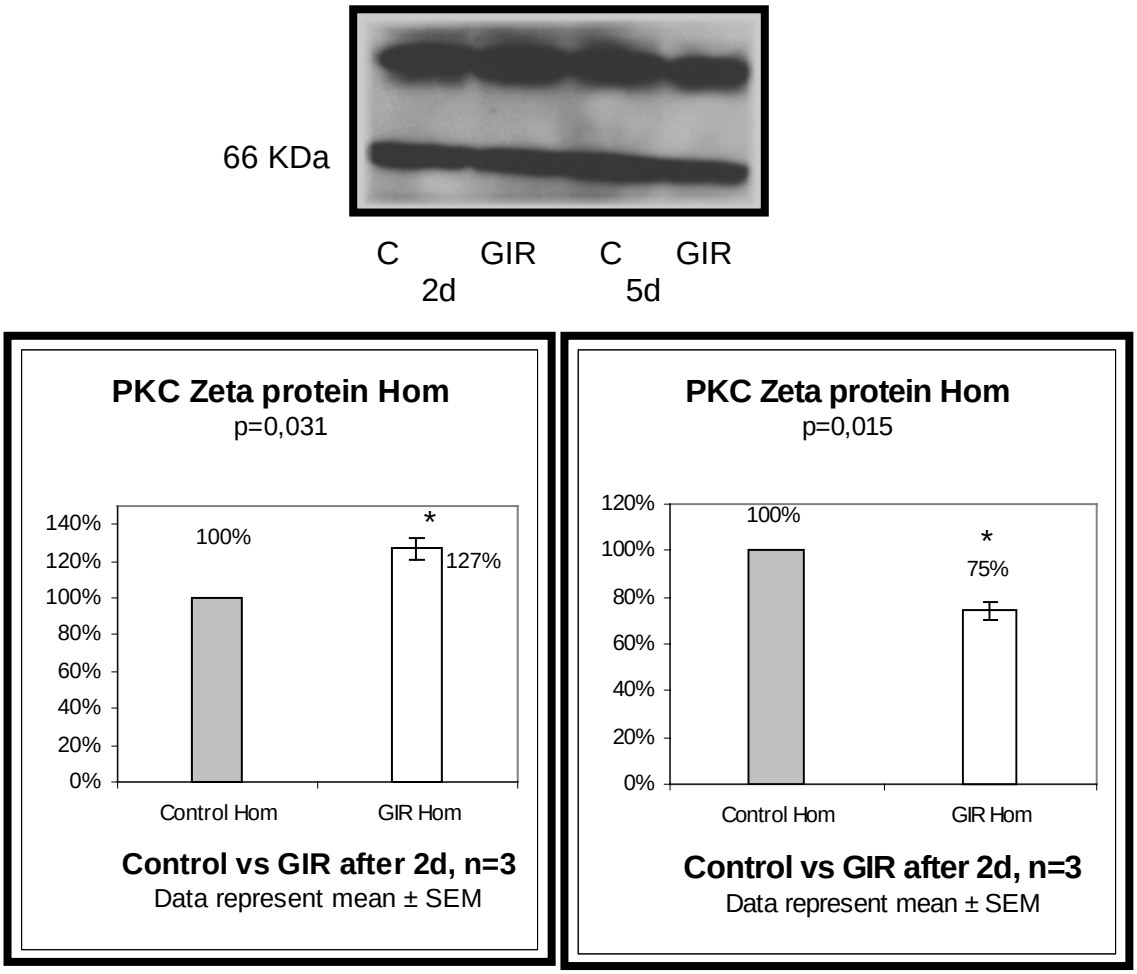

Figure 4.6.25 Representative Western-Blot of PKC ζ in mixed hind limb muscle homogenate and results of scanning densitometry.

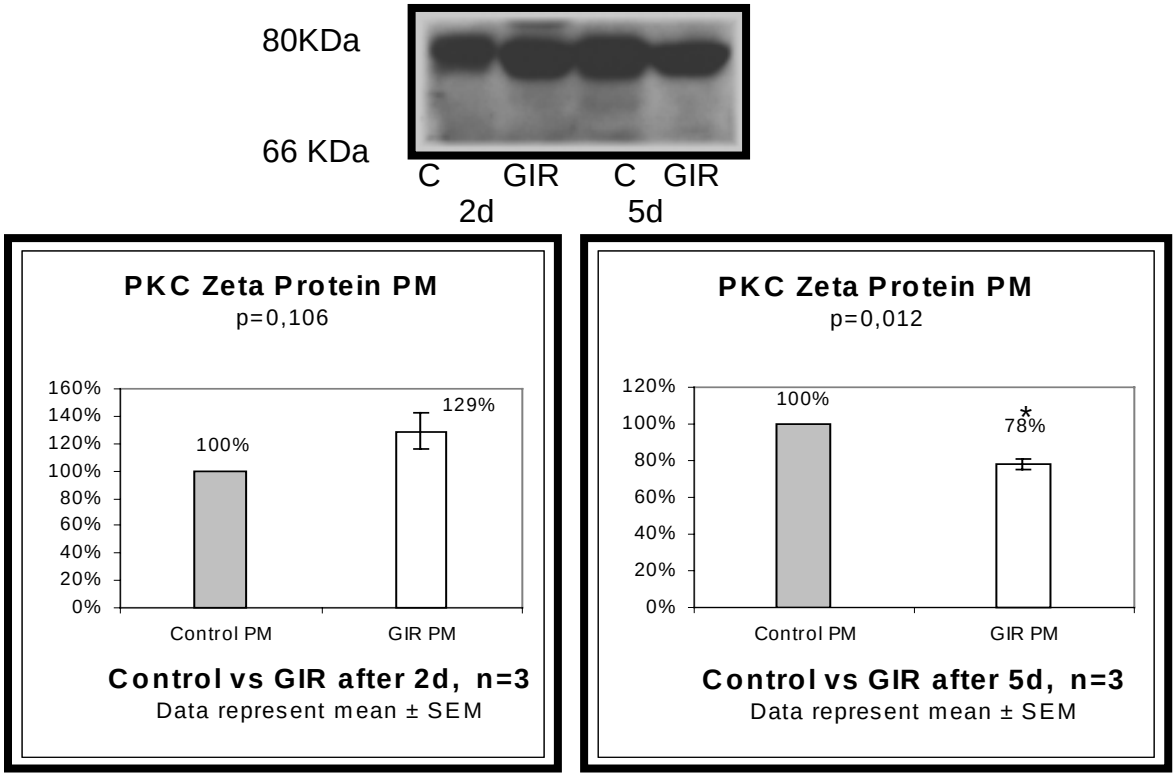

Figure 4.6.26 Representative Western-Blot of PKCζ in total membrane fraction of mixed hind limb muscle and results of scanning densitometry.

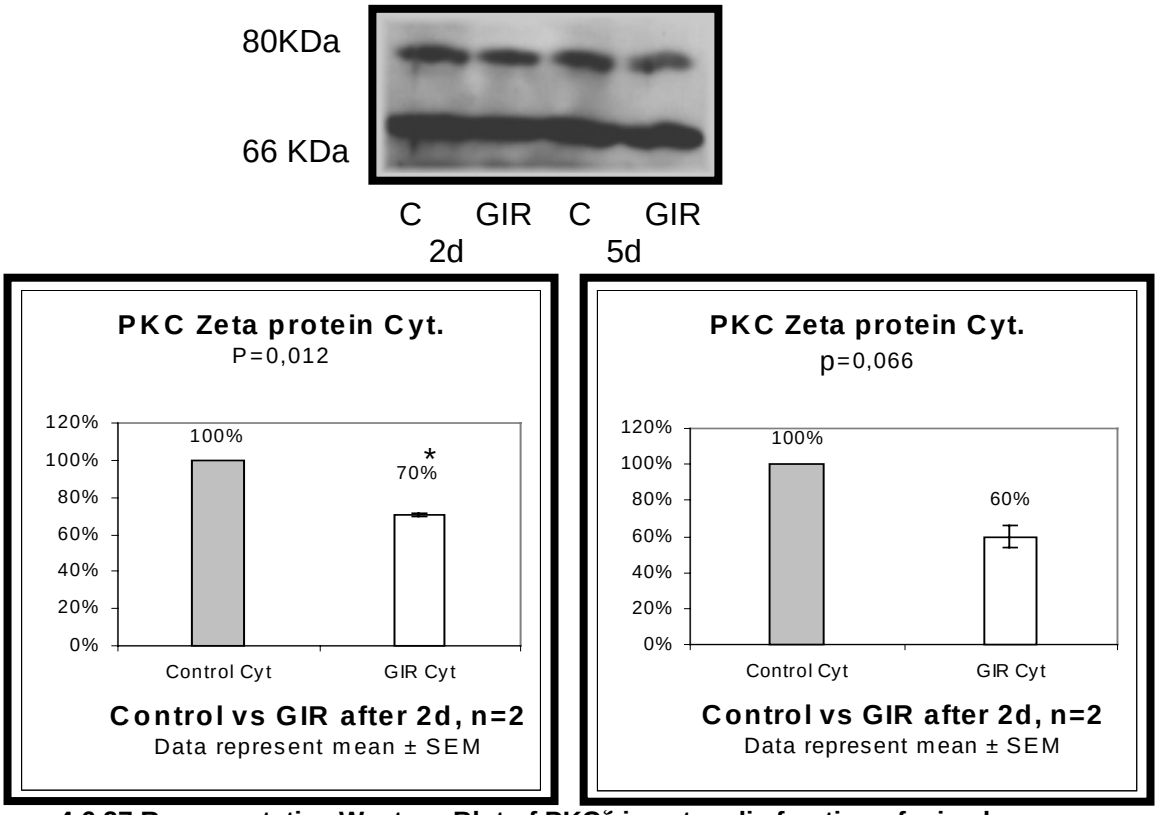

Figure 4.6.27 Representative Western-Blot of PKCζ in cytosolic fraction of mixed hind limb muscle and results of scanning densitometry.

No significant translocation from cytosolic fraction to plasma membrane fraction was seen after 2d, nor after 5d.

C.1.2 Effects of Glucose Infusion on Protein Kinase C Isoform ζ mRNA-Expression (PKCζ)

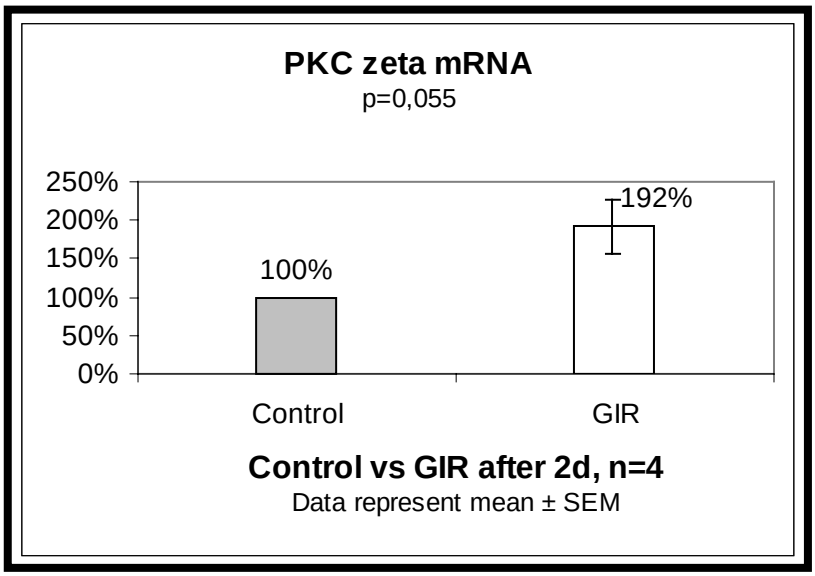

Figure 4.6.28 mRNA-expression of PKCζ after 2d of glucose infusion.

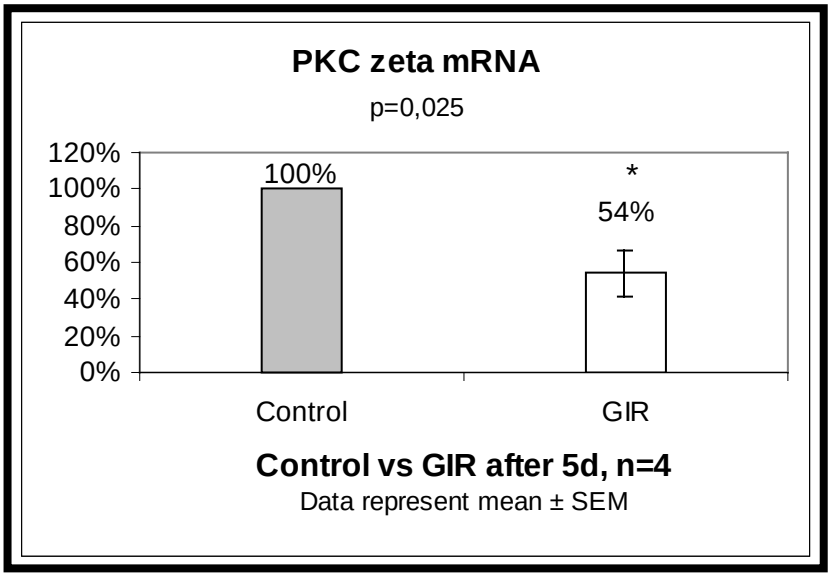

Figure 4.6.29 mRNA-expression of PKCζ after 5d of glucose infusion.

A significant decrease after 5d of infusion can be reported.

C.2 Effects of Glucose Infusion on Protein Kinase C Isoform λ Expression (PKCλ)

PKCλ was not detectable by Western-Blotting at 100µg/Lane.
The following results are restricted to mRNA-expression.

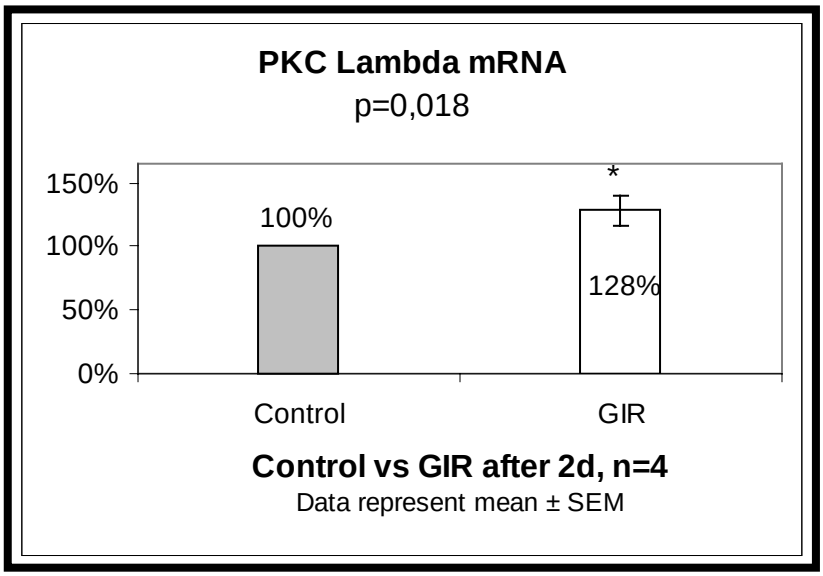

Figure 4.6.30 mRNA-expression of PKCλ after 2d of glucose infusion.

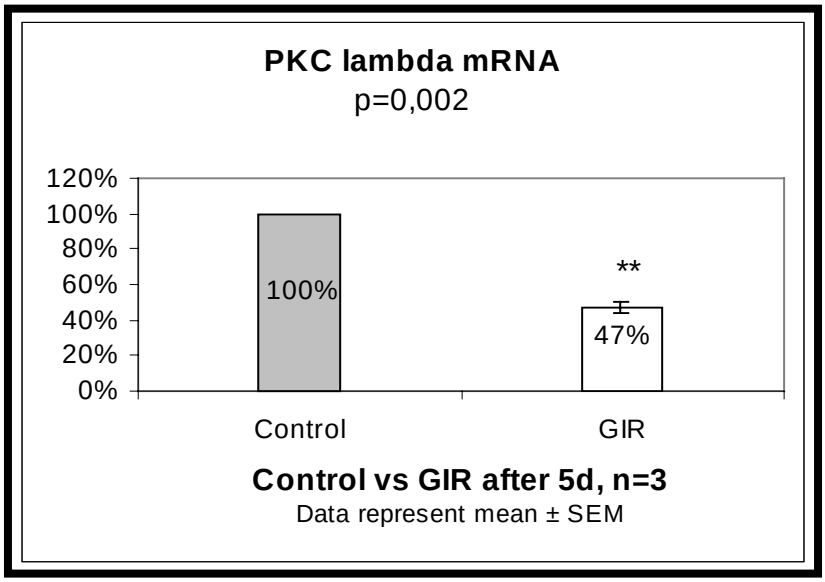

Figure 4.6.31 mRNA-expression of PKCλ after 5d of glucose infusion.

mRNA-expression was increased after 2d of infusion and decreased significantly after 5d of infusion.

4.7 Effects of Glucose Infusion on Glutamine:Fructose-6-phosphate- Amidotransferase (GFAT)

4.7.1 Protein Expression in Crude Homogenate

The effect of glucose infusion on the protein expression of GFAT in crude homogenate of mixed hind limb muscle was investigated. The protein expression was highly increased after 2d as well as after 5d of glucose infusion.

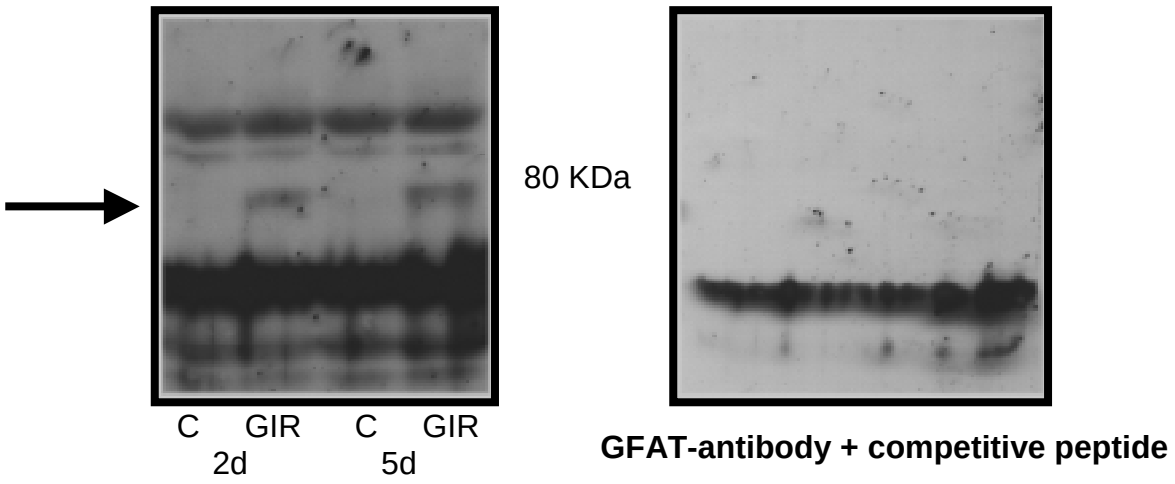

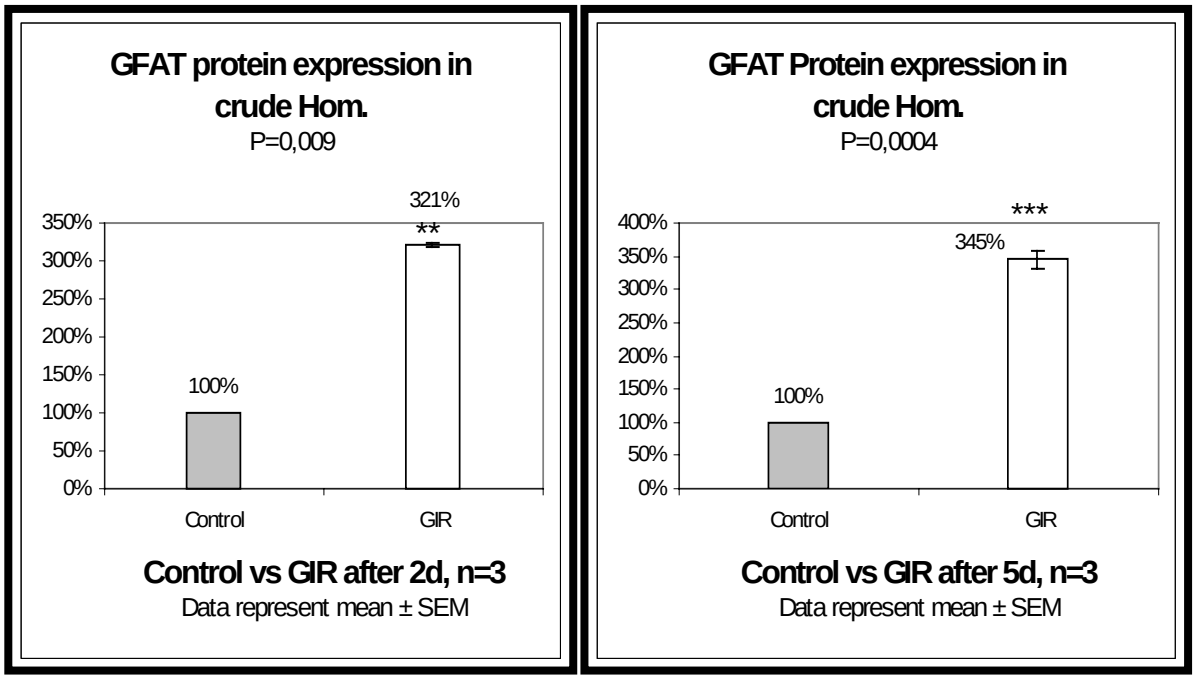

Figure 4.7.1 Representative Western-Blot of GFAT in mixed hind limb muscle, specificity proof of the antibody and results of scanning densitomery.

4.7.2 Effects of Glucose Infusion on GFAT mRNA-Expression

The mRNA-expression increased after 2d of infusion and decreased after 5d of glucose infusion.

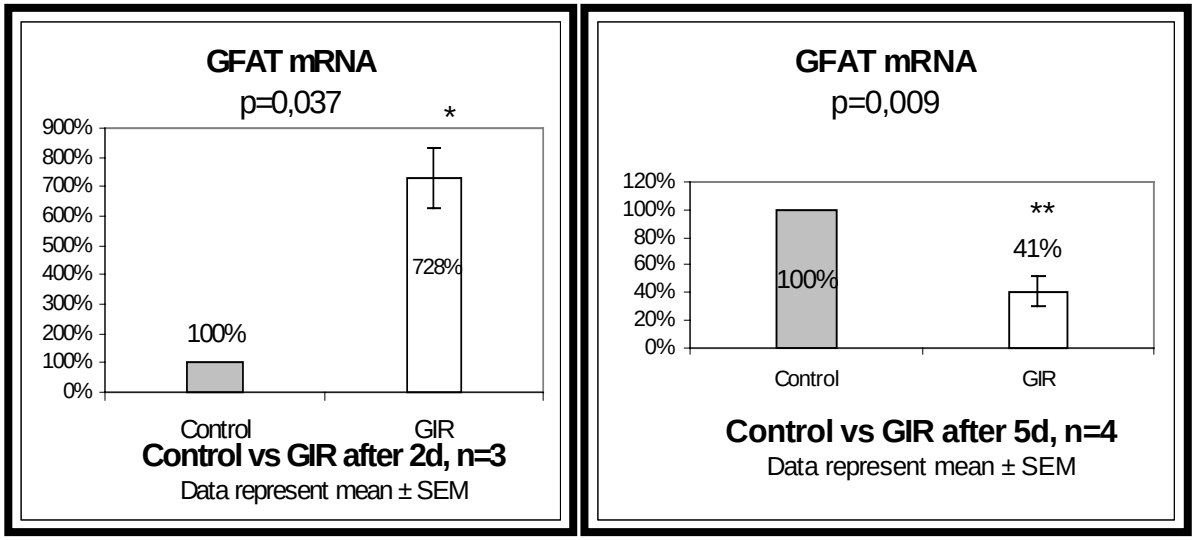

Figure 4.7.2 GFAT mRNA-expression after 2d and after 5d of infusion.

4.7.3 DNA Sequencing of GFAT from Rat Skeletal Muscle

DNA sequencing of PCR-product of GFAT was performed. Sequence is delineated below:

5´-TCTGATGTGTGATGACAGAATCTCCATGCNAGAAAGACGCAAAGAGATCATGCTGGGACTGAAGCGACTGCC
GGACTTGATTAAGGAAGTGTTGAGCATGGATGATGAAATTCAGAAGCTGGCTGACAGAGCTTTACCACCAGA
AGTCGGTCCTGATAATGGGCCGAGGCTATCATTATGCTACATGTCTNGAAGGAGCCCTGAAAATCNNGGAGA
TTACATATATACCACNCACCCCTNCCCCNCCTCNAAAANNNNACACNCCCNTTTTTNTNCNANCCCCNNANC
CNACAACCNNCCCTCCCAATNNANTNTNCNCTCCCCCNNCCNCNNNTACCCANTCNNCANTCACCANNNCTN
CGACCNCCACCNCCNCNCACANTNCNAACTCNCNCCTCCTNNCNACCNCTTCACCTNCTACGCCCTCNCTCC
CGNTANNNNCNN**-3´**

4.8 Effects of Glucose Infusion on Tissue Concentrations of UDP-Glc, UDP-Gal, UDP-GlcNAc and UDP-GalNAc by Capillary Zone Electrophoresis

The tissue concentrations of the four UDP-sugars were investigated.
Tissue concentrations of UDP-sugars increased after 2d, only UDP-GlcNAc was decreased.

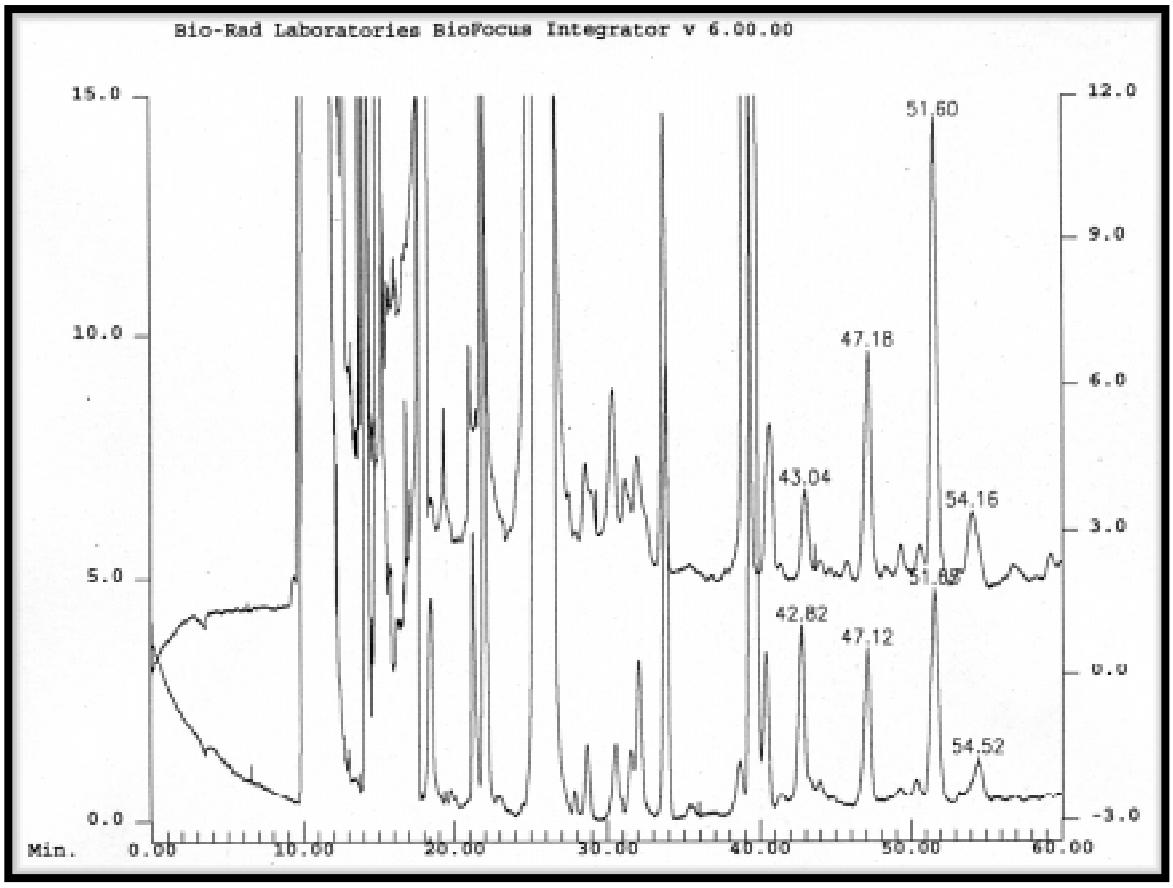

Figure 4.8.1 Electropherograms of separated UDP-sugars from extracts of mixed hind limb muscle.
The upper electropherogram was obtained from GIR after 2d of glucose infusion.
The lower electropherogram was obtained from SIR after 2d of infusion (control).
Separation profile: UDP-GlcNAc, followed by UDP-GalNAc, UDP-Glc and UDP-Gal, respectively.

UDP-sugar	UDP-GlcNAc		UDP-Glc		UDP-GalNAc		UDP-Gal	
	AUC	conc.	AUC	conc.	AUC	conc.	AUC	conc.
Control	603.38	**26,01**	529.77	**16,72**	842.53	**33,75**	245.7	**5,93**
GIR	308.84	**13,29**	824.38	**25,97**	1.480.2	**59,02**	429.6	**10,01**

Table 4.8.2 Integration of the labeled peaks in figure 4.8.1 and calculated corresponding concentrations (pmol/mg).

UDP-sugars tissue concentrations also increased after 5d of infusion. Again only the tissue concentration of UDP-GlcNAc was decreased.

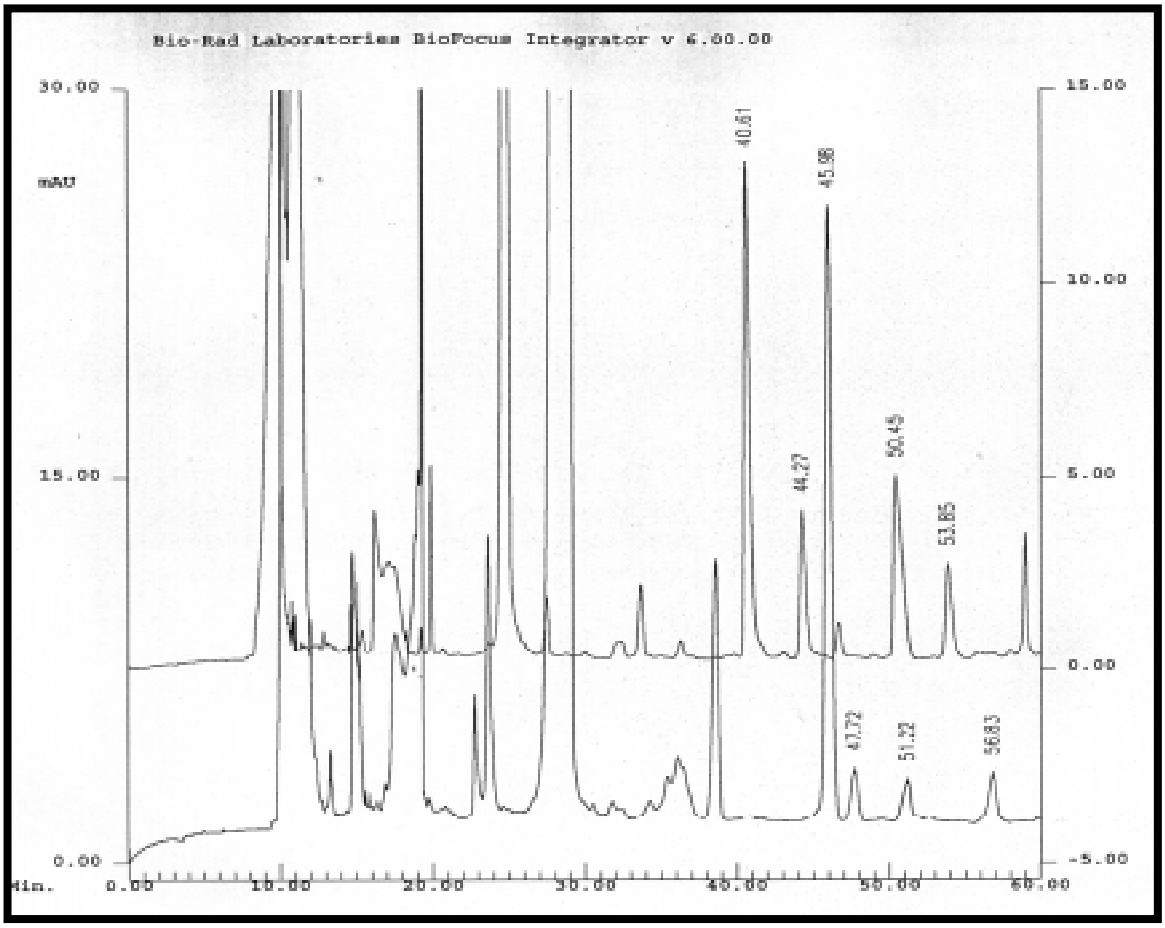

Figure 4.8.3 Electropherograms of separated UDP-sugars from extracts of mixed hind limb muscle.
The upper electropherogram was obtained from GIR after 5d of glucose infusion.
The lower electropherogram was obtained from SIR after 5d of infusion (control).
Separation profile: UDP-GlcNAc, followed by UDP-GalNAc, UDP-Glc and UDP-Gal, respectively.

UDP-sugar	UDP-GlcNAc		UDP-Glc		UDP-GalNAc		UDP-Gal	
	AUC	conc.	AUC	conc.	AUC	conc.	AUC	conc.
Control	7.490	**323,43**	694.07	**21,88**	746.02	**29,92**	1.498	**33,69**
GIR	7.001	**302,33**	2.228	**70,05**	3.887.7	**154,45**	1.557	**34,99**

Table 4.8.4 Integration of the labeled peaks in figure 4.8.3 and calculated corresponding concentrations (pmol/mg).

4.9 O-linked N-Acetylglucosamine Modification of Early Post Insulin Receptor Signal Transduction:

To determine whether O-GlcNAc glycosylation may obscure phosphorylation sites and act as a mediator of signaling, total extracts of SIRs and GIRs were separated on SDS-PAGE and incubated with an anti-O-linked GlcNAc Glycoproteins antibody.
The antibody recognized several bands representing O-GlcNAc glycoproteins.
The "O-GlcNAc glycosylation state" was monitored and no changes were seen compared to control animals.

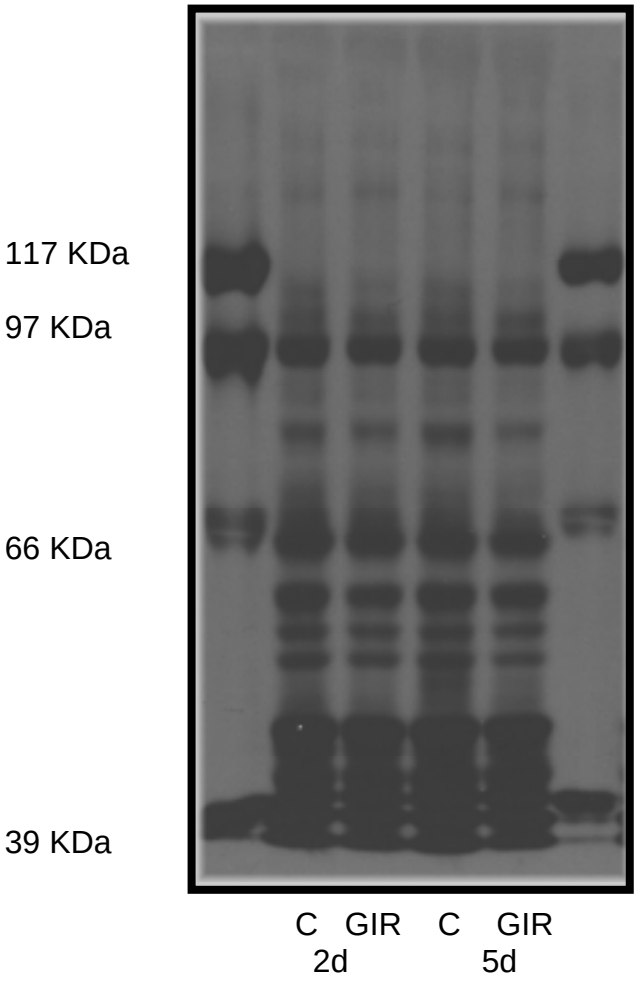

Figure 4.9.1 Representative Western-Blot of n=3 different experiments of O-GlcNAc glycosylation in mixed hind limb muscle of the rat after 2d and 5d of glucose infusion.

4.10 Effects of Glucose Infusion on Glucose Transporter Isoform 4 (GLUT4)

The effect of glucose infusion on total expression of GLUT4 was investigated.
The translocation of GLUT4 was then studied using subcellular fractionation of mixed hind limb muscle.

4.10.1 Effects of Glucose Infusion on Expression of GLUT4 in Crude Homogenate of Skeletal Muscle

The total expression of GLUT4 strongly increased after 2d of infusion and was slightly increased after 5d of infusion (158% vs. 111%).

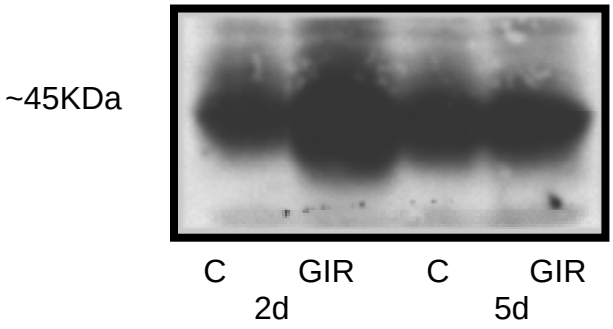

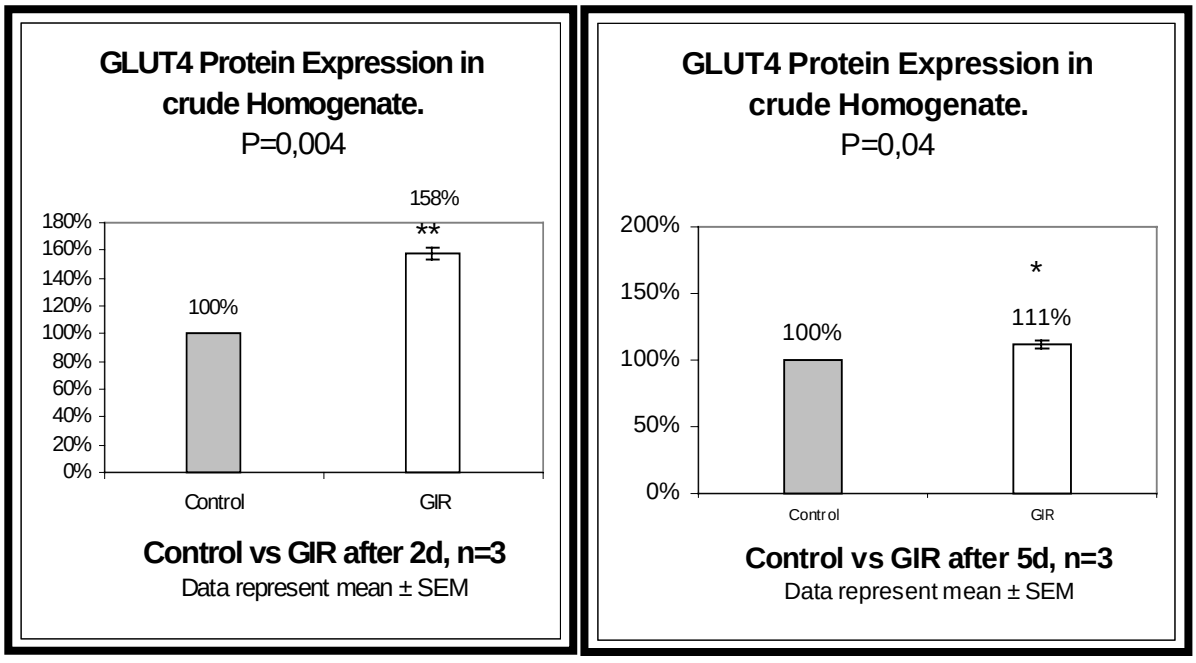

Figure 4.10.1 Representative Western-Blot of GLUT4 in crude homogenate of mixed hind limb muscle and results of scanning densitometry.

4.10.2 Effects of Glucose Infusion on the Translocation of the Glucose Transporter Isoform 4 (GLUT4) to the Plasma Membrane PM

A strong Translocation of GLUT4 to different plasma membrane regions as well as to the transversal tubules region after 2d of glucose infusion can be clearly shown:

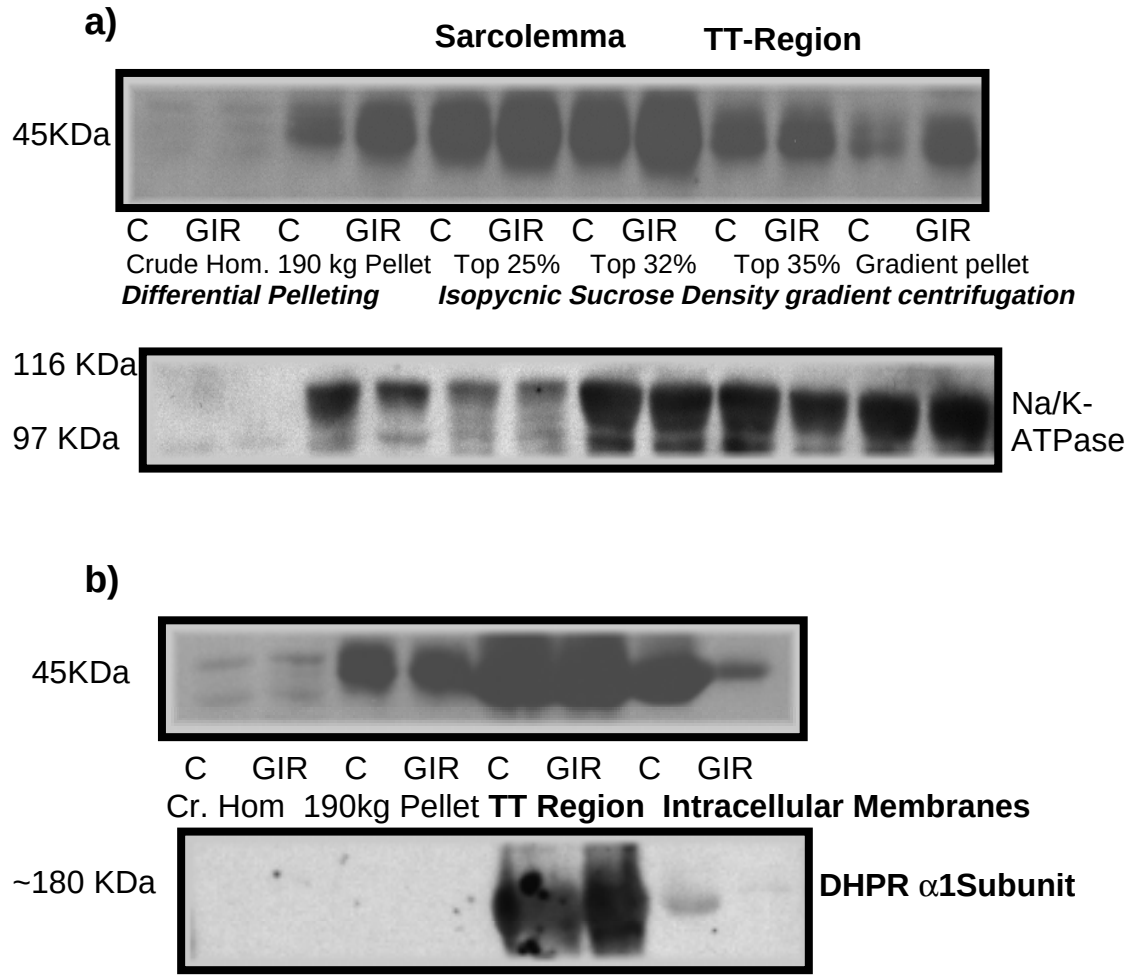

Figure 4.10.2. a) Representative Western-Blot of subcellular fractionation of n=3 different animals after 2d of glucose infusion: total plasma membranes were first collected using differential centrifugation and the PM pellet was loaded on the top of a sucrose step gradient. Bands from the interfaces were collected and similar amounts of protein were separated on 7.5% SDS-PAGE and blotted with anti-GLUT4 antibodies.

b) refers to the low spin pellet, which was treated with LiBr and further centrifuged to yield a fraction enriched in TT and an intracellular fraction enriched in glucose transporter.

Na/K-ATPase α1 subunit and DHPR α1 subunit were used as enzyme markers to characterize fractions yielded during subcellular centrifugation. 190 kg pellet: 190000 Xg pellet referring to total plasma membrane pellet.

Translocation of GLUT4 to plasma membrane region can be also shown for glucose infused rats (GIR) after 5d.

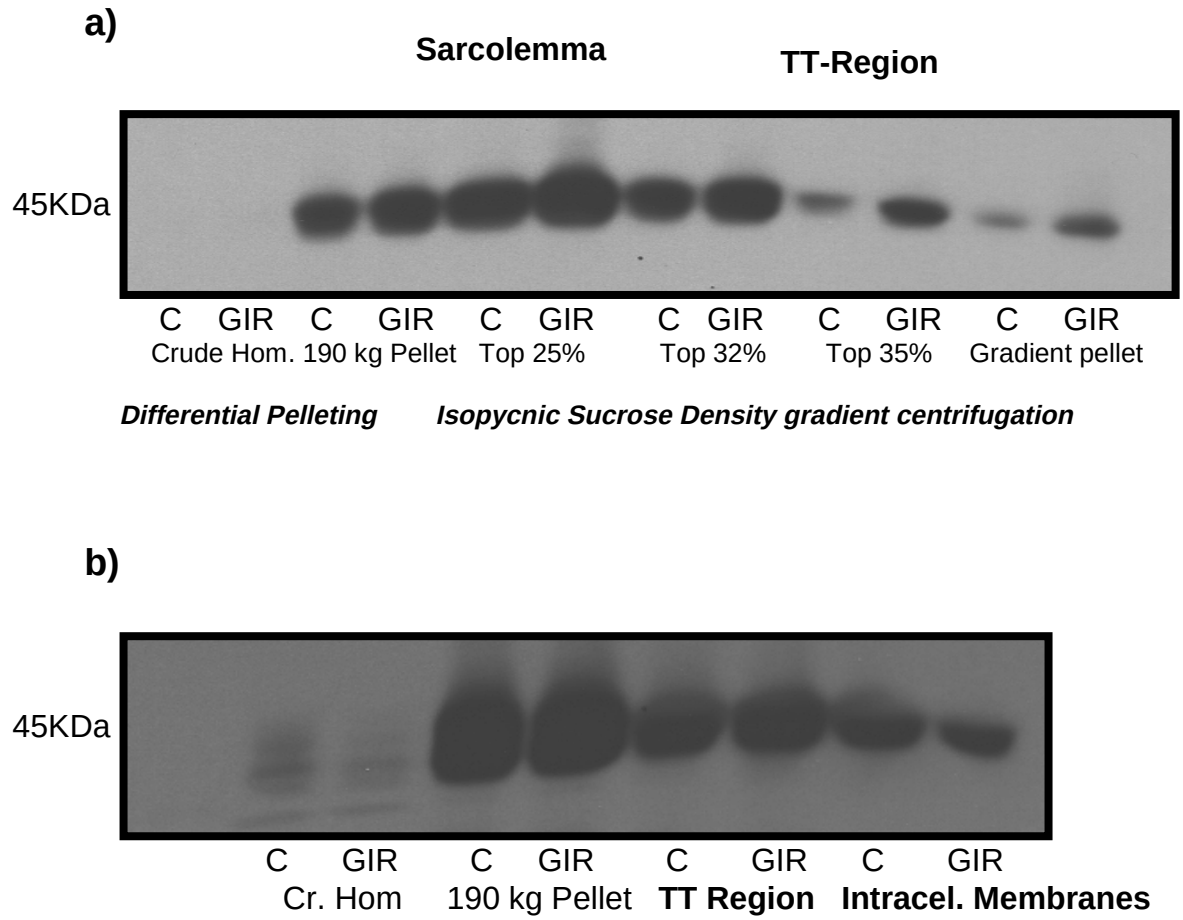

Figure 4.10.3. a) Representative Western-Blot of subcellular fractionation of n=3 different animals after 5d of glucose infusion: total plasma membranes were first collected using differential centrifugation and the PM pellet was loaded on the top of a sucrose step gradient. Bands from the interfaces were collected and similar amounts of protein were separated on 7.5% SDS-PAGE and blotted with anti-GLUT4 antibodies.

b) refers to the low spin pellet, which was treated with LiBr and further centrifuged to yield a fraction enriched in TT and an intracellular fraction enriched in glucose transporter.

4.11 Effects of Glucose Infusion on Glucose Transporter Isoform 1 (GLUT1)

The effect of glucose infusion on total expression of GLUT1 was investigated.
The translocation of GLUT1 was then studied using subcellular fractionation of mixed hind limb muscle.

4.11.1 Effects of Glucose Infusion on Expression of GLUT1 in Crude Homogenate of Skeletal Muscle

No changes in the total protein expression of GLUT1 were seen.

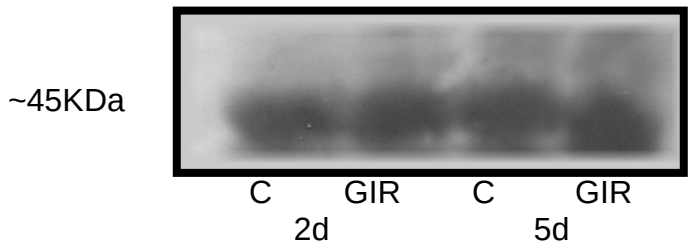

Figure 4.11.1 Representative Western-Blot of GLUT1 in crude homogenate of mixed hind limb muscle. N=3 blots were performed and resulted in no changes in expression at protein level.

4.11.2 Effects of Glucose Infusion on mRNA-Expression of GLUT1

The mRNA-expression decreased after 2d of infusion and was then restored to normal levels after 5d of infusion.

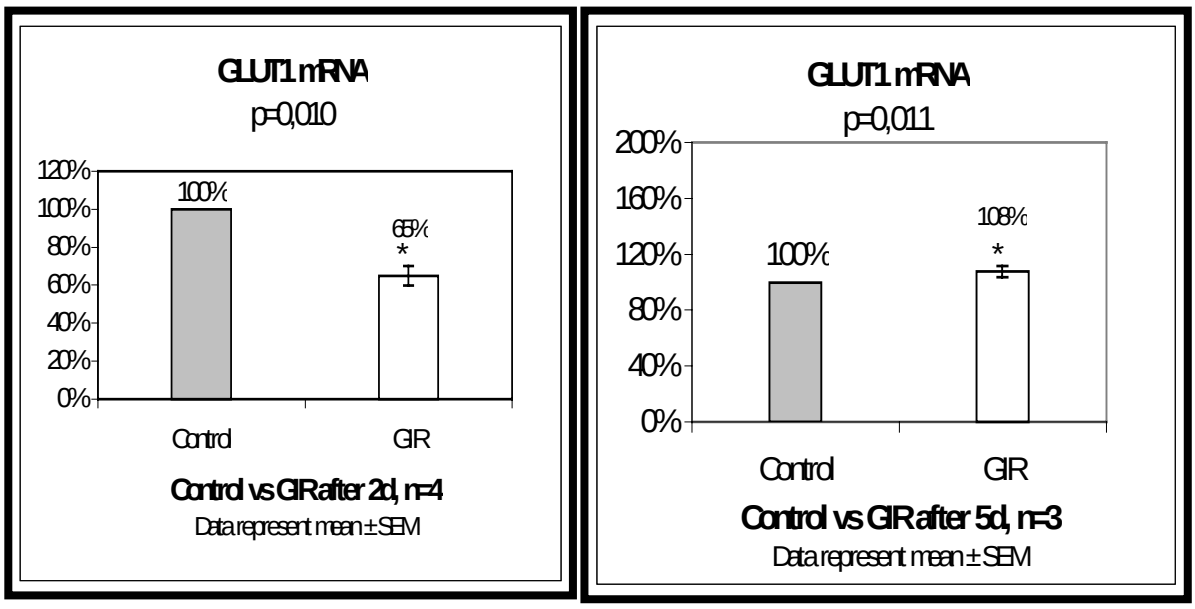

Figure 4.11.2 mRNA-expression of GLUT1 in mixed hind limb muscle after 2d and 5d of glucose infusion.

4.11.3 Effects of Glucose Infusion on the Translocation of the Glucose Transporter Isoform 1 (GLUT1) to the Plasma Membrane PM

In two cases (figure 4.10.3 a & b) translocation of GLUT1 to plasma membrane can be shown, whereas in a third subcellular fractionation (figure 4.1.3 c) no translocation occurred:

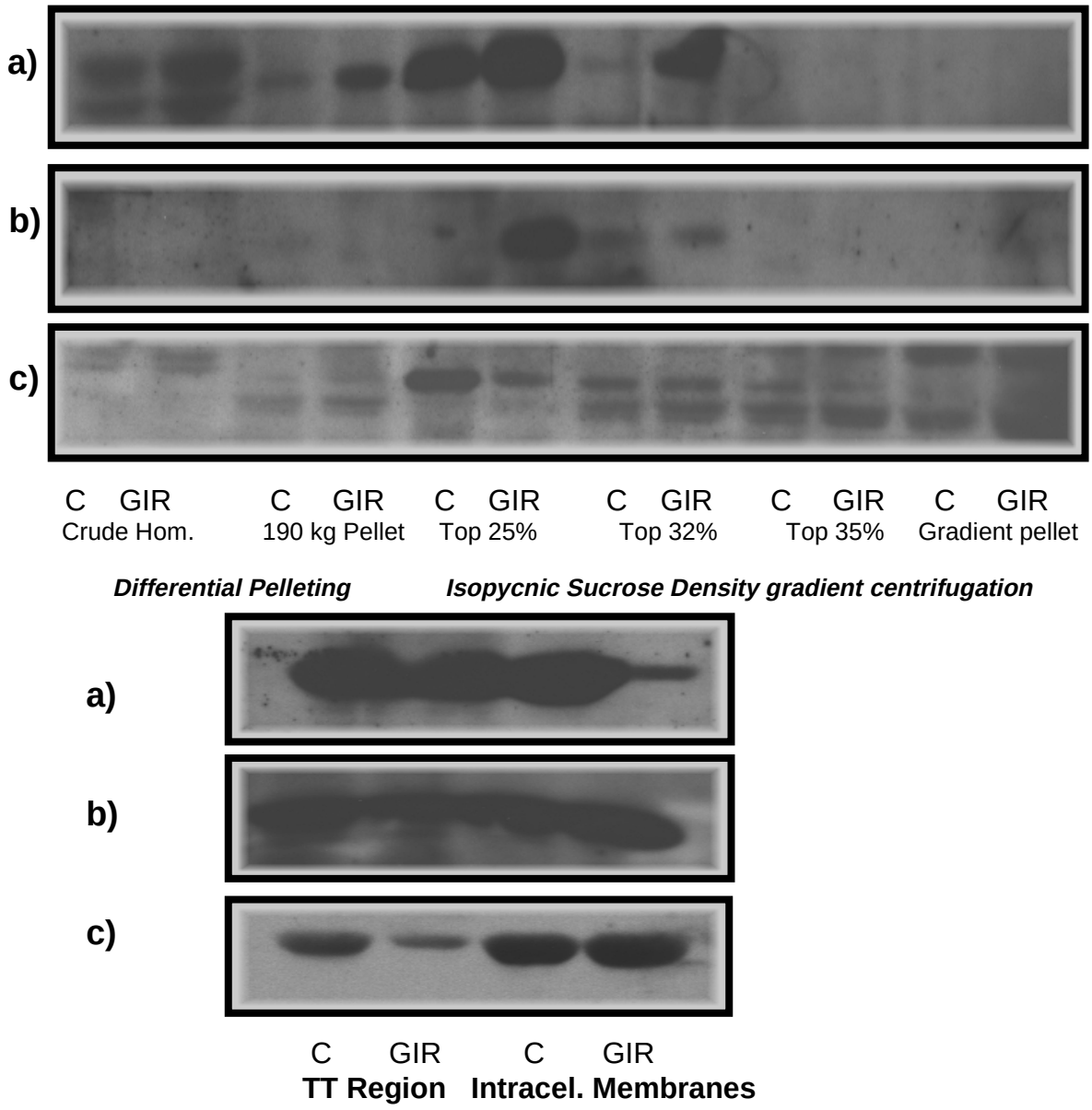

Figure 4.11.3 Western-Blot of subcellular fractionation of n=3 different animals after 2d of glucose infusion: total plasma membranes were first collected using differential centrifugation and the PM pellet was loaded on the top of a sucrose step gradient. Bands from the interfaces were collected and similar amounts of protein were separated on 7.5% SDS-PAGE and blotted with anti-GLUT1 antibodies.
The low spin pellet was treated with LiBr and further centrifuged to yield a fraction enriched in TT and an intracellular fraction enriched in glucose transporter.

a, b and c refer to different subcellular centrifugations, each from two different rats.

No translocation of GLUT1 to the plasma membrane can be shown after 5d of infusion.

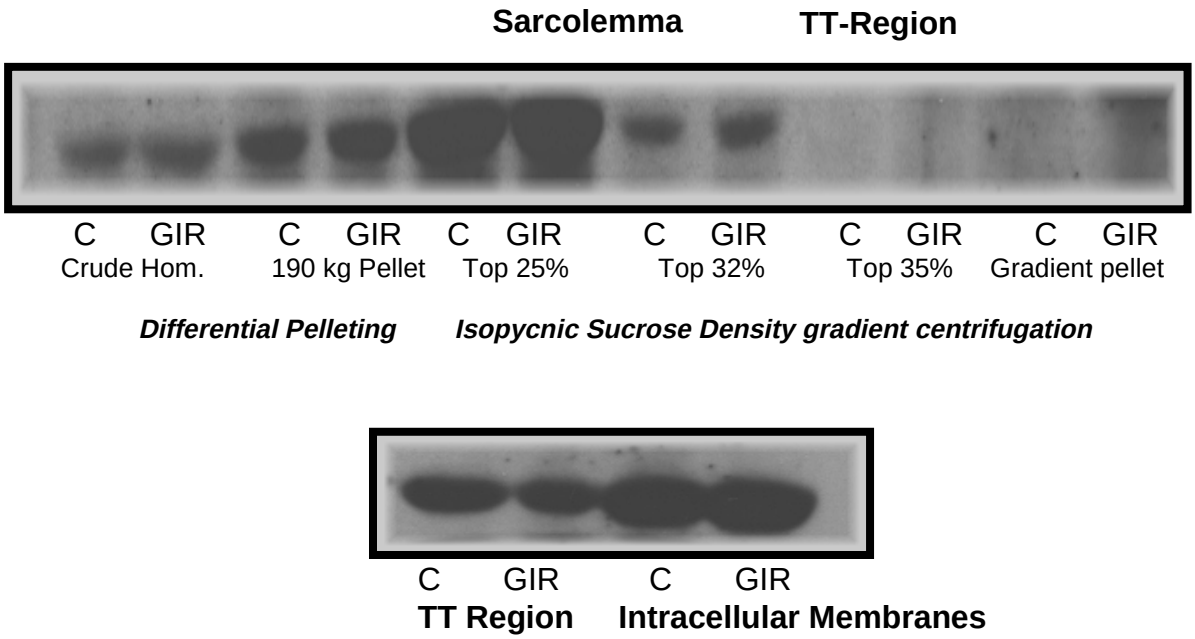

Figure 4.11.4 Representative Western-Blot of subcellular fractionation of n=3 different animals after 5d of glucose infusion: total plasma membranes were first collected using differential centrifugation and the PM pellet was loaded on the top of a sucrose step gradient. Bands from the interfaces were collected and similar amounts of protein were separated on 7.5% SDS-PAGE and blotted with anti-GLUT1 antibodies.
The low spin pellet was treated with LiBr and further centrifuged to yield a fraction enriched in TT and an intracellular fraction enriched in glucose transporter.

4.12 Effects of Glucose Infusion on Glycogen Content in Rat Skeletal Muscle

The effects of glucose infusion on glycogen content in rat skeletal muscle was investigated.
Glycogen content evidently increased after 2d of glucose infusion and was increased at a lesser extent after 5d of glucose infusion.

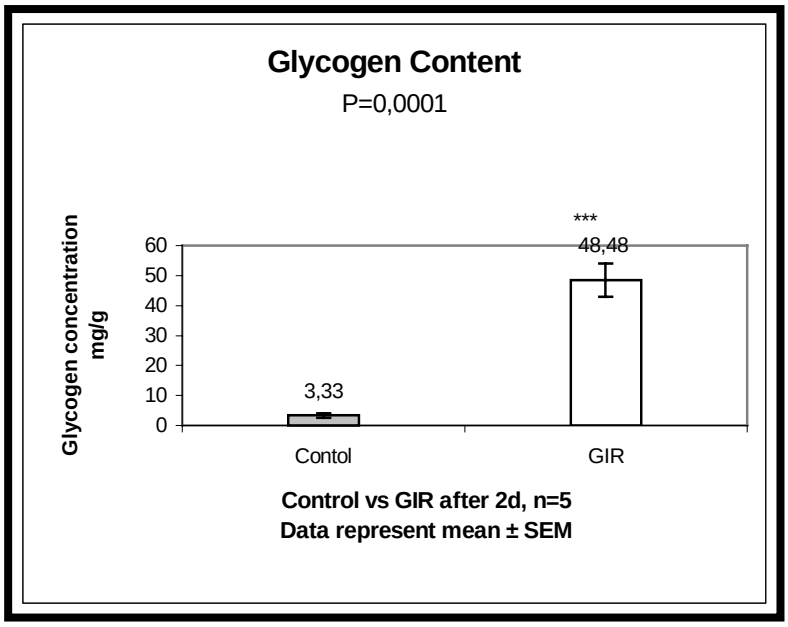

Figure 4.12.1 Glycogen content in rat skeletal muscle after 2d of glucose infusion.

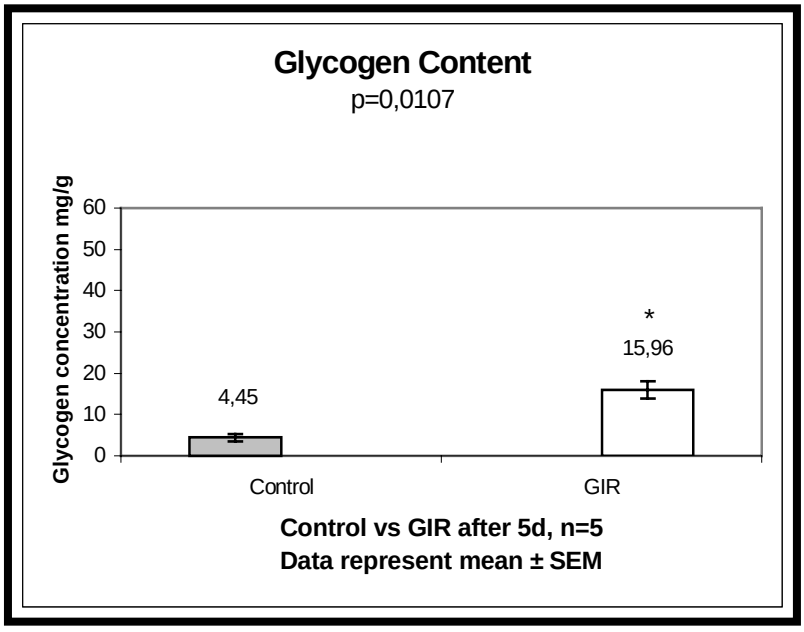

Figure 4.12.2 Glycogen content in rat skeletal muscle after 5d of glucose infusion.

5 DISCUSSION

5.1 Experimental Design

Animal models represent a powerful means for the investigation of a metabolic disease like diabetes. GLUT1 expression is increased in all cell culture lines (Gould & Holman 1993), thus limiting the ability of cell culture experiments to represent a real life situation as encountered in tissues. In addition, paracrine hormonal effects and other influences, e.g. endocrine, nervous and hemodynamic effects can not be considered in cell culture models.
Numerous of animal models have been described for type 1 diabetes (IDDM) (Cheta 1998), (Mathe 1995) and for type 2 diabetes (NIDDM) (Shafrir 1992), (Mathe 1995).
The diversity of pathogenic factors used to induce diabetes in these animals (Chattopadhyay, Ramanathan, et al. 1997) often does not correspond to human diabetes and thus restricts the validity of conclusions made from these models for man.
Thus, in our experimental design, glucose infusion into normal conscious rats was chosen, which might in addition address the question to whether pathophysiological effects of hyperglycemia per se will be reproducible in nondiabetic animals.

5.2 Effect of Glucose Infusion on Plasma Glucose and Serum Insulin Concentrations

Chronic infusion of saline showed no effect on plasma glucose, nor on serum insulin.
Glucose infusion increased plasma glucose concentrations to peak after 24h. Despite further continuous glucose infusion, plasma glucose levels decreased continuously to reach normoglycemia after 5d. Moreover, normoglycemia was maintained after 7 days of continuous glucose infusion. Serum insulin concentrations followed a similar pattern. Hyperinsulinemia persisted in GIR during the whole infusion period, though.
These findings are in accordance with previous results reported from other groups (Ammon, Bacher, et al. 1998), (Ammon 1997), (Hager, Jochen, et al. 1991), (Leahy, Cooper, et al. 1987), (Laybutt, Thompson, et al. 1997).
Rats were sacrificed after 2d or 5d of infusion, which represent hyperglycemic hyperinsulinemic (2d) and normoglycemic mild hyperinsulinemic (5d) metabolic states, respectively.

5.3 Effect of Glucose Infusion on Glucose Transporter Expression and Translocation

Since glucose excretion in the urine of GIR was only positively monitored on the 2nd day of infusion, whereas no urine glucose was measured on the 5th day of infusion and since GIR significantly gained more body weight than controls, despite of less food consumption, it can be concluded that GIR were able to dispose excessively infused glucose not only by the fashion of glucosuria (urinary excretion).

Since skeletal muscle represents 40% of body weight. 60% of basal glucose uptake and 80% of insulin-stimulated glucose uptake are accounted for by muscle (Yki yärvinen 1993) and since leg muscles are representative for all skeletal muscles and 64% of leg tissue is muscle (Stolwijk & Hardy 1966), rat hind limb muscle was used for our investigations.
If rats are able to dispose of infused glucose by increasing muscle glucose uptake, we would expect alterations in glucose transporter expression and/or their intracellular distribution.
In fact, our findings show that the expression of total cellular GLUT4 was highly increased in GIR at hyperglycemic hyperinsulinemic conditions on the 2nd day of glucose infusion and was still higher than in control rats after 5 days of infusion.
In contrast, total cellular expression of GLUT1 was not changed during the whole infusion period, whereas its messenger RNA-expression was decreased on the 2nd day of glucose infusion in GIR and was restored slightly above normal level as normoglycemia was reached on the 5th day of infusion.
Furthermore, redistribution of GLUT4 to PM and TT regions and concomitant decrease in IM-fraction can be shown in GIR on the 2nd day of glucose infusion Translocation of GLUT1 was less evident. On the 5th day of glucose infusion, translocation can be shown only for GLUT4.
Our findings suggest that glucose infusion increased expression of GLUT4 and translocation of both GLUT1 And GLUT4 to the plasma membrane reflecting a mechanism, by which GIR manage to dispose of infused glucose and decline plasma glucose levels.
In fact, the role of GLUT4 expression on glucose uptake has not been confirmed yet. Sato et al. reported in accordance to our findings increased GLUT4 levels and normal GLUT1 levels in an animal model of NIDDM (Sato, Man, et al. 1997).
Furthermore, Laybutt et al. have shown that whole body glucose uptake and more interesting skeletal muscle glucose disposal were elevated in glucose infused rats after 1d and after 4d of glucose infusion (Laybutt, Chisholm, et al. 1997). Davidson et al. showed that plasma membrane GLUT4 content was doubled in glucose infused rats after 48h of glucose infusion (Davidson, Bouch, et al. 1994). GLUT4 content was also doubled in rat adipose tissue after 24h of hyperinsulinemia (Postic, Leturque, et al. 1993).
Furthermore, Zierath's group showed that GLUT4 expression was increased in NIDDM patients when compared with controls (Zierath, He, et al. 1996). Moreover, upregulation of GLUT4 was shown to enhance whole body glucose utilization and to prevent fasting hyperglycemia induced by high-sugar diet (Marshall, Hansen, et al. 1999) or by high fat diet (Gnudi, Shepherd, et al. 1996).
Overexpression of GLUT4 in muscle of normal, db/db and streptozotocin diabetic mice produced animals of superior glycemic control (Katz, Burcelin, et al. 1996). Finally, exercise increases GLUT4 expression and enhances glucose tolerance (Hayashi, Wojtaszewski, et al. 1997).

Thus increased GLUT4 expression in GIR enhances glucose uptake in skeletal muscle.

We previously reported the translocation of GLUT4 due to hyperglycemia in C_2C_{12} cells and in rat skeletal muscle (Galante, Mosthaf, et al. 1995).
Findings in this work and previous findings challange the results of Wallberg-Hendriksson (Nolte, Rincon, et al. 1995), (Kawano, Rincon, et al. 1999) in terms of glucose-induced translocation of glucose transporter. Wallberg-Hendriksson suggested modification of cell surface glucose transporter activity, instead of glucose transporter translocation.
In fact, it can not be ruled out, that the activity of cell surface glucose transporter was also altered in GIR, since activity studies were not performed.
However, increased glucose transport is obvious in our model since glycogen content was highly increased in GIR during the infusion period.
Increased muscle glycogen content due to hyperglycemia was also reported by others (Vaag, Damsbo, et al. 1992). The increase in glycogen content in GIR on the 5^{th} day was less than on day 2 of glucose infusion and might be due to differential effects of hyperinsulinemia (day 5) or combined hyperinsulinemia and hyperglycemia (day 2) as previously reported (Sugden, Holness, et al. 1997).

The decrease in mRNA levels of GLUT1 seen on 2^{nd} day might be due to altered mRNA stability (Qi & Pekala 1999). In concomitance, hyperglycemia was reported to decrease GLUT1 mRNA levels in rat skeletal muscle (Simmons, Flozak, et al. 1993).
In contrast, Simmons et al. reported decreased GLUT1 protein expression either. The divergence might be due to a lack of simultaneous hyperinsulinemia as it was monitored in GIR. Simultaneous hyperinsulinemia might prevent hyperglycemia's effect of lowering GLUT1 expression.
Furthermore, Vinals et al. showed no change in GLUT1 expression in human endothelial cells when preincubated with high glucose concentrations (Vinals, Gross, et al. 1999).

In sum, it can be concluded that glucose infusion into normal rats leading to hyperglycemic, hyperinsulinemic metabolic states increases glucose flux and glycogen content in skeletal muscle.

5.4 Increased Glucose Flux in Muscle Impaired Insulin Signal Transduction

Increased glucose flux in skeletal muscle was reported to impair insulin-stimulated glucose transport (Etgen-GJ, Zavadoski, et al. 1999), (Hansen, Wang, et al. 1998), (Buse, Robinson, et al. 1996).
To determine whether increased glucose flux in rat skeletal muscle impairs insulin-stimulated glucose uptake, insulin signaling was studied.
The protein and messenger expression of the insulin receptor as well as its autophosphorylation was investigated. Our results show no significant change in messenger nor in protein expression of IR on the 2nd day of infusion.
The autophosphorylation of IR was not changed either. In terms of insulin resistance, these findings are in fact surprising, since highest serum insulin concentrations measured permanently in GIR were not able to induce autophosphorylation of IR above control levels. Moreover, insulin receptor messenger and protein expression as well as autophosphorylation in GIR decreased after 5d of infusion when compared to controls.

The significance of insulin autophosphorylation for the transmission of insulin signal was reported by studies showing the inability of mutated insulin receptor to mediate insulin effects (McClain, Maegawa, et al. 1987).
High glucose conditions were reported to decrease insulin receptor autophosphorylation (Ide, Maegawa, et al. 1995), (Berti, Mosthaf, et al. 1994), (Haring, Kellerer, et al. 1994) and IR protein expression was decreased compared to controls in insulin resistant diabetic mice (Bonini, Colca, et al. 1995). Thus decreased IR expression and autophosphorylation might be involved in hyperglycemia-induced insulin resistance.
However, certain insulin receptor antibodies mediate insulin stimulation of glucose transport without autophosphorylation of IR (Simpson & Hedo 1984).
Chinese hamster ovary cells transfected with insulin receptor mutants unable of autophosphorylation respond to insulin by an increase in glucose transport (Moller, Benecke, et al. 1991). Additionally, muscle specific insulin receptor knockout mice (MIRKO) showed normal glucose uptake (Wojtaszewski, Higaki, et al. 1999).
Thus modulation of insulin signaling at the post receptor level might be a site of modulation in insulin action.
IRS-1 plays a major role in insulin action in skeletal muscle (Kido, Burks, et al. 2000). IRS-2 plays a role in insulin action in liver (Kido, Burks, et al. 2000) and is not necessary for insulin stimulated glucose transport in skeletal muscle (Higaki, Wojtaszewski, et al. 1999). IRS-3 and IRS-4 are not expressed in skeletal muscle (Lavan, Lane, et al. 1997).
Altered expression of IRS-1 contributes to insulin resistance (deVente, Carey, et al. 1996) and phosphorylation of IRS-1 on serine or threonine residues by PKC is required to inhibit tyrosine kinase activity of the insulin receptor (Kellerer, Mushack, et al. 1998).
In this work, glucose infusion showed no effects on the protein expression, nor messenger expression of IRS-1. The tyrosine phosphorylation of IRS-1 was not changed from control animals.

These findings are in accordance with findings of others (Bjornholm, Kawano, et al. 1997). In the latter approach, no changes on protein expression, nor on insulin stimulation of IRS-1 phosphorylation were found in NIDDM muscle.
Furthermore, both expression and enzyme activity of PI3-K to generate PIP_3 is altered in insulin resistance (Shepherd, Withers, et al. 1998). The functional consequences of these alterations on insulin action is not fully understood. Decreased insulin stimulation of IRS-1 associated PI3-K activity was reported in NIDDM (Bjornholm, Kawano, et al. 1997).
Direct binding of PI3-K to the C-terminus of phosphorylated insulin receptor was also reported, but may not play a major role in insulin-stimulated PI3-K activity (Shepherd, Withers, et al. 1998).
The Zierath's group demonstrated a decrease in phosphotyrosine-associated PI3-K activity in NIDDM muscle upon stimulation with insulin when compared to controls (Bjornholm, Kawano, et al. 1997).
However, the decrease in insulin-stimulated glucose uptake after 1 day of muscle denervation was not associated with changes in PI3-K expression, nor activity (Elmendorf, Damrau, et al. 1997). And englitazone enhances insulin action without affecting PI3-K activity (Stevenson, Kreutter, et al. 1998). Moreover, inhibition of PI3-K by wortmannin did not affect hyperglycemia-induced glucose uptake (Nolte, Rincon, et al. 1995).
Thus hyperglycemia-induced effects on insulin signaling might not involve PI3-K.

In concomitance, our findings suggest no alteration in PI3-K protein expression, nor in its IRS-1-associated enzyme activity and furthermore rule out an activation of PI3-K to be involved in glucose-induced glucose uptake in GIR.

Activation of downstream targets of PI3-K, particularly PKB was decreased in rat liver of hyperglycemic diabetic rats (Nawano, Ueta, et al. 1999), (Krook, Kawano, et al. 1997). Insulin-stimulated PKB activity was reduced in NIDDM muscle (Krook, Roth, et al. 1998) and phlorizin improvement of glycemia restored PKB activity suggesting possible affecting of PKB by hyperglycemia.
In contrast, our results suggest no effect of glucose infusion on PKB expression, nor activation upon phosphorylation on serine residue 473.
In fact, the role of PKB in glucose uptake is (temporarily) controversial. Kasuga et al (Kitamura, Ogawa, et al. 1998) challenged the role of PKB to be necessary for insulin-stimulated glucose uptake, since mutations on phosphorylation sites threonine 308 and serine 473 had no effect on insulin-stimulated glucose uptake.
On the other hand, insulin-activated PKB enhances insulin-induced glucose transport (Ueki, Yamamoto-Honda, et al. 1998) and stimulate the translocation of GLUT4 (Foran, Fletcher, et al. 1999), (Kohn, Summers, et al. 1996).
Serine phosphorylation of IRS-1 by PKB enables IRS-1 to maintain its active tyrosine-phosphorylated conformation (Paz, Liu, et al. 1999).
Our results favor no involvement of PKB in glucose-induced glucose uptake.

Thus, it can be concluded that glucose infusion in conscious rats enhances glucose uptake in skeletal muscle via an insulin-independent mechanism and increased glucose flux desensitizes insulin action by modulation at the level of receptor autophosphorylation.

5.5 Glucose Infusion in Conscious Rats Activates the Redistribution of PKC Isoforms

PKC Isoform	Protein expression		mRNA-expression		Translocation	
Infusion period	2d	5d	2d	5d	2d	5d
PKC α	↑	↓	n.s.	↓	↑	n.s.
PKC βI	↑	n.s.	↑↑	↓	↑↑	n.s.
PKC βII	n.s.	↓	n.d.	n.d.	↑↑	n.s.
PKC θ	↑	↑	n.d.	n.d.	↑	n.s.
PKCζ	↑	↓	n.s.	↓	n.s.	n.s.
PKCδ	↑	n.s.	n.s.	↓	n.s.	n.s.
PKCε	n.d.	n.d.	↑	↓	n.d.	n.d.
PKCλ	n.d.	n.d.	↑	↓	n.d.	n.d.

Table 5.5.1 summarizes results obtained for PKC isoforms. n.s., not significant, n.d., not determined (for PKC βII and PKCθ mRNA expression) or not detecable for the rest.

The majority of all investigated PKCs showed an increase at similar extent in both protein- and mRNA-expression on the 2nd day of glucose infusion compared to control rats.
The increased protein levels might be involved in the increased glucose uptake in these animals.
The process of PKC activation involves their translocation to the plasma membrane followed by proteolysis, possibly by calpain (Verret, Poussard, et al. 1999), (Hong, Huan, et al. 1995) and the parallel increase in messenger levels on the 2nd glucose infusion day might be a regulatory process to compensate for protein amounts being degraded after translocation as suggested by (Avignon, Standaert, et al. 1995), (Ishizuka, Kajita, et al. 1996).
After 5d of infusion, where normoglycemia was reached and PKC translocation ceased to be higher than control animals, PKC protein expression and mRNA expression returned to normal levels or were even more decreased to levels lower than in control animals. Long-term activation of PKCs might have caused down regulation of PKC. In fact, long-term exposure to TPA, which activates PKC leads to downregulation of PKC (Hong, Huan, et al. 1995). Furthermore, decreased PKC expression in GIR after 5d of glucose infusion might be related to glucose-induced insulin resistance in these animals, since PKC protein levels and mRNA expression were decreased in muscle of insulin resistant rats (Cooper, Watson, et al. 1993), (van-de-Werve, Zaninetti, et al. 1987).
Moreover, hyperglycemia, which is a potent inductor of PKC redistribution (Galante, Mosthaf, et al. 1995) was normalized after 5d of infusion.

Thus, activation of PKC via both increased expression and translocation was only evident when rats were hyperglycemic.

The translocation of PKCβI and PKCβII was most evident and less obvious in PKCα and PKCθ on the 2nd day of glucose infusion.
PKCβ was repeatedly reported to be involved in mediating effects of hyperglycemia on glucose transport. Hyperglycemia increased translocation of PKCβ in smooth muscle (Ganz & Seftel 2000) and in rat skeletal muscle (Galante, Mosthaf, et al. 1995), (Kawano, Rincon, et al. 1999) leading to increased glucose uptake in an insulin-independent fashion (Galante, Mosthaf, et al. 1995), possibly involving Ca^{2+} (Nolte, Rincon, et al. 1995), (Kawano, Rincon, et al. 1999), (Khayat, Tsakiridis, et al. 1998), (Keranen & Newton 1997).
Overexpression of PKCβI and PKCβII inhibits the tyrosine kinase activity of the insulin receptor (Bossenmaier, Mosthaf, et al. 1997) and mediates hyperglycemia-induced diabetic complications (Koya & King 1998), (Wakasaki, Koya, et al. 1997). Moreover, a specific inhibitor of the PKCβ isoform normalized renal and retinal dysfunctions induced by hyperglycemia (Koya, Jirousek, et al. 1997).

Thus, it can be concluded that increased expression and translocation of PKCβI and PKCβII measured in GIR on the 2nd day of glucose infusion activates glucose uptake independently of insulin and mediate hyperglycemia induced insulin resistance.

PKCα (Berti, Mosthaf, et al. 1994), (Koya, Jirousek, et al. 1997), (Ishizuka, Kajita, et al. 1999) and PKCθ (Kellerer, Mushack, et al. 1998) may furthermore contribute to increased glucose-induced glucose uptake and hyperglycemia-induced insulin resistance.

5.6 Glucose Infusion in Conscious Rats Activates the Hexosamine Biosynthesis Pathway

Activation of the hexosamine pathway induces insulin resistance (Virkamaki, Daniels, et al. 1997), (Patti, Virkamaki, et al. 1999) and hyperglycemia activates the hexosamine pathway (Kolm, Sauer, et al. 1998), (Robinson, Weinstein, et al. 1995).
GFAT, which activates the rate limiting step in this pathway, is highly expressed in skeletal muscle (Nerlich, Sauer, et al. 1998). Hyperglycemia increases GFAT activity (Daniels, Ciaraldi, et al. 1996) and GFAT activity is increased in hyperglycemic obese mice (Buse, Robinson, et al. 1997) and hyperglycemic NIDDMs (Yki-Yärvinen, Daniels, et al. 1996).
Here, we are the first group to show increased GFAT expression in rat skeletal muscle of GIR, particularly with the antisera, produced in our laboratory (Nerlich, Sauer, et al. 1998).
GFAT expression was increased to the same level in skeletal muscle of GIR on both 2^{nd} and 5^{th} day of glucose infusion.
Increased GFAT activity reported from other groups might be due to increased GFAT protein expression, since activity studies were usually not paralleled by studies of GFAT protein expression.
The increased GFAT protein expression was associted with an increase in messenger expression only under hyperglycemic conditions (on day 2) and decreased significantly after 5d.
Elevated levels of GFAT proteins in GIR, despite the decrement of messenger expression on the 5^{th} day of glucose infusion might be due to a long turnover of GFAT protein. However, GFAT turnover was reported to be short of approximately (half-life time $t_{1/2}$ 45 min) (Marshall, Bacote, et al. 1991).
Thus, the discrepancy might be due to post-transcriptional modification stabilizing GFAT. In fact, UDP-HexNAc concentrations (see below) were also elevated in GIR after 5d suggesting increased GFAT activity.
Furthermore, levels of mRNA and protein did not correlate in rat skeletal muscle (Robinson, Weinstein, et al. 1995), nor in liver of diabetic rats (Yki, Nyman, et al. 1999).
In addition, this discrepancy might reflect differential regulation of GFAT1 and GFAT2, since our antisera recognize both GFAT1 and GFAT2, whereas analysis of mRNA expression was made for GFAT1.

For further characterization of the GFAT-PCR product, DNA sequencing of GFAT-PCR product was performed and pair comparison was made using BLAST2 search in the GenBank (www.ncbi.nlm.nih.gov/blast/). Pair comparison revealed high alignment to mouse GFAT1 and human GFAT1 as delineated below:

Pair comparison with mouse GFAT1:

```
href="http://www.ncbi.nlm.nih.gov:80/entrez/query.fcgi?cmd=Retrieve&db=Nucl
eotide&list_uids=00414424&dopt=GenBank">gb|U00932.1|U00932</a> Mus musculus
glutamine:fructose-6-phosphate amidotransferase mRNA, complete cds,
Length = 2046
Score =  278 bits (140), Expect = 1e-72
Identities = 203/224 (90%), Gaps = 1/224 (0%)
Strand = Plus / Plus (Query:Rat GFAT, subject: Mouse GFAT1)

Query: 3   tgatgtgtgatgacagaatctccatgcnagaaagacgcaaagagatcatgctggactga 62
           ||||||||||||||| |||||||||| ||| |||||||||||||||||||| |||||||
Sbjct:1472 tgatgtgtgatgacaggatctccatgcaagagagacgcaaagagatcatgctcggactga1531

Query: 63  agcgactgccggacttgattaaggaagtgttgagcatggatgatgaaattcagaagctgg 122
           |||||||||||||||||||||||| ||| |||||||||||||||||| |||||||| |
Sbjct:1532 agcgactgccggacttgattaaggaggtgctgagcatggatgatgaaatccagaagctag1591

Query: 123 ctgacagagctttaccaccagaagtcggtcctgataatgggccgaggctatcattatgct 182
           |  || |||||||||||||||||||||||||||||||||| || ||||| |||||||||
Sbjct:1592 c-aacggagctttaccaccagaagtcggtcctgataatggggcgggctaccattatgct1650

Query: 183  acatgtctngaaggagccctgaaaatcnnggagattacatatat 226
            ||||| || ||||| || |||||||||  ||||||||| |||||
Sbjct: 1651 acatgccttgaaggggctctgaaaatcaaggagattacttatat 1694
```

Pair comparison with human GFAT1:

```
href="http://www.ncbi.nlm.nih.gov:80/entrez/query.fcgi?cmd=Retrieve&db=Nucl
eotide&list_uids=04503980&dopt=GenBank">ref|NM_002056.1||</a> Homo sapiens
glutamine-fructose-6-phosphate transaminase 1 (GFPT1)mRNA, Length = 3082
Score =  192 bits (97), Expect = 7e-47
Identities = 180/207 (86%), Gaps = 1/207 (0%)
Strand = Plus / Plus (Query:Rat GFAT, subject: human GFAT1)

Query: 3   tgatgtgtgatgacagaatctccatgcnagaaagacgcaaagagatcatgctggagactga 62
           |||||||||||||  | |||||||||| ||||||||||||||||||||||| ||| |||
Sbjct:1594 tgatgtgtgatgatcggatctccatgcaagaaagacgcaaagagatcatgcttggattga1653

Query: 63  agcgactgccggacttgattaaggaagtgttgagcatggatgatgaaattcagaagctgg 122
           | || ||||| || |||||||||||||  |||||||||||| |||||||||| || |
Sbjct:1654 aacggctgcctgatttgattaaggaagtactgagcatggatgacgaaattcagaaactag1713

Query: 123 ctgacagagctttaccaccagaagtcggtcctgataatgggccgaggctatcattatgct 182
           |  ||||| ||||| || |||||||| || |||||||||| ||||||||||||||||||
Sbjct:1714 c-aacagaactttatcatcagaagtcagttctgataatgggacgaggctatcattatgct1772

Query: 183  acatgtctngaaggagccctgaaaatc 209
            || ||||| ||||| || |||||||||
Sbjct: 1773 acttgtcttgaaggggcactgaaaatc 1799
```

Pair comparison with human GFAT2 (GenBank Accession Nr. AB016789) revealed a much lesser alignment:

Score = 46.8 bits (24), Expect = 0.002
Identities = 41/50 (82%), Positives = 41/50 (82%)

```
Query:159  atgggccgaggctatcattatgctacatgtctngaaggagccctgaaaat 208
           ||||| || |||||  | ||||| || || || ||||||||||||||||
sbct :1729 atggggcggggctacaactatgccacctgcctggaaggagccctgaaaat 1778
```

Thus it can be shown that the measured GFAT mRNA levels involved only GFAT1 mRNA.

UDP-Glc is precursor for glycogen. CE analysis revealed increased tissue UDP-Hexose (UDP-Hex: UDP-Glc and UDP-Gal). This is in concomitance with the increased glycogen content in GIR on both 2nd and 5th day of glucose infusion.
In fact, overexpression of GFAT was shown to increase basal glycogen synthase activity in rat-1-fibroblasts (Crook, Daniels, et al. 1993).
Again the accumulation of glycogen and the increased availability of UDP-Hex in GIR reflect the increased glucose flux in rat skeletal muscle of GIR.
The ratio UPD-HexNAc/UDP-Hex for GIRs revealed 76% and 68% of controls after 2 and 5d, respectively. This indicates increased metabolization of glucose flux towards glycogen synthesis.
Although the overall concentrations of UDP-HexNAc was elevated, which is in agreement with increased GFAT expression in GIRs and which was repeatedly reported by others (Buse, Robinson, et al. 1996), (Hawkins, Angelov, et al. 1997), (Robinson, Weinstein, et al. 1995), the tissue concentrations of UDP-GlcNAc were decreased in GIR on both the 2nd and the 5th day of infusion when compared with control animals.

Thus, it seems that under conditions of increased glucose flux, the equilibrium between UPD-GlcNAc and UDP-GalNAc is favored unidirectional to produce more UDP-GalNAc.

On the other hand, UDP-GlcNAc might be depleted by O-linked attachment to serine and threonine residue on intracellular proteins (Patti, Virkamaki, et al. 1999).
O-GlcNAc transferase activity, however, does not appear to be increased in muscle of NIDDM (Yki-Yärvinen, Vogt, et al. 1997). Furthermore, in GIR O-linked glycosylation was not found to be increased in comparison to control animals.
Moreover, keeping UDP-GlcNAc at low concentrations favors its own production by GFAT, since feed-back-inhibition of GFAT by UDP-GlcNAc (Nerlich, Sauer, et al. 1998), (Yki-Yärvinen, Daniels, et al. 1996) is kept at a minimum.

Thus, increased glucose flux in rat skeletal muscle involves activation of the hexosamine pathway by increasing GFAT protein expression and tissue concentrations of UDP-HexNAc.

Taken together, glucose infusion increased glucose flux in rat skeletal muscle by increasing the total expression of GLUT4 and inducing its translocation (and translocation of GLUT1) to the plasma membrane. The mechanism of increased glucose flux altered insulin receptor phosphorylation.
Increased glucose flux in rat skeletal muscle involved elevated PKC expression and translocation as well as the activation of hexosamine pathway.
As normoglycemia was reached, increased glucose flux persisted, increased GLUT4 expression and translocation, GFAT expression and hexosamine pathway activation were retained, but not PKC activation.

6 SUMMARY

6.1 INTRODUCTION

Hyperglycemia is a common feature of diabetes mellitus.
Hyperglycemia per se is a potent regulator of insulin action. Inhibition of insulin action by hyperglycemia in diabetes is a phenomenon referred to as glucose toxicity.
Under hyperglycemic conditions, skeletal muscle can be protected from glucose oversupply due to adaptation in the insulin-stimulated glucose uptake, which limits the glucose flux into this tissue (insulin resistance).
Hyperglycemia increases glucose uptake in skeletal muscle in a concentration-dependent fashion (glucose mass-action effect)
The mechanism(s), by which hyperglycemia induces glucose uptake and increases glucose flux in skeletal muscle is important for the development of insulin resistance and is temporarily a matter of intensive investigations.
One of the plausible mechanisms proposed to underlie hyperglycemia-induced insulin resistance involves the activation of PKCs.
An alternative hypothesis for hyperglycemia-induced insulin resistance suggests increased flux of glucose through the hexosamine biosynthesis pathway.
The elucidation of the “sinister scenario” of hyperglycemia to positively or negatively alter glucose uptake in skeletal muscle is of highest interest to diabetic research.

6.2 AIM

The aim of this thesis was to elucidate pathological effects of prolonged glucose infusion on insulin signal transduction towards glucose transport in normal conscious rats.
The central hypothesis is that infused glucose interacts with its own metabolism in skeletal muscle and propagates its uptake in an insulin independent fashion leading to insulin resistance.
In particular, the following questions have been addressed:

- Does infused glucose influence insulin signaling towards glucose transporter translocation to the plasma membrane?

- Does infused glucose activate PKC isoforms?

- Does the hexosamine pathway mediate effects of infused glucose on its own uptake in skeletal muscle?

6.3 RESULTS

Glucose uptake in rat skeletal muscle was increased in glucose-infused rats when compared to saline-infused rats as evidenced by the measurement of UDP-Hexose concentrations and glycogen content.
Glucose-infused rats managed to normalize plasma glucose concentrations, despite of 5d of continuous glucose infusion.

The mechanism of hyperglycemia-induced glucose uptake in skeletal muscle was shown to involve increased expression of the glucose transporter isoform 4 and the translocation of both glucose transporter isoform 1 and 4.
Glucose infusion increased the protein expression of several PKC isoforms and their translocation to the plasma membrane indicating that their activation may play a role in the glucose-induced glucose uptake.
In agreement with other groups, we confirm the role for PKCβ in hyperglycemia-induced insulin resistance and in enhancing insulin-independent glucose uptake in rat skeletal muscle.
Furthermore, hyperglycemia activated the hexosamine biosynthesis pathway via increasing the expression of GFAT. The activation of the hexosamine pathway increased the tissue concentrations of UDP-HexNAc.

Increased glucose flux in skeletal muscle via activation of PKC and hexosamine pathway may induce insulin resistance in skeletal muscle by modulation at the level of autophosphorylation of the insulin receptor, whereas no effects can be reported for post receptor signaling.

Thus, our data has put more spotlight on mechanisms involved in muscle glucose uptake and could fairly show the involvement of hyperglycemia in induction of insulin resistance apparently by inhibition of insulin signaling cascade. We could furthermore report an increased hyperglycemia-induced, insulin-independent glucose uptake in rat skeletal muscle.
Since activation of PKC, particularly PKCβ, has been shown to inhibit insulin signaling and evidence exists that it also may stimulate cellular glucose uptake, our data indicate that PKC activation may shift glucose uptake from an insulin-dependent to an insulin-independent pathway.

Akimoto K, Takahashi R, Moriya S, Nishioka N, Takayanagi J, Kimura K, Fukui Y, Osada S, Mizuno K, Hirai S, Kazlauskas A, Ohno S: EGF or PDGF receptors activate atypical PKClambda through phosphatidylinositol 3-kinase. *EMBO J* 15:788-798, 1996

Aledo JC, Lavoie L, Volchuk A, Keller SR, Klip A, Hundal HS: Identification and characterization of two distinct intracellular GLUT4 pools in rat skeletal muscle: evidence for an endosomal and an insulin-sensitive GLUT4 compartment. *Biochem J* 325:727-732, 1997

Ammon HP, Bacher M, Brandle WF, Waheed A, Roenfeldt M, el-Sayed ME, Ahmed AA, Wahl MA: Effect of forty-eight-hour glucose infusion into rats on islet ion fluxes, ATP/ADP ratio and redox ratios of pyridine nucleotides. *J Endocrinol* 156:583-590, 1998

Ammon HP: Hyper- and hypoinsulinemia in type-2 diabetes: what may be wrong in the secretory mechanism of the B-cell. *Exp Clin Endocrinol Diabetes* 105 Suppl 2:43-47, 1997

Auboeuf D, Vidal H: The use of the reverse transcription-competitive polymerase chain reaction to investigate the in vivo regulation of gene expression in small tissue samples. *Anal Biochem* 245:141-148, 1997

Avignon A, Standaert ML, Yamada K, Mischak H, Spencer B, Farese RV: Insulin increases mRNA levels of protein kinase C-alpha and -beta in rat adipocytes and protein kinase C-alpha, -beta and -theta in rat skeletal muscle. *Biochem J* 308:181-187, 1995

Avignon A, Yamada K, Zhou X, Spencer B, Cardona O, Saba SS, Galloway L, Standaert ML, Farese RV: Chronic activation of protein kinase C in soleus muscles and other tissues of insulin-resistant type II diabetic Goto-Kakizaki (GK), obese/aged, and obese/Zucker rats. A mechanism for inhibiting glycogen synthesis. *Diabetes* 45:1396-1404, 1996

Bader S, Scholz R, Kellerer M, Tippmer S, Rett K, Mathaei S, Freund P, Haring HU: Normal insulin receptor tyrosine kinase activity and glucose transporter (GLUT 4) levels in the skeletal muscle of hyperinsulinaemic hypertensive rats. *Diabetologia* 35:712-718, 1992

Bak JF: Insulin receptor function and glycogen synthase activity in human skeletal muscle. Physiology and pathophysiology. *Dan Med Bull* 41:179-192, 1994

Baltensperger K, Kozma LM, Cherniack AD, Klarlund JK, Chawla A, Banerjee U, Czech MP: Binding of the Ras activator son of sevenless to insulin receptor substrate-1 signaling complexes. *Science* 260:1950-1952, 1993

Bandyopadhyay G, Standaert ML, Galloway L, Moscat J, Farese RV: Evidence for involvement of protein kinase C (PKC)-zeta and noninvolvement of diacylglycerol-sensitive PKCs in insulin-stimulated glucose transport in L6 myotubes. *Endocrinology* 138:4721-4731, 1997

Baron AD, Zhu JS, Zhu JH, Weldon H, Maianu L, Garvey WT: Glucosamine induces insulin resistance in vivo by affecting GLUT 4 translocation in skeletal muscle. Implications for glucose toxicity. *J Clin Invest* 96:2792-2801, 1995

Bell GI, Kayano T, Buse JB, Burant CF, Takeda J, Lin D, Fukumoto H, Seino S: Molecular biology of mammalian glucose transporters. *Diabetes Care* 13:198-208, 1990

Bers DM, Philipson KD, Nishimoto AY: Sodium-calcium exchange and sidedness of isolated cardiac sarcolemmal vesicles. *Biochim Biophys Acta* 601:358-371, 1980

Bers DM: Isolation and characterization of cardiac sarcolemma. *Biochim Biophys Acta* 555:131-146, 1979

Berti L, Mosthaf L, Kroder G, Kellerer M, Tippmer S, Mushack J, Seffer E, Seedorf K, Haring H: Glucose-induced translocation of protein kinase C isoforms in rat-1 fibroblasts is paralleled by inhibition of the insulin receptor tyrosine kinase. *J Biol Chem* 269:3381-3386, 1994

Bjornholm M, Kawano Y, Lehtihet M, Zierath JR: Insulin receptor substrate-1 phosphorylation and phosphatidylinositol 3-kinase activity in skeletal muscle from NIDDM subjects after in vivo insulin stimulation. *Diabetes* 46:524-527, 1997

Bollag GE, Roth RA, Beaudoin J, Mochly RD, Koshland-DE J: Protein kinase C directly phosphorylates the insulin receptor in vitro and reduces its protein-tyrosine kinase activity. *Proc Natl Acad Sci U S A* 83:5822-5824, 1986

Bonini JA, Colca JR, Dailey C, White M, Hofmann C: Compensatory alterations for insulin signal transduction and glucose transport in insulin-resistant diabetes. *Am J Physiol* 269:E759-E765, 1995

Bornemann A, Ploug T, Schmalbruch H: Subcellular localization of GLUT4 in nonstimulated and insulin-stimulated soleus muscle of rat. *Diabetes* 41:215-221, 1992

Bossenmaier B, Mosthaf L, Mischak H, Ullrich A, Haring HU: Protein kinase C isoforms beta 1 and beta 2 inhibit the tyrosine kinase activity of the insulin receptor. *Diabetologia* 40:863-866, 1997

Brozinick-JT J, Etgen-GJ J, Yaspelkis BB, Ivy JL: Glucose uptake and GLUT-4 protein distribution in skeletal muscle of the obese Zucker rat. *Am J Physiol* 267:R236-R243, 1994

Bruning JC, Michael MD, Winnay JN, Hayashi T, Horsch D, Accili D, Goodyear LJ, Kahn CR: A muscle-specific insulin receptor knockout exhibits features of the metabolic syndrome of NIDDM without altering glucose tolerance. *Mol Cell* 2:559-569, 1998

Burdett E, Beeler T, Klip A: Distribution of glucose transporters and insulin receptors in the plasma membrane and transverse tubules of skeletal muscle. *Arch Biochem Biophys* 253:279-286, 1987

Burgering BM, Coffer PJ: Protein kinase B (c-Akt) in phosphatidylinositol-3-OH kinase signal transduction [see comments]. *Nature* 376:599-602, 1995

Buse MG, Robinson KA, Gettys TW, McMahon EG, Gulve EA: Increased activity of the hexosamine synthesis pathway in muscles of insulin-resistant ob/ob mice. *Am J Physiol* 272:E1080-E1088, 1997

Buse MG, Robinson KA, Marshall BA, Mueckler M: Differential effects of GLUT1 or GLUT4 overexpression on hexosamine biosynthesis by muscles of transgenic mice. *J Biol Chem* 271:23197-23202, 1997

Carpentier JL: Insulin-induced and constitutive internalization of the insulin receptor. *Horm Res* 38:13-18, 1992

Carr RS, Neff JM: Quantitative semi-automated enzymatic assay for tissue glycogen. *Comp Biochem Physiol B* 77:447-449, 1984

Caruso M, Miele C, Oriente F, Maitan A, Bifulco G, Andreozzi F, Condorelli G, Formisano P, Beguinot F: In L6 skeletal muscle cells, glucose induces cytosolic translocation of protein kinase C-alpha and trans-activates the insulin receptor kinase. *J Biol Chem* 274:28637-28644, 1999

Chattopadhyay S, Ramanathan M, Das J, Bhattacharya SK: Animal models in experimental diabetes mellitus. *Indian J Exp Biol* 35:1141-1145, 1997

Chen H, Ing BL, Robinson KA, Feagin AC, Buse MG, Quon MJ: Effects of overexpression of glutamine:fructose-6-phosphate amidotransferase (GFAT) and glucosamine treatment on translocation of GLUT4 in rat adipose cells. *Mol Cell Endocrinol* 135:67-77, 1997

Chen KS, Friel JC, Ruderman NB: Regulation of phosphatidylinositol 3-kinase by insulin in rat skeletal muscle. *Am J Physiol* 265:E736-E742, 1993

Cheta D: Animal models of type I (insulin-dependent) diabetes mellitus. *J Pediatr Endocrinol Metab* 11:11-19, 1998

Cline GW, Petersen KF, Krssak M, Shen J, Hundal RS, Trajanoski Z, Inzucchi S, Dresner A, Rothman DL, Shulman GI: Impaired glucose transport as a cause of decreased insulin-stimulated muscle glycogen synthesis in type 2 diabetes [see comments]. *N Engl J Med* 341:240-246, 1999

Cong LN, Chen H, Li Y, Zhou L, McGibbon MA, Taylor SI, Quon MJ: Physiological role of Akt in insulin-stimulated translocation of GLUT4 in transfected rat adipose cells. *Mol Endocrinol* 11:1881-1890, 1997

Cooksey RC, Hebert-LF J, Zhu JH, Wofford P, Garvey WT, McClain DA: Mechanism of hexosamine-induced insulin resistance in transgenic mice overexpressing glutamine:fructose-6-phosphate amidotransferase: decreased glucose transporter GLUT4 translocation and reversal by treatment with thiazolidinedione. *Endocrinology* 140:1151-1157, 1999

Cooper DR, Watson JE, Dao ML: Decreased expression of protein kinase-C alpha, beta, and epsilon in soleus muscle of Zucker obese (fa/fa) rats. *Endocrinology* 133:2241-2247, 1993

Cooper DR, Watson JE, Patel N, Illingworth P, Acevedo-Duncan M, Goodnight J, Chalfant CE, Mischak H: Ectopic expression of protein kinase CbetaII, -delta, and -epsilon, but not -betaI or -zeta, provide for insulin stimulation of glucose uptake in NIH-3T3 cells. *Arch Biochem Biophys* 372:69-79, 1999

Corvera S, D'Arrigo A, Stenmark H: Phosphoinositides in membrane traffic. *Curr Opin Cell Biol* 11:460-465, 1999

Crook ED, Daniels MC, Smith TM, McClain DA: Regulation of insulin-stimulated glycogen synthase activity by overexpression of glutamine: fructose-6-phosphate amidotransferase in rat-1 fibroblasts. *Diabetes* 42:1289-1296, 1993

Crook ED, McClain DA: Regulation of glycogen synthase and protein phosphatase-1 by hexosamines. *Diabetes* 45:322-327, 1996

Crook ED, Zhou J, Daniels M, Neidigh JL, McClain DA: Regulation of glycogen synthase by glucose, glucosamine, and glutamine:fructose-6-phosphate amidotransferase. *Diabetes* 44:314-320, 1995

Czech MP: Molecular actions of insulin on glucose transport. *Annu Rev Nutr* 15:441-471, 1995

Daniels MC, Ciaraldi TP, Nikoulina S, Henry RR, McClain DA: Glutamine:fructose-6-phosphate amidotransferase activity in cultured human skeletal muscle cells: relationship to glucose disposal rate in control and non-insulin-dependent diabetes mellitus subjects and regulation by glucose and insulin. *J Clin Invest* 97:1235-1241, 1996

Davidson MB, Bouch C, Venkatesan N, Karjala RG: Impaired glucose transport in skeletal muscle but normal GLUT-4 tissue distribution in glucose-infused rats. *Am J Physiol* 267:E808-E813, 1994

DeFronzo RA: Lilly lecture 1987. The triumvirate: beta-cell, muscle, liver. A collusion responsible for NIDDM. *Diabetes* 37:667-687, 1988

Denton RM, Tavare JM: Does mitogen-activated-protein kinase have a role in insulin action? The cases for and against. *Eur J Biochem* 227:597-611, 1995

Derubertis FR, Craven PA: Activation of protein kinase C in glomerular cells in diabetes. Mechanisms and potential links to the pathogenesis of diabetic glomerulopathy. *Diabetes* 43:1-8, 1994

deVente JE, Carey JO, Bryant WO, Pettit GJ, Ways DK: Transcriptional regulation of insulin receptor substrate 1 by protein kinase C. *J Biol Chem* 271:32276-32280, 1996

Dimitrakoudis D, Vranic M, Klip A: Effects of hyperglycemia on glucose transporters of the muscle: use of the renal glucose reabsorption inhibitor phlorizin to control glycemia [editorial]. *J Am Soc Nephrol* 3:1078-1091, 1992

Dinter A, Berger EG: The regulation of cell- and tissue-specific expression of glycans by glycosyltransferases. *Adv Exp Med Biol* 376:53-82, 1995

Dombrowski L, Marette A: Marked depletion of GLUT4 glucose transporters in transverse tubules of skeletal muscle from streptozotocin-induced diabetic rats. *FEBS Lett* 374:43-47, 1995

Dombrowski L, Roy D, Marcotte B, Marette A: A new procedure for the isolation of plasma membranes, T tubules, and internal membranes from skeletal muscle. *Am J Physiol* 270:E667-E676, 1996

Dombrowski L, Roy D, Marette A: Selective impairment in GLUT4 translocation to transverse tubules in skeletal muscle of streptozotocin-induced diabetic rats. *Diabetes* 47:5-12, 1998

Downward J: Mechanisms and consequences of activation of protein kinase B/Akt. *Curr Opin Cell Biol* 10:262-267, 1998

Elmendorf JS, Damrau AA, Smith TR, David TS, Turinsky J: Phosphatidylinositol 3-kinase and dynamics of insulin resistance in denervated slow and fast muscles in vivo. *Am J Physiol* 272:E661-E670, 1997

Etgen GJ, Valasek KM, Broderick CL, Miller AR: In vivo adenoviral delivery of recombinant human protein kinase C-zeta stimulates glucose transport activity in rat skeletal muscle. *J Biol Chem* 274:22139-22142, 1999

Etgen-GJ J, Zavadoski WJ, Holman GD, Gibbs EM: Insulin-sensitive regulation of glucose transport and GLUT4 translocation in skeletal muscle of GLUT1 transgenic mice. *Biochem J* 337:51-57, 1999

Filippis A, Clark S, Proietto J: Increased flux through the hexosamine biosynthesis pathway inhibits glucose transport acutely by activation of protein kinase C. *Biochem J* 324:981-985, 1997

Fischer Y, Thomas J, Sevilla L, Munoz P, Becker C, Holman G, Kozka IJ, Palacin M, Testar X, Kammermeier H, Zorzano A: Insulin-induced recruitment of glucose transporter 4 (GLUT4) and GLUT1 in isolated rat cardiac myocytes. Evidence of the existence of different intracellular GLUT4 vesicle populations. *J Biol Chem* 272:7085-7092, 1997

Foran PG, Fletcher LM, Oatey PB, Mohammed N, Dolly JO, Tavare JM: Protein kinase B stimulates the translocation of GLUT4 but not GLUT1 or transferrin receptors in 3T3-L1 adipocytes by a pathway involving SNAP-23, synaptobrevin-2, and/or cellubrevin. *J Biol Chem* 274:28087-28095, 1999

Friedman JE, Dudek RW, Whitehead DS, Downes DL, Frisell WR, Caro JF, Dohm GL: Immunolocalization of glucose transporter GLUT4 within human skeletal muscle. *Diabetes* 40:150-154, 1991

Galante P, Maerker E, Scholz R, Rett K, Herberg L, Mosthaf L, Haring HU: Insulin-induced translocation of GLUT 4 in skeletal muscle of insulin-resistant Zucker rats. *Diabetologia* 37:3-9, 1994

Galante P, Mosthaf L, Kellerer M, Berti L, Tippmer S, Bossenmaier B, Fujiwara T, Okuno A, Horikoshi H, Haring HU: Acute hyperglycemia provides an insulin-independent inducer for GLUT4 translocation in C2C12 myotubes and rat skeletal muscle. *Diabetes* 44:646-651, 1995

Ganz MB, Seftel A: Glucose-induced changes in protein kinase C and nitric oxide are prevented by vitamin E. *Am J Physiol Endocrinol Metab* 278:E146-E152, 2000

Garvey WT: Glucose transport and NIDDM. *Diabetes Care* 15:396-417, 1992

Gnudi L, Shepherd PR, Kahn BB: Over-expression of GLUT4 selectively in adipose tissue in transgenic mice: implications for nutrient partitioning. *Proc Nutr Soc* 55:191-199, 1996

Gould GW, Holman GD: The glucose transporter family: structure, function and tissue-specific expression. *Biochem J* 295:329-341, 1993

Grover MM, Walsh SA, Thompson SA: Glucose transporter 3 (GLUT3) protein is present in human myocardium. *Biochim Biophys Acta* 1416:145-154, 1999

Guma A, Camps M, Palacin M, Testar X, Zorzano A: Protein kinase C activators selectively inhibit insulin-stimulated system A transport activity in skeletal muscle at a post-receptor level. *Biochem J* 268:633-639, 1990

Guma A, Zierath JR, Wallberg HH, Klip A: Insulin induces translocation of GLUT-4 glucose transporters in human skeletal muscle. *Am J Physiol* 268:E613-E622, 1995

Hager SR, Jochen AL, Kalkhoff RK: Insulin resistance in normal rats infused with glucose for 72 h. *Am J Physiol* 260:E353-E362, 1991

Han DH, Hansen PA, Host HH, Holloszy JO: Insulin resistance of muscle glucose transport in rats fed a high-fat diet: a reevaluation. *Diabetes* 46:1761-1767, 1997

Handberg A, Kayser L, Hoyer PE, Micheelsen J, Vinten J: Elevated GLUT 1 level in crude muscle membranes from diabetic Zucker rats despite a normal GLUT 1 level in perineurial sheaths [published erratum appears in Diabetologia 1994 Jul;37(7):732]. *Diabetologia* 37:443-448, 1994

Hansen PA, Corbett JA, Holloszy JO: Phorbol esters stimulate muscle glucose transport by a mechanism distinct from the insulin and hypoxia pathways. *Am J Physiol* 273:E28-E36, 1997

Hansen PA, Wang W, Marshall BA, Holloszy JO, Mueckler M: Dissociation of GLUT4 translocation and insulin-stimulated glucose transport in transgenic mice overexpressing GLUT1 in skeletal muscle. *J Biol Chem* 273:18173-18179, 1998

Haring HU, Kasuga M, Kahn CR: Insulin receptor phosphorylation in intact adipocytes and in a cell- free system. *Biochem Biophys Res Commun* 108:1538-1545, 1982

Haring HU, Kellerer M, Mosthaf L: Modulation of insulin receptor signalling: significance of altered receptor isoform patterns and mechanism of hyperglycaemia-induced receptor modulation. *Diabetologia* 37 Suppl 2:S149-S154, 1994

Haring HU, Tippmer S, Kellerer M, Mosthaf L, Kroder G, Bossenmaier B, Berti L: Modulation of insulin receptor signaling. Potential mechanisms of a cross talk between bradykinin and the insulin receptor. *Diabetes* 45 Suppl 1:S115-S119, 1996

Hart GW: Glycosylation. *Curr Opin Cell Biol* 4:1017-1023, 1992

Hawkins M, Angelov I, Liu R, Barzilai N, Rossetti L: The tissue concentration of UDP-N-acetylglucosamine modulates the stimulatory effect of insulin on skeletal muscle glucose uptake. *J Biol Chem* 272:4889-4895, 1997

Hawkins M, Hu M, Yu J, Eder H, Vuguin P, She L, Barzilai N, Leiser M, Backer JM, Rossetti L: Discordant effects of glucosamine on insulin-stimulated glucose metabolism and phosphatidylinositol 3-kinase activity. *J Biol Chem* 274:31312-31319, 1999

Hayashi T, Wojtaszewski JF, Goodyear LJ: Exercise regulation of glucose transport in skeletal muscle. *Am J Physiol* 273:E1039-E1051, 1997

Heart E, Choi WS, Sung CK: Glucosamine-induced insulin resistance in 3T3-L1 adipocytes. *Am J Physiol Endocrinol Metab* 278:E103-E112, 2000

Hebert-LF J, Daniels MC, Zhou J, Crook ED, Turner RL, Simmons ST, Neidigh JL, Zhu JS, Baron AD, McClain DA: Overexpression of glutamine:fructose-6-phosphate amidotransferase in transgenic mice leads to insulin resistance. *J Clin Invest* 98:930-936, 1996

Henry RR, Gumbiner B, Flynn T, Thorburn AW: Metabolic effects of hyperglycemia and hyperinsulinemia on fate of intracellular glucose in NIDDM. *Diabetes* 39:149-156, 1990

Higaki Y, Wojtaszewski JF, Hirshman MF, Withers DJ, Towery H, White MF, Goodyear LJ: Insulin receptor substrate-2 is not necessary for insulin- and exercise-stimulated glucose transport in skeletal muscle. *J Biol Chem* 274:20791-20795, 1999

Holman GD, Kasuga M: From receptor to transporter: insulin signalling to glucose transport. *Diabetologia* 40:991-1003, 1997

Holman GD, Kozka IJ, Clark AE, Flower CJ, Saltis J, Habberfield AD, Simpson IA, Cushman SW: Cell surface labeling of glucose transporter isoform GLUT4 by bis- mannose photolabel. Correlation with stimulation of glucose transport in rat adipose cells by insulin and phorbol ester. *J Biol Chem* 265:18172-18179, 1990

Hong DH, Huan J, Ou BR, Yeh JY, Saido TC, Cheeke PR, Forsberg NE: Protein kinase C isoforms in muscle cells and their regulation by phorbol ester and calpain. *Biochim Biophys Acta* 1267:45-54, 1995

Horgan DJ, Kuypers R: Biochemical properties of purified transverse tubules isolated from skeletal muscle triads. *Arch Biochem Biophys* 260:1-9, 1988

Hother NO, Beck NH: Basal glucose metabolism in type 2 diabetes. A critical review. *Diabete Metab* 17:136-145, 1991

Hresko RC, Heimberg H, Chi MM, Mueckler M: Glucosamine-induced insulin resistance in 3T3-L1 adipocytes is caused by depletion of intracellular ATP. *J Biol Chem* 273:20658-20668, 1998

Hundal HS, Darakhshan F, Kristiansen S, Blakemore SJ, Richter EA: GLUT5 expression and fructose transport in human skeletal muscle. *Adv Exp Med Biol* 441:35-45, 1998

Hundal HS, Marette A, Mitsumoto Y, Ramlal T, Blostein R, Klip A: Insulin induces translocation of the alpha 2 and beta 1 subunits of the Na+/K(+)-ATPase from intracellular compartments to the plasma membrane in mammalian skeletal muscle. *J Biol Chem* 267:5040-5043, 1992

Hunter T: Protein kinases and phosphatases: the yin and yang of protein phosphorylation and signaling. *Cell* 80:225-236, 1995

Ide R, Maegawa H, Kashiwagi A, Kikkawa R, Shigeta Y: High glucose condition desensitizes insulin action at the levels of receptor kinase. *Endocr J* 42:1-8, 1995

Inoguchi T, Battan R, Handler E, Sportsman JR, Heath W, King GL: Preferential elevation of protein kinase C isoform beta II and diacylglycerol levels in the aorta and heart of diabetic rats: differential reversibility to glycemic control by islet cell transplantation. *Proc Natl Acad Sci U S A* 89:11059-11063, 1992

Ishizuka T, Kajita K, Miura A, Ishizawa M, Kanoh Y, Itaya S, Kimura M, Muto N, Mune T, Morita H, Yasuda K: DHEA improves glucose uptake via activations of protein kinase C and phosphatidylinositol 3-kinase. *Am J Physiol* 276:E196-E204, 1999

Ishizuka T, Kajita K, Yamada K, Miura A, Kanoh Y, Ishizawa M, Wada H, Itaya S, Yamamoto M, Yasuda K, Nagata K, Okano Y: Insulin regulated PKC isoform mRNA in rat adipocytes. *Diabetes Res Clin Pract* 33:159-167, 1996

Jones PM, Persaud SJ: Protein kinases, protein phosphorylation, and the regulation of insulin secretion from pancreatic beta-cells. *Endocr Rev* 19:429-461, 1998

Kahn BB, Rossetti L, Lodish HF, Charron MJ: Decreased in vivo glucose uptake but normal expression of GLUT1 and GLUT4 in skeletal muscle of diabetic rats. *J Clin Invest* 87:2197-2206, 1991

Kandror K, Pilch PF: Identification and isolation of glycoproteins that translocate to the cell surface from GLUT4-enriched vesicles in an insulin-dependent fashion. *J Biol Chem* 269:138-142, 1994

Kasuga M, Zick Y, Blith DL, Karlsson FA, Haring HU, Kahn CR: Insulin stimulation of phosphorylation of the beta subunit of the insulin receptor. Formation of both phosphoserine and phosphotyrosine. *J Biol Chem* 257:9891-9894, 1982

Katz EB, Burcelin R, Tsao TS, Stenbit AE, Charron MJ: The metabolic consequences of altered glucose transporter expression in transgenic mice. *J Mol Med* 74:639-652, 1996

Kawano Y, Rincon J, Soler A, Ryder JW, Nolte LA, Zierath JR, Wallberg-Henriksson H: Changes in glucose transport and protein kinase Cbeta(2) in rat skeletal muscle induced by hyperglycaemia. *Diabetologia* 42:1071-1079, 1999

Kayano T, Burant CF, Fukumoto H, Gould GW, Fan YS, Eddy RL, Byers MG, Shows TB, Seino S, Bell GI: Human facilitative glucose transporters. Isolation, functional characterization, and gene localization of cDNAs encoding an isoform (GLUT5) expressed in small intestine, kidney, muscle, and adipose tissue and an unusual glucose transporter pseudogene-like sequence (GLUT6). *J Biol Chem* 265:13276-13282, 1990

Kellerer M, Lammers R, Haring HU: Insulin signal transduction: possible mechanisms for insulin resistance. *Exp Clin Endocrinol Diabetes* 107:97-106, 1999

Kellerer M, Mushack J, Mischak H, Haring HU: Protein kinase C (PKC) epsilon enhances the inhibitory effect of TNF alpha on insulin signaling in HEK293 cells. *FEBS Lett* 418:119-122, 1998

Kellerer M, Mushack J, Seffer E, Mischak H, Ullrich A, Haring HU: Protein kinase C isoforms alpha, delta and theta require insulin receptor substrate-1 to inhibit the tyrosine kinase activity of the insulin receptor in human kidney embryonic cells (HEK 293 cells). *Diabetologia* 41:833-838, 1997

Keranen LM, Newton AC: Ca2+ differentially regulates conventional protein kinase Cs' membrane interaction and activation. *J Biol Chem* 272:25959-25967, 1997

Khayat ZA, Tsakiridis T, Ueyama A, Somwar R, Ebina Y, Klip A: Rapid stimulation of glucose transport by mitochondrial uncoupling depends in part on cytosolic Ca2+ and cPKC. *Am J Physiol* 275:C1487-C1497, 1998

Kido Y, Burks DJ, Withers D, Bruning JC, Kahn CR, White MF, Accili D: Tissue-specific insulin resistance in mice with mutations in the insulin receptor, IRS-1, and IRS-2. *J Clin Invest* 105:199-205, 2000

King GL, Brownlee M: The cellular and molecular mechanisms of diabetic complications. *Endocrinol Metab Clin North Am* 25:255-270, 1996

Kitamura T, Ogawa W, Sakaue H, Hino Y, Kuroda S, Takata M, Matsumoto M, Maeda T, Konishi H, Kikkawa U, Kasuga M: Requirement for activation of the serine-threonine kinase Akt (protein kinase B) in insulin stimulation of protein synthesis but not of glucose transport. *Mol Cell Biol* 18:3708-3717, 1998

Klip A, Ramlal T, Bilan PJ, Cartee GD, Gulve EA, Holloszy JO: Recruitment of GLUT-4 glucose transporters by insulin in diabetic rat skeletal muscle. *Biochem Biophys Res Commun* 172:728-736, 1990

Kohn AD, Summers SA, Birnbaum MJ, Roth RA: Expression of a constitutively active Akt Ser/Thr kinase in 3T3-L1 adipocytes stimulates glucose uptake and glucose transporter 4 translocation. *J Biol Chem* 271:31372-31378, 1996

Kohout TA, Rogers TB: Use of a PCR-based method to characterize protein kinase C isoform expression in cardiac cells. *Am J Physiol* 264:C1350-C1359, 1993

Kolm L, V, Sauer U, Nerlich A, Lehmann R, Schleicher ED: High glucose-induced transforming growth factor beta1 production is mediated by the hexosamine pathway in porcine glomerular mesangial cells. *J Clin Invest* 101:160-169, 1998

Kolm L, V, Tippmer S, Haring HU, Schleicher E: Glucosamine induces translocation of protein kinase C isoenzymes in mesangial cells. *Exp Clin Endocrinol Diabetes* 106:377-383, 1998

Konishi H, Kuroda S, Kikkawa U: The pleckstrin homology domain of RAC protein kinase associates with the regulatory domain of protein kinase C zeta. *Biochem Biophys Res Commun* 205:1770-1775, 1994

Koya D, Jirousek MR, Lin YW, Ishii H, Kuboki K, King GL: Characterization of protein kinase C beta isoform activation on the gene expression of transforming growth factor-beta, extracellular matrix components, and prostanoids in the glomeruli of diabetic rats. *J Clin Invest* 100:115-126, 1997

Koya D, King GL: Protein kinase C activation and the development of diabetic complications. *Diabetes* 47:859-866, 1998

Krook A, Kawano Y, Song XM, Efendic S, Roth RA, Wallberg-Henriksson H, Zierath JR: Improved glucose tolerance restores insulin-stimulated Akt kinase activity and glucose transport in skeletal muscle from diabetic Goto-Kakizaki rats. *Diabetes* 46:2110-2114, 1997

Krook A, Roth RA, Jiang XJ, Zierath JR, Wallberg-Henriksson H: Insulin-stimulated Akt kinase activity is reduced in skeletal muscle from NIDDM subjects. *Diabetes* 47:1281-1286, 1998

Laemmli UK: Cleavage of structural proteins during the assembly of the head of bacteriophage T4. *Nature* 227:680-685, 1970

Landers JP, Oda RP, Madden BJ, Spelsberg TC: High-performance capillary electrophoresis of glycoproteins: the use of modifiers of electroosmotic flow for analysis of microheterogeneity. *Anal Biochem* 205:115-124, 1992

Lavan BE, Lane WS, Lienhard GE: The 60-kDa phosphotyrosine protein in insulin-treated adipocytes is a new member of the insulin receptor substrate family. *J Biol Chem* 272:11439-11443, 1997

Laville M, Auboeuf D, Khalfallah Y, Vega N, Riou JP, Vidal H: Acute regulation by insulin of phosphatidylinositol-3-kinase, Rad, Glut 4, and lipoprotein lipase mRNA levels in human muscle. *J Clin Invest* 98:43-49, 1996

Lawrence JCJ, Hiken JF, James DE: Stimulation of glucose transport and glucose transporter phosphorylation by okadaic acid in rat adipocytes. *J Biol Chem* 265:19768-19776, 1990

Laybutt DR, Chisholm DJ, Kraegen EW: Specific adaptations in muscle and adipose tissue in response to chronic systemic glucose oversupply in rats. *Am J Physiol* 273:E1-E9, 1997

Laybutt DR, Thompson AL, Cooney GJ, Kraegen EW: Selective chronic regulation of GLUT1 and GLUT4 content by insulin, glucose, and lipid in rat cardiac muscle in vivo. *Am J Physiol* 273:H1309-H1316, 1997

Leahy JL, Cooper HE, Weir GC: Impaired insulin secretion associated with near normoglycemia. Study in normal rats with 96-h in vivo glucose infusions. *Diabetes* 36:459-464, 1987

Lehmann R, Voelter W, Liebich HM: Capillary electrophoresis in clinical chemistry. *J Chromatogr B Biomed Sci Appl* 697:3-35, 1997

Lehmann R, Huber M, Beck A, Schindera T, Rinkler T, Houdali B, Weigert C, Haring HU, Voelter W, Schleicher ED: Simultaneous, quantitaive analysis of UDP-N-acetylglucosamine, UDP-Nacetylgalactosamine, UDP-glucose and UDP-galactose in human peripheral blood cells, muscle biopsies and cultured mesangial cells by capillary zone electrophoresis, Electrophoresis, in press

Lund S, Flyvbjerg A, Holman GD, Larsen FS, Pedersen O, Schmitz O: Comparative effects of IGF-I and insulin on the glucose transporter system in rat muscle. *Am J Physiol* 267:E461-E466, 1994

Maegawa H, Ide R, Hasegawa M, Ugi S, Egawa K, Iwanishi M, Kikkawa R, Shigeta Y, Kashiwagi A: Thiazolidine derivatives ameliorate high glucose-induced insulin resistance via the normalization of protein-tyrosine phosphatase activities. *J Biol Chem* 270:7724-7730, 1995

Maegawa H, Shigeta Y, Egawa K, Kobayashi M: Impaired autophosphorylation of insulin receptors from abdominal skeletal muscles in nonobese subjects with NIDDM. *Diabetes* 40:815-819, 1991

Marette A, Burdett E, Douen A, Vranic M, Klip A: Insulin induces the translocation of GLUT4 from a unique intracellular organelle to transverse tubules in rat skeletal muscle. *Diabetes* 41:1562-1569, 1992

Marette A, Krischer J, Lavoie L, Ackerley C, Carpentier JL, Klip A: Insulin increases the Na(+)-K(+)-ATPase alpha 2-subunit in the surface of rat skeletal muscle: morphological evidence. *Am J Physiol* 265:C1716-C1722, 1993

Marette A, Richardson JM, Ramlal T, Balon TW, Vranic M, Pessin JE, Klip A: Abundance, localization, and insulin-induced translocation of glucose transporters in red and white muscle. *Am J Physiol* 263:C443-C452, 1992

Marshall BA, Hansen PA, Ensor NJ, Ogden MA, Mueckler M: GLUT-1 or GLUT-4 transgenes in obese mice improve glucose tolerance but do not prevent insulin resistance. *Am J Physiol* 276:E390-E400, 1999

Marshall S, Bacote V, Traxinger RR: Complete inhibition of glucose-induced desensitization of the glucose transport system by inhibitors of mRNA synthesis. Evidence for rapid turnover of glutamine:fructose-6-phosphate amidotransferase. *J Biol Chem* 266:10155-10161, 1991

Marshall S, Bacote V, Traxinger RR: Discovery of a metabolic pathway mediating glucose-induced desensitization of the glucose transport system. Role of hexosamine biosynthesis in the induction of insulin resistance. *J Biol Chem* 266:4706-4712, 1996

Mathe D: Dyslipidemia and diabetes: animal models. *Diabete Metab* 21:106-111, 1995

McCarty MF: Up-regulation of intracellular signalling pathways may play a central pathogenic role in hypertension, atherogenesis, insulin resistance, and cancer promotion--the 'PKC syndrome'. *Med Hypotheses* 46:191-221, 1996

McClain DA, Maegawa H, Lee J, Dull TJ, Ulrich A, Olefsky JM: A mutant insulin receptor with defective tyrosine kinase displays no biologic activity and does not undergo endocytosis. *J Biol Chem* 262:14663-14671, 1987

Mellor H, Parker PJ: The extended protein kinase C superfamily. *Biochem J* 332:281-292, 1996

Miele C, Formisano P, Condorelli G, Caruso M, Oriente F, Andreozzi F, Tocchetti CG, Riccardi G, Beguinot F: Abnormal glucose transport and GLUT1 cell-surface content in fibroblasts and skeletal muscle from NIDDM and obese subjects. *Diabetologia* 40:421-429, 1997

Miles PD, Higo K, Romeo OM, Lee MK, Rafaat K, Olefsky JM: Troglitazone prevents hyperglycemia-induced but not glucosamine-induced insulin resistance. *Diabetes* 47:395-400, 1998

Moller DE, Benecke H, Flier JS: Biologic activities of naturally occurring human insulin receptor mutations. Evidence that metabolic effects of insulin can be mediated by a kinase-deficient insulin receptor mutant. *J Biol Chem* 266:10995-11001, 1991

Mosthaf L, Kellerer M, Muhlhofer A, Mushack J, Seffer E, Haring HU: Insulin leads to a parallel translocation of PI-3-kinase and protein kinase C zeta [see comments]. *Exp Clin Endocrinol Diabetes* 104:19-24, 1996

Mueckler M: Facilitative glucose transporters. *Eur J Biochem* 219:713-725, 1994

Muller HK, Kellerer M, Ermel B, Muhlhofer A, Obermaier KB, Vogt B, Haring HU: Prevention by protein kinase C inhibitors of glucose-induced insulin-receptor tyrosine kinase resistance in rat fat cells. *Diabetes* 40:1440-1448, 1991

Munoz P, Rosemblatt M, Testar X, Palacin M, Thoidis G, Pilch PF, Zorzano A: The T-tubule is a cell-surface target for insulin-regulated recycling of membrane proteins in skeletal muscle. *Biochem J* 312:393-400, 1996

Munoz P, Rosemblatt M, Testar X, Palacin M, Zorzano A: Isolation and characterization of distinct domains of sarcolemma and T-tubules from rat skeletal muscle. *Biochem J* 307:273-280, 1995.

Murphy M, McGinty A, Godson C: Protein kinases C: potential targets for intervention in diabetic nephropathy. *Curr Opin Nephrol Hypertens* 7:563-570, 1998

Myers MGJ, Backer JM, Sun XJ, Shoelson S, Hu P, Schlessinger J, Yoakim M, Schaffhausen B, White MF: IRS-1 activates phosphatidylinositol 3'-kinase by associating with src homology 2 domains of p85. *Proc Natl Acad Sci U S A* 89:10350-10354, 1992

Nawano M, Ueta K, Oku A, Arakawa K, Saito A, Funaki M, Anai M, Kikuchi M, Oka Y, Asano T: Hyperglycemia impairs the insulin signaling step between PI 3-kinase and Akt/PKB activations in ZDF rat liver. *Biochem Biophys Res Commun* 266:252-256, 1999

Nerlich AG, Sauer U, Kolm L, V, Wagner E, Koch M, Schleicher ED: Expression of glutamine:fructose-6-phosphate amidotransferase in human tissues: evidence for high variability and distinct regulation in diabetes. *Diabetes* 47:170-178, 1998

Newton AC: Protein kinase C: structure, function, and regulation. *J Biol Chem* 270:28495-28498, 1995

Newton AC: Regulation of protein kinase C. *Curr Opin Cell Biol* 9:161-167, 1997

Nolte LA, Rincon J, Wahlstrom EO, Craig BW, Zierath JR, Wallberg HH: Hyperglycemia activates glucose transport in rat skeletal muscle via a Ca(2+)-dependent mechanism. *Diabetes* 44:1345-1348, 1995

Obermaier-Kusser B, White MF, Pongratz DE, Su Z, Ermel B, Muhlbacher C, Haring HU: A defective intramolecular autoactivation cascade may cause the reduced kinase activity of the skeletal muscle insulin receptor from patients with non-insulin-dependent diabetes mellitus. *J Biol Chem* 264:9497-9504, 1989

Oki T, Yamazaki K, Kuromitsu J, Okada M, Tanaka I: cDNA cloning and mapping of a novel subtype of glutamine:fructose-6-phosphate amidotransferase (GFAT2) in human and mouse. *Genomics* 57:227-234, 1999

Patti ME, Virkamaki A, Landaker EJ, Kahn CR, Yki JH: Activation of the hexosamine pathway by glucosamine in vivo induces insulin resistance of early postreceptor insulin signaling events in skeletal muscle. *Diabetes* 48:1562-1571, 1999

Paz K, Liu YF, Shorer H, Hemi R, LeRoith D, Quan M, Kanety H, Seger R, Zick Y: Phosphorylation of insulin receptor substrate-1 (IRS-1) by protein kinase B positively regulates IRS-1 function. *J Biol Chem* 274:28816-28822, 1999

Pierce GN, Dhalla NS: Sarcolemmal Na+-K+-ATPase activity in diabetic rat heart. *Am J Physiol* 245:C241-C247, 1983

Ploug T, Ralston E: Anatomy of glucose transporters in skeletal muscle. Effects of insulin and contractions. *Adv Exp Med Biol* 441:17-26, 1998

Postic C, Leturque A, Rencurel F, Printz RL, Forest C, Granner DK, Girard J: The effects of hyperinsulinemia and hyperglycemia on GLUT4 and hexokinase II mRNA and protein in rat skeletal muscle and adipose tissue. *Diabetes* 42:922-929, 1993

Qi C, Pekala PH: The influence of mRNA stability on glucose transporter (GLUT1) gene expression. *Biochem Biophys Res Commun* 263:265-269, 1999

Ramlal T, Sarabia V, Bilan PJ, Klip A: Insulin-mediated translocation of glucose transporters from intracellular membranes to plasma membranes: sole mechanism of stimulation of glucose transport in L6 muscle cells. *Biochem Biophys Res Commun* 157:1329-1335, 1988

Rett K, Wicklmayr M, Dietze GJ, Haring HU: Insulin-induced glucose transporter (GLUT1 and GLUT4) translocation in cardiac muscle tissue is mimicked by bradykinin. *Diabetes* 45 Suppl 1:S66-S69, 1996

Rickard EC, Strohl MM, Nielsen RG: Correlation of electrophoretic mobilities from capillary electrophoresis with physicochemical properties of proteins and peptides. *Anal Biochem* 197:197-207, 1991

Robinson KA, Sens DA, Buse MG: Pre-exposure to glucosamine induces insulin resistance of glucose transport and glycogen synthesis in isolated rat skeletal muscles. Study of mechanisms in muscle and in rat-1 fibroblasts overexpressing the human insulin receptor [published erratum appears in Diabetes 1993 Oct;42(10):1547]. *Diabetes* 42:1333-1346, 1993

Robinson KA, Weinstein ML, Lindenmayer GE, Buse MG: Effects of diabetes and hyperglycemia on the hexosamine synthesis pathway in rat muscle and liver. *Diabetes* 44:1438-1446, 1995

Rodnick KJ, Slot JW, Studelska DR, Hanpeter DE, Robinson LJ, Geuze HJ, James DE: Immunocytochemical and biochemical studies of GLUT4 in rat skeletal muscle. *J Biol Chem* 267:6278-6285, 1992

Rossetti L, Giaccari A, DeFronzo RA: Glucose toxicity. *Diabetes Care* 13:610-630, 1990

Sato T, Man ZW, Toide K, Asahi Y: Plasma membrane content of insulin-regulated glucose transporter in skeletal muscle of the male Otsuka Long-Evans Tokushima Fatty rat, a model of non-insulin-dependent diabetes mellitus. *FEBS Lett* 407:329-332, 1997

Schmitz PC, Browne CL, Biden TJ: Characterization of two forms of protein kinase C alpha, with different substrate specificities, from skeletal muscle. *Biochem J* 320:207-214, 1997

Schmitz PC, Browne CL, Oakes ND, Watkinson A, Chisholm DJ, Kraegen EW, Biden TJ: Alterations in the expression and cellular localization of protein kinase C isozymes epsilon and theta are associated with insulin resistance in skeletal muscle of the high-fat-fed rat. *Diabetes* 46:169-178, 1996

Shafrir E: Animal models of non-insulin-dependent diabetes. *Diabetes Metab Rev* 8:179-208, 1992

Shepherd PR, Withers DJ, Siddle K: Phosphoinositide 3-kinase: the key switch mechanism in insulin signalling. *Biochem J* 333:471-490, 1998

Shoelson SE, Chatterjee S, Chaudhuri M, White MF: YMXM motifs of IRS-1 define substrate specificity of the insulin receptor kinase. *Proc Natl Acad Sci U S A* 89:2027-2031, 1992

Simmons RA, Flozak AS, Ogata ES: Glucose regulates glut 1 function and expression in fetal rat lung and muscle in vitro. *Endocrinology* 132:2312-2318, 1993

Simpson IA, Hedo JA: Insulin receptor phosphorylation may not be a prerequisite for acute insulin action. *Science* 223:1301-1304, 1984

Smith TR, Elmendorf JS, David TS, Turinsky J: Growth hormone-induced insulin resistance: role of the insulin receptor, IRS-1, GLUT-1, and GLUT-4. *Am J Physiol* 272:E1071-E1079, 1997

Sofue M, Yoshimura Y, Nishida M, Kawada J: ADP modifies the function of the glucose transporter: studies with reconstituted liposomes. *Biochem J* 292:877-881, 1993

Song XM, Ryder JW, Kawano Y, Chibalin AV, Krook A, Zierath JR: Muscle fiber type specificity in insulin signal transduction. *Am J Physiol* 277:R1690-R1696, 1999

Standaert ML, Bandyopadhyay G, Perez L, Price D, Galloway L, Poklepovic A, Sajan MP, Cenni V, Sirri A, Moscat J, Toker A, Farese RV: Insulin activates protein kinases C-zeta and C-lambda by an autophosphorylation-dependent mechanism and stimulates their translocation to GLUT4 vesicles and other membrane fractions in rat adipocytes. *J Biol Chem* 274:25308-25316, 1999

Standaert ML, Bandyopadhyay G, Sajan MP, Cong L, Quon MJ, Farese RV: Okadaic acid activates atypical protein kinase C (zeta/lambda) in rat and 3T3/L1 adipocytes. An apparent requirement for activation of Glut4 translocation and glucose transport. *J Biol Chem* 274:14074-14078, 1999

Stevenson RW, Kreutter DK, Andrews KM, Genereux PE, Gibbs EM: Possibility of distinct insulin-signaling pathways beyond phosphatidylinositol 3-kinase-mediating glucose transport and lipogenesis. *Diabetes* 47:179-185, 1998

Stolwijk JA, Hardy JD: Temperature regulation in man--a theoretical study. *Pflugers Arch Gesamte Physiol Menschen Tiere* 291:129-162, 1966

Sugden MC, Holness MJ, Fryer LG: Differential regulation of glycogen synthase by insulin and glucose in vivo in skeletal muscles of the rat. *Am J Physiol* 273:E479-E487, 1997

Thorens B, Charron MJ, Lodish HF: Molecular physiology of glucose transporters. *Diabetes Care* 13:209-218, 1990

Ueki K, Yamamoto-Honda R, Kaburagi Y, Yamauchi T, Tobe K, Burgering BM, Coffer PJ, Komuro I, Akanuma Y, Yazaki Y, Kadowaki T: Potential role of protein kinase B in insulin-induced glucose transport, glycogen synthesis, and protein synthesis. *J Biol Chem* 273:5315-5322, 1998

Utriainen T, Takala T, Luotolahti M, Ronnemaa T, Laine H, Ruotsalainen U, Haaparanta M, Nuutila P, Yki JH: Insulin resistance characterizes glucose uptake in skeletal muscle but not in the heart in NIDDM. *Diabetologia* 41:555-559, 1998

Vaag A, Damsbo P, Hother NO, Beck NH: Hyperglycaemia compensates for the defects in insulin-mediated glucose metabolism and in the activation of glycogen synthase in the skeletal muscle of patients with type 2 (non-insulin-dependent) diabetes mellitus. *Diabetologia* 35:80-88, 1992

van-de-Werve G, Zaninetti D, Lang U, Vallotton MB, Jeanrenaud B: Identification of a major defect in insulin-resistant tissues of genetically obese (fa/fa) rats. Impaired protein kinase C. *Diabetes* 36:310-314, 1987

Vanhaesebroeck B, Alessi DR: The PI3K-PDK1 connection: more than just a road to PKB. *Biochem J* 346:561-576, 2000

Verret C, Poussard S, Touyarot K, Donger C, Savart M, Cottin P, Ducastaing A: Degradation of protein kinase Malpha by mu-calpain in a mu-calpain-protein kinase Calpha complex. *Biochim Biophys Acta* 1430:141-148, 1999

Vinals F, Gross A, Testar X, Palacin M, Rosen P, Zorzano A: High glucose concentrations inhibit glucose phosphorylation, but not glucose transport, in human endothelial cells. *Biochim Biophys Acta* 1450:119-129, 1999

Virkamaki A, Daniels MC, Hamalainen S, Utriainen T, McClain D, Yki JH: Activation of the hexosamine pathway by glucosamine in vivo induces insulin resistance in multiple insulin sensitive tissues. *Endocrinology* 138:2501-2507, 1997

Vogt B, Muhlbacher C, Carrascosa J, Obermaier KB, Seffer E, Mushack J, Pongratz D, Haring HU: Subcellular distribution of GLUT 4 in the skeletal muscle of lean type 2 (non-insulin-dependent) diabetic patients in the basal state. *Diabetologia* 35:456-463, 1992

Vuorinen MH, Koivisto VA, Yki JH: Mechanisms of hyperglycemia-induced insulin resistance in whole body and skeletal muscle of type I diabetic patients. *Diabetes* 41:571-580, 1992

Wakasaki H, Koya D, Schoen FJ, Jirousek MR, Ways DK, Hoit BD, Walsh RA, King GL: Targeted overexpression of protein kinase C beta2 isoform in myocardium causes cardiomyopathy. *Proc Natl Acad Sci U S A* 94:9320-9325, 1997

Wang Q, Bilan PJ, Tsakiridis T, Hinek A, Klip A: Actin filaments participate in the relocalization of phosphatidylinositol3-kinase to glucose transporter-containing compartments and in the stimulation of glucose uptake in 3T3-L1 adipocytes. *Biochem J* 331:917-928, 1998

Wang W, Hansen PA, Marshall BA, Holloszy JO, Mueckler M: Insulin unmasks a COOH-terminal Glut4 epitope and increases glucose transport across T-tubules in skeletal muscle. *J Cell Biol* 135:415-430, 1996

White MF: The insulin signalling system and the IRS proteins. *Diabetologia* 40 Suppl 2:S2-17, 1997

Wojtaszewski JF, Higaki Y, Hirshman MF, Michael MD, Dufresne SD, Kahn CR, Goodyear LJ: Exercise modulates postreceptor insulin signaling and glucose transport in muscle-specific insulin receptor knockout mice. *J Clin Invest* 104:1257-1264, 1999

Yamada K, Avignon A, Standaert ML, Cooper DR, Spencer B, Farese RV: Effects of insulin on the translocation of protein kinase C-theta and other protein kinase C isoforms in rat skeletal muscles. *Biochem J* 308:177-180, 1995

Yki JH, Daniels MC, Virkamaki A, Makimattila S, DeFronzo RA, McClain D: Increased glutamine:fructose-6-phosphate amidotransferase activity in skeletal muscle of patients with NIDDM. *Diabetes* 45:302-307, 1996

Yki JH, Makimattila S: Insulin resistance due to hyperglycaemia: an adaptation protecting insulin-sensitive tissues. *Diabetologia* 40 Suppl 2:S141-S144, 1997

Yki JH, Nyman T, Rissanen E, Leino M, Hamalainen S, Virkamaki A, Hauguel-de MS: Glutamine: fructose-6-phosphate amidotransferase activity and gene expression are regulated in a tissue-specific fashion in pregnant rats. *Life Sci* 65:215-223, 1999

Yki JH, Vogt C, Lozzo P, Pipek R, Daniels MC, Virkamaki A, Makimattila S, Mandarino L, DeFronzo RA, McClain D, Gottschalk WK: UDP-N-acetylglucosamine transferase and glutamine: fructose 6-phosphate amidotransferase activities in insulin-sensitive tissues. *Diabetologia* 40:76-81, 1997

Yki JH: Action of insulin on glucose metabolism in vivo. *Baillieres Clin Endocrinol Metab* 7:903-927, 1993

Yki JH: Acute and chronic effects of hyperglycaemia on glucose metabolism: implications for the development of new therapies. *Diabet Med* 14 Suppl 3:S32-S37, 1996

Yki JH: Glucose toxicity. *Endocr Rev* 13:415-431, 1996

Yki-Jarvinen H, Sahlin K, Ren JM, Koivisto VA: Localization of rate-limiting defect for glucose disposal in skeletal muscle of insulin-resistant type I diabetic patients. *Diabetes* 39:157-167, 1990

Zaninetti D, Greco PR, Assimacopoulos JF, Jeanrenaud B: Dysregulation of glucose transport and transporters in perfused hearts of genetically obese (fa/fa) rats. *Diabetologia* 32:56-60, 1989

Zhou L, Chen H, Xu P, Cong LN, Sciacchitano S, Li Y, Graham D, Jacobs AR, Taylor SI, Quon MJ: Action of insulin receptor substrate-3 (IRS-3) and IRS-4 to stimulate translocation of GLUT4 in rat adipose cells. *Mol Endocrinol* 13:505-514, 1999

Zierath JR, He L, Guma A, Odegoard WE, Klip A, Wallberg HH: Insulin action on glucose transport and plasma membrane GLUT4 content in skeletal muscle from patients with NIDDM. *Diabetologia* 39:1180-1189, 1996

Zierath JR, Houseknecht KL, Gnudi L, Kahn BB: High-fat feeding impairs insulin-stimulated GLUT4 recruitment via an early insulin-signaling defect. *Diabetes* 46:215-223, 1997

Zierler K: Does insulin-induced increase in the amount of plasma membrane GLUTs quantitatively account for insulin-induced increase in glucose uptake? *Diabetologia* 41:724-730, 1998

Zorzano A, Munoz P, Camps M, Mora C, Testar X, Palacin M: Insulin-induced redistribution of GLUT4 glucose carriers in the muscle fiber. In search of GLUT4 trafficking pathways. *Diabetes* 45 Suppl 1:S70-S81, 1996